An optogenetic investigation of mechanisms of ictogenesis

Zahra Shiri

Degree of Doctor of Philosophy

Integrated Program in Neuroscience
McGill University
Montreal, QC, Canada

December 2016

A thesis submitted to the faculty of Graduate Studies and Research in partial fulfillment of the requirements of the degree of Doctor of Philosophy

Acknowledgements

Although words don't suffice to express my gratitude to those who have helped me reach where I am today, I would like to acknowledge their help and support here.

First and foremost, I would like to express my most sincere gratitude to my supervisor, Dr. Massimo Avoli, who believed in me and was always there to redirect me when I felt lost and disoriented. I cannot thank him enough for the support and guidance he has provided me over the past four years. Working in his lab and under his supervision has been a blessing I am glad to say I never took for granted.

I would also like to thank Dr. Sylvain Williams who welcomed me in his lab for over two years and gave me ample time and resources to feed my curiosity in exploring the never ending opportunities of the optogenetic world.

I am ever so grateful to my committee member, Dr. Phillipe Séguéla, for always being available and greeting me with a smile even as I stopped him in the hallways time and time again.

I would like to thank Dr. Maxime Lévesque who always stayed positive and happily spent hours perfecting Matlab scripts for my analyses. I am grateful to my colleagues Dr. Pariya Salami, Dr. Charles Behr, Dr. Rochelle Herrington, and Li-Yuan Chen for making the lab a pleasant environment. I would like to particularly thank Dr. Shabnam Hamidi for patiently teaching me the nitty gritty details of electrophysiology and still finding the time to be a great friend and support throughout these years.

From the wonderful team I got to work with at the Douglas Institute, I want to thank Dr. Bénédicte Amilhon, Dr. Christian Kortleven, Jennifer Robinson, and Heather Nichol who welcomed me as one of their own. I would especially like to thank Dr. Frédérique Manseau

for sharing his valuable time and knowledge with me so generously.

I am thankful to Toula Papadopoulos for her reliability and her assistance. I must thank everyone at the MNI Animal Care Facility for always being available to help with a wonderful extra smile.

Last but most certainly not least, I would like to thank my family without who I could not have become who I am today. To my parents, your unconditional love, never-ending support, and sacrifice were essential to my succeeding in life. To my sister and my brother, having such strong role models to grow up with and look up to provided me with all the strength I needed to become the woman I am today. Finally, I cannot thank enough my wonderful spouse, friend, and mentor who always talked me into pushing myself a little further and who believed in me and supported me through rain and shine. This is for you!

Table of Contents

Abstract

Epilepsy is a neurological disorder characterized by excessive neuronal activity in the brain that manifests as spontaneous seizures. Mesial temporal lobe epilepsy (MTLE) is the most common form of focal epilepsy involving seizures that originate from the hippocampus and parahippocampal structures. Seizures occurring in MTLE patients and in experimental models mimicking this neurological disorder can be classified based on their onset pattern, into low-voltage, fast (LVF) and hypersynchronous (HYP) onset seizures. Experimental evidence suggests that LVF-onset seizures mainly result from the synchronous activity of GABA releasing cells while HYP-onset seizures tend to rely on glutamatergic signaling as well. However, despite many advances made in understanding the pathophysiology of epileptic disorders, seizures remain poorly controlled in approximately one third of MTLE patients. Therefore, my graduate studies were focused on deciphering the contributions of different cell populations to epileptiform activity in the *in vitro* 4-aminopyridine (4AP) model using the powerful optogenetic technique. The main findings of my studies are summarized below.

First, I tested the hypothesis that synchronous activation of GABA releasing parvalbumin (PV)-positive interneurons can initiate seizures with an LVF onset pattern similar to those occurring spontaneously in the 4AP model by employing optogenetic stimulation of PV-interneurons in the entorhinal cortex of slices obtained from mice constitutively expressing ChR2 in all PV cells in the brain. These experiments demonstrated the involvement of interneuronal networks in the initiation of LVF-onset seizures.

Second, I compared the role of PV-interneurons and somatostatin (SOM)-interneurons in the initiation of LVF discharges. For this comparison, I confirmed the contribution of PV interneurons to LVF discharges using a novel strain of mice with a PV-Cre background in

which we expressed the enhanced ChR2 opsin, ChETA, using a stereotaxic virus injection procedure. I then used the same procedure in a different transgenic line to obtain mice expressing the ChETA opsin in SOM-interneurons of the entorhinal cortex. Here, I demonstrated that the same optogenetic stimulation pattern targeted to either interneuron subtype can similarly lead to seizures with an LVF onset pattern.

Third, to test the hypothesis that distinct patterns of seizure onset (HYP and LVF) rely on the activity of different neuronal networks, I employed the optogenetic stimulation of calmodulin-dependent protein kinase-positive (CaMKII) pyramidal cells of the entorhinal cortex in the *in vitro* 4AP model. These results demonstrated that the glutamatergic network is mainly responsible for the initiation of HYP onset seizures.

Finally, I wanted to explore the potential ability of optogenetic low-frequency stimulation (LFS) to abate seizures in real-time. Therefore, I used the optogenetic stimulation of CaMKII-positive principal cells and of PV- or SOM-positive interneurons at 1 Hz to compare, for the first time, the effects induced by activation of these specific cell subtypes on 4AP-induced ictal discharges generated from the entorhinal cortex of the transgenic mouse in an *in vitro* brain slice preparation. We found that 1 Hz stimulation of any of these cell types reduced the frequency and duration of ictal discharges.

Collectively, my results demonstrate that (i) under similar experimental conditions, the initiation of LVF and of HYP onset seizures in the entorhinal cortex depends on the preponderant involvement of interneuronal and principal cell networks, respectively, and that (ii) optogenetic LFS of either interneurons or principal cells can control 4AP-induced ictogenesis *in vitro*.

Résumé

L'épilepsie est un désordre neurologique caractérisé par une activité neuronale excessive qui se manifeste par des crises. L'épilepsie temporale mésiale (ETM) est la forme la plus commune d'épilepsie focale et inclut des crises dont l'origine se situe dans l'hippocampe et les structures parahippocampiques. Les crises survenant chez les patients atteints d'ETM et dans les modèles expérimentaux imitant ce désordre neurologique peuvent être classées en deux groupes basés sur l'activité EEG lors de leur initiation, soit les crises à bas voltage haute fréquence (ou « low-voltage fast onset », LVF) et les crises hypersynchrones (HYP). Des études en laboratoire suggèrent que les crises LVF résulteraient de l'activité synchrone des neurones GABAergiques tandis que les crises HYP proviendraient de l'activité des neurones glutamatergiques. Cependant, malgré les avancées réalisées dans l'étude de la pathophysiologie des désordres épileptiques, les crises demeurent peu contrôlées chez approximativement un tiers des patients atteints d'ÉTM. Lors de mes études graduées, j'ai tenté de mieux comprendre, à l'aide de l'optogénétique, la contribution des différentes populations de cellules à l'activité épileptiforme induite *in vitro* par la 4-aminopyridine (4AP). Les principaux résultats de mes études sont résumés ci-dessous.

Premièrement, en employant la stimulation optogénétique des interneurones du cortex entorhinal provenant de tranches de souris exprimant la protéine Channelrodopsine-2 (ChR2) dans les cellules positives à la parvalbumine (PV), j'ai testé l'hypothèse selon laquelle l'activité synchrone des interneurones PV GABAergiques génère des décharges ictales LVF similaires à celles qui surviennent dans le modèle à la 4AP. Ces travaux ont montré l'implication des réseaux d'interneurones dans l'initiation des décharges ictales de type LVF.

Deuxièmement, j'ai comparé le rôle des interneurones PV et des interneurones positifs à la somatostatine (SOM) dans l'initiation des décharges ictales de type LVF. J'ai d'abord confirmé la contribution des interneurones PV lors de l'initiation des décharges de type LVF en utilisant une nouvelle souche de souris PV-Cre dans lesquelles nous avons fait exprimer une nouvelle variante de l'opsine ChR2 (ChETA) en utilisant une procédure d'injection stéréotaxique de virus. J'ai ensuite utilisé la même procédure mais dans une lignée transgénique différente de souris exprimant l'opsine ChETA dans les interneurones SOM du cortex entorhinal. J'ai montré, en utilisant la même méthode de stimulation optogénétique, que l'activation d'un type ou l'autre d'interneurone induit des décharges ictales de type LVF.

Troisièmement, j'ai testé dans le modèle à la 4AP l'hypothèse selon laquelle les décharges ictales de type LVF et HYP dépendent de l'activité de réseaux neuronaux différents en employant la stimulation optogénétique des cellules pyramidales positives à la protéine kinase calmoduline-dépendante (CaMKII) dans le cortex entorhinal. Les résultats obtenus ont montré que le réseau glutamatergique est principalement impliqué lors de l'initiation des décharges ictales de type HYP.

Enfin, j'ai voulu explorer la capacité de la stimulation optogénétique à basse fréquence (« low-frequency stimulation ») à bloquer l'occurrence de décharges ictales. J'ai alors appliqué une stimulation optogénétique à 1 Hz des cellules pyramidales CAMKII et des interneurones PV et SOM afin de comparer, pour la première fois, les effets induits par l'activation en *in vitro* de ces trois types de cellules sur les décharges ictales induites par la 4AP dans des tranches du cortex entorhinal provenant de souris transgéniques. Nous avons découvert que la stimulation à 1 Hz de l'un ou l'autre type de ces cellules induit une diminution de la fréquence et de la durée des décharges ictales.

Dans l'ensemble, mes résultats montrent (i) qu'en conditions expérimentales, l'initiation des décharges ictales LVF et HYP dans le cortex entorhinal dépend respectivement de l'implication des réseaux d'interneurones et de neurones pyramidaux et (ii) que la stimulation optogénétique à basse fréquence des réseaux d'interneurones ou de neurones pyramidaux peut contrôler l'occurrence des décharges ictales induites par la 4AP en *in vitro*.

Contributions of Authors

Chapter 2:

Shiri Z, Manseau F, Lévesque M, Williams S, Avoli M. Interneuron activity leads to initiation of low-voltage fast-onset seizures. *Annals of Neurology*, 2015, 77:541-546.

ZS, SW, and MA designed the study. ZS and FM performed the experiments. ZS and ML analyzed the data. ZS wrote the first draft of the manuscript. ZS, FM, ML, SW, and MA reviewed the manuscript.

Chapter 3:

Shiri Z, Manseau F, Lévesque M, Williams S, Avoli M. Activation of specific neuronal networks leads to different seizure onset types. *Annals of Neurology*, 2016, 79:354-365.

ZS, SW, and MA designed the study. ZS and FM performed the experiments. ZS and ML analyzed the data. ZS wrote the first draft of the manuscript. ZS, FM, ML, SW, and MA reviewed the manuscript.

Chapter 4:

Shiri Z, Lévesque M, Williams S, Avoli M. Optogenetic low-frequency stimulation of specific neuronal populations abates ictogenesis. *Journal of Neuroscience*, submitted.

ZS, SW, and MA designed the study. ZS performed the experiments. ZS and ML analyzed the data. ZS wrote the first draft of the manuscript. ZS, ML, SW, and MA reviewed the manuscript.

Chapter 1: Introduction

In chapter 1, a brief introduction to epilepsy and in particular to mesial temporal lobe epilepsy is provided; this is followed by the fundamentals of epileptiform synchronization with a particular emphasis on mechanisms of ictogenesis. In this chapter, the related articles are reviewed and a broad overview of the contents of this thesis can be found.

1.1. Temporal Lobe Epilepsy

According to the world health organization, about one percent of the world population has some form of epilepsy (Engel et al., 2008). Epilepsy is a neurological disorder characterized by excessive neuronal activity in the brain that manifests as spontaneous seizures. Seizures present different characteristics depending on the brain regions involved in their generation. Based on these characteristics, they can be classified into two groups: generalized or focal epilepsies (Engel, 2005).

Mesial temporal lobe epilepsy (MTLE) is the most common form of focal epilepsy involving seizures that originate from the hippocampus and parahippocampal structures such as the amygdala and the rhinal cortices (Gloor, 1997). Most of our current knowledge on the pathophysiology of this disease is based on animal models that reproduce a sequence of events similar to what is seen in MTLE patients. These events include an initial *status epilepticus* followed by a seizure-free latent period of variable duration, which is associated with reorganization of neural networks and changes in cellular excitability (a process called 'epileptogenesis') (Pitkänen and Sutula, 2002). Following this latent period, spontaneously recurring seizures emerge, which identify the start of the chronic period (Curia et al., 2008; Engel, 2001; Gloor, 1990; Lévesque and Avoli, 2013).

In the past century, researchers have used various tools to study epileptic networks, which has led to considerable improvements in the treatment of epilepsy and in the development of antiepileptic drugs (see for review: Brodie, 2010). However, almost two thirds of MTLE patients do not respond to antiepileptic drugs that are currently available. Due to this refractoriness and the unpredictable nature of the disease, the quality of life of these patients is quite low as they report problems with memory, socialization, and fear of leaving their home (Wiebe et al., 2001).

If antiepileptic drugs do not provide sufficient seizure control and a seizure onset zone can be reliably identified, surgical removal of the epileptogenic zone can be performed (Blume and Parrent, 2006; Wiebe, 2004). Unfortunately, in spite of the progress made in diagnostic techniques, in one third of surgical resections, patients do not become seizure free. In these cases, an alternative approach for treating patients with intractable epilepsy rests on stimulation that can be delivered through either transcranial magnetic or deep-brain electrical procedures (Fisher and Velasco, 2014). However, electrical stimulation is nonspecific and targets all cell types, making it difficult to identify the key cells involved in the generation of seizures (a process called 'ictogenesis') as well as to control unwanted effects of a global stimulation.

What is evident is that we do not yet have a full understanding of the conditions required for seizures to start, propagate, or stop. Thus, it is of paramount importance to shine light on the mechanisms underlying both ictogenesis and epileptogenesis to prevent the occurrence of seizures and to develop new treatments for controlling them. One possible mechanism that could account for epileptiform discharges is attributed to abnormally enhanced excitability

and pathological neuronal synchronization, which is referred to as hypersynchronous activity. This concept is further discussed in the next section.

1.2. Epileptiform Synchronization

Coordinated neural activity, be it between neurons, within local networks or between limbic structures is a hallmark of a healthy brain and supports physiological states such as cognitive functions and sleep (Buzsáki and Draguhn, 2004). Neuronal synchronization depends on chemical and electrical synaptic as well as ephaptic interactions (Timofeev et al., 2012). These interactions, which range from milliseconds to hours, can occur locally to generate local field potentials or over long intracerebral distances to contribute to EEG synchronization (Jiruska et al., 2013). In the abnormal brain, the coordination of neuronal activity becomes pathological and constitutes an important mechanistic role in epileptic disorders including MTLE.

Pathological neuronal synchronization has been studied extensively in seizure-prone limbic structures, and specifically, it has been shown that seizure occurrence could be a consequence of alterations in glutamatergic and GABAergic neurotransmission, i.e., an imbalance between excitatory and inhibitory synaptic transmission (Huberfeld et al., 2011). Other studies have however suggested that seizures arise from the synchronization of a large neuronal population by inhibitory interneurons (Avoli and de Curtis, 2011a; de Curtis and Avoli, 2016; Gnatkovsky et al., 2008).

In the epileptic brain, synchronization can become pathological via several synaptic mechanisms. One such mechanism involves divergent connections of CA3 pyramidal cells onto local pyramidal cells producing hypersynchronous depolarizations (Jefferys et al.,

2012a). Under specific conditions, pyramidal cells can fire bursts of action potentials, recruiting a critical number of neurons to produce epileptiform activity (Traub and Wong, 1982). Overtime, synchronous pathways and excessive cell loss leads to sprouting of new connections that may strengthen these synaptic networks in the chronic epileptic brain (Chen et al., 2013).

A second synaptic mechanism involves a network of inhibitory neurons that can contribute to ictogenesis by entraining populations of excitatory neurons to generate hypersynchronous activity (Mann and Mody, 2008). Furthermore, synchronous activity of interneuonal networks can lead to an accumulation of intracellular chloride and a subsequent increased extrusion of chloride and potassium into the extracellular space (Viitanen et al., 2010). In this manner, excessive interneuronal activity can lead to an increase in extracellular potassium concentrations that can depolarize principal cells and recruit them into seizure activity (McNamara, 1994). Alternatively, synchronous interneuronal activity can constrain the activity of principal cells into specific time windows. Recovery from such strong hyperpolarizing inhibition causes rebound excitation which generates epileptiform discharges (Jefferys et al., 2012a).

Epileptiform activity, however, has been shown to persist under conditions that block synaptic transmission (low extracellular Ca^{2+}) suggesting that non-synaptic mechanisms may also contribute to these events (Jefferys and Haas, 1982). For example, gap junctions can synchronize pairs of interneurons promoting synchronous firing of interneuronal populations (Beierlein et al., 2000). Also, neuronal activity generates electric fields that can modulate neuronal excitability in coupled neurons. Such ephaptic interactions may result in hypersynchronous activity (Jefferys, 1995).

To study these and other mechanisms, epileptiform synchronization may be experimentally induced via several pharmacological manipulations: (i) blocking GABAergic inhibition (using drugs such as bicuculline or picrotoxin); (ii) enhancing glutamatergic excitation (using low-Mg^{2+} artificial cerebrospinal fluid); (iii) increasing intrinsic excitability (using low-Ca^{2+} artificial cerebrospinal fluid); or (iv) enhancing both excitatory and inhibitory transmission (using the K^+ channel blocker 4-aminopyridine (4AP)) (Avoli, 1996; Stanton et al., 1987; Swartzwelder et al., 1988). These manipulations can be used *in vitro* and *in vivo* to induce epileptiform activity to study interictal spikes, ictal discharges, and high frequency oscillations (HFOs), which are described in the following sections.

1.3. Interictal Spikes

Interictal spikes or discharges are brief hypersynchronous events (de Curtis and Avanzini, 2001) that occur between seizures on the EEG of patients with partial epileptic disorders as well as in animal models of epilepsy. The role of these epileptiform events remains elusive as they are not associated with any detectable clinical symptoms. However, they have been shown to impair memory consolidation by disrupting communication between the hippocampus and the prefrontal cortex (Gelinas et al., 2016). Furthermore, seemingly contradictory interactions with ictal discharges have been reported for interictal events in the literature. Specifically, while it has been suggested that interictal discharges herald the onset of ictal events (Ayala et al., 1973), it has also been reported that they can interfere with the occurrence of ictal events (Engel and Ackermann, 1980). Despite this ambiguity, it has been widely accepted that interictal spikes are an important biomarker of epilepsy and can be used reliably for diagnostic purposes (Wirrell, 2010).

Animal models of limbic seizures that are electrographically close to those seen in MTLE patients have allowed researchers to closely examine these interictal events to shine light on their contributions to seizures (Jensen and Yaari, 1988). In particular, studying these interictal discharges in brain slices *in vitro* during bath application of the potassium channel blocker 4AP has revealed two distinct types of discharges. The first type of interictal discharges are long-lasting 'slow' events, they have a low rate of occurrence, appear in all limbic areas, initiate at various sites, and spread slowly to other regions (Perreault and Avoli, 1992; Voskuyl and Albus, 1985). The second type are 'fast' discharges, they have a higher rate of occurrence, originate in the hippocampus, and can propagate to other seizure-prone areas more quickly (Benini et al., 2003). Pharmacological manipulations have suggested that slow interictal discharges reflect the postsynaptic response of principal cells to GABA released by interneurons (*cf.* Capogna et al., 1993) while fast interictal discharges depend on the activity of non-NMDA glutamatergic receptors (Perreault and Avoli, 1991).

The contradicting views on the contribution of interictal discharges to ictal events may be explained in light of these electrophysiologically and pharmacologically different types of interictal events. Indeed, findings obtained in the *in vitro* 4AP model indicate that ictal onset is characterized by one or more events that share similar features with the slow interictal discharges described above (Avoli and de Curtis, 2011a). In addition, it has been shown that both isolated slow interictal discharges and those preceding ictal discharges are accompanied by transient elevations in extracellular potassium concentrations that are $GABA_A$ receptor dependent (Avoli et al., 1996a; Morris et al., 1996). These studies were also in line with previous findings obtained from guinea-pig hippocampal slices (Barolet and Morris, 1991).

Contrarily, it has been shown that fast interictal discharges can control the propensity of parahippocampal structures to generate ictal discharges (Swartzwelder et al., 1987). This process was elegantly demonstrated by Barbarosie and Avoli (1997) in slices bathed in 4AP or Mg^{2+}-free medium where ictal discharges eventually disappear from the entorhinal cortex (EC) while fast interictal events persist for several hours. Subsequent cutting of the Schaffer collateral, which abolishes the spread of hippocampal fast interictal discharges to the EC, restores the ictal activity in the latter region suggesting that these fast events control limbic seizures.

Experimental evidence suggests that the propensity of fast interictal discharges to control ictogenesis rests on their ability to hamper the transient elevations in extracellular potassium associated with slow interictal discharges which were shown to contribute to ictal onset (Avoli et al., 1996b). Fast interictal discharges thus may limit excessive levels of synchronization by down-regulating GABA release and the associated elevations in extracellular potassium during the slow interictal events, thereby controlling ictogenesis. This hypothesis is supported by experiments where parahippocampal structures are stimulated electrically at frequencies similar to that of fast interictal discharges (approximately 1 Hz) to control ictal discharge occurrence in the target structures (Avoli et al., 2013a). These findings also support the ability of low frequency stimulation to reduce seizures in epileptic patients (Yamamoto et al., 2006).

1.4. Ictal Discharges

Seizures are characterized by prolonged periods of hypersynchronous activity that disrupt normal brain function. The electrographic counterpart of a seizure consists of a series of fast

EEG transients that can vary in amplitude and origin, and are easily distinguished from background activity and from interictal spikes. Seizure-like events can also be recorded in *in vitro* models where they are referred to as "ictal discharges". Ictal discharges recorded from epileptic patients, as well as from *in vivo* and *in vitro* animal models are remarkably similar in terms of their electrographic patterns. However, despite the availability of such models and of pharmacological and surgical interventions, how the brain transitions between physiological and pathological states remains obscure.

Studies addressing the progression of seizures demonstrate that neuronal synchrony changes as the seizure progresses. Specifically, during the pre-ictal phase, a decrease in synchronization between brain structures has been reported (Mormann et al., 2003) followed by a subsequent increase in synchrony between brain regions in the moments leading up to a seizure (Bartolomei et al., 2004). Seizures then evolve into a phase of sustained oscillatory activity of high frequency ('tonic' phase) which is characterized by the uncoupling of brain regions involved in its generation (Bartolomei et al., 2004). The seizure then progresses into rhythmic bursting discharges of higher amplitude and lower frequency ('clonic' phase) where synchronicity increases once again between structures (Schindler et al., 2007). Hypersynchronous neuronal activity at seizure termination is then followed by a period of spontaneous electrical activity ('postictal depression').

Seizures in MTLE patients studied with intracranial electrodes reveal various EEG features (Perucca et al., 2014). Evidence obtained from these patients in the last decade indicates the existence of two predominant patterns of seizure-onset, namely low-voltage fast (LVF) onset seizures and hypersynchronous (HYP) onset seizures (Ogren et al., 2009; Velasco et al., 2000). Similar seizure onset types occur in animal models of MTLE both *in vivo* (Bragin et

al., 2005a; Grasse et al., 2013; Lévesque et al., 2012a; Salami et al., 2015a) and *in vitro* (Avoli et al., 1996a; Boido et al., 2014; Derchansky et al., 2008; Köhling et al., 2016; Lopantsev and Avoli, 1998; Zhang et al., 2012). LVF seizures are characterized at onset by the occurrence of a positive- or negative-going spike followed by low amplitude activity in the gamma range whereas HYP seizures are characterized at onset by a pattern of focal (pre-ictal) spiking at a frequency of approximately 1-2 Hz.

LVF and HYP seizures are thought to depend on the activity of distinct neural networks. Indeed, evidence obtained using animal models of MTLE have revealed that LVF seizures more often originate from the hippocampus and EC and they frequently propagate to other limbic and paralimbic structures (Bragin et al., 2005a). On the other hand, HYP onset seizures initiate predominantly from the hippocampus and tend to remain focal (Bragin et al., 1999a; Velasco et al., 2000b). In agreement with this hypothesis, patients with HYP seizures show patterns of atrophy that are consistent with hippocampal sclerosis whereas LVF seizures are linked to a more diffuse and bilateral distribution of nonspecific atrophy (Ogren et al., 2009). Overall, evidence obtained from epileptic patients indicate that these two seizure-onset patterns should reflect different histopathological conditions, which supports the involvement of different types of neuronal networks and mechanisms.

Acutely, LVF seizures can also be triggered *in vivo* with the systemic administration of substances that enhance GABAergic transmission (Lévesque et al., 2013a); while HYP seizures are recorded under conditions of $GABA_A$ receptor blockade (Salami et al., 2015a). Electrographic activity closely resembling LVF- and HYP-onset seizures recorded in patients and in *in vivo* animal models can also be reproduced in brain slices *in vitro*. In the *in vitro* 4AP model where $GABA_A$ receptor signaling is enhanced, mostly LVF-onset seizures are

recorded (Avoli and de Curtis, 2011a). Intracellular recordings from principal neurons have shown that these ictal events are initiated by a long-lasting GABAergic potential that reflects the synchronous activity of interneurons (Avoli and de Curtis, 2011). These findings are supported by studies that show a blockade of both interneuron synchrony and ictal discharge occurrence under conditions of $GABA_A$ receptor antagonism (Avoli et al., 1996a). Conversely, HYP discharges can be recorded from hippocampal tissue perfused with medium containing low Mg^{2+} (Derchansky et al., 2008; Zhang et al., 2012) as well as from the perirhinal cortex under 4AP administration (Köhling et al., 2016). This pattern of ictal discharge has been linked to repeated firing of principal cells at onset which persist under conditions of $GABA_B$ receptor antagonism (Bragin et al., 2005a; Köhling et al., 2016; Lévesque et al., 2012a).

1.5. High Frequency Oscillations

HFOs are sinusoid-like field potentials that can occur in the limbic structures and neocortex during slow-wave sleep, consummatory behaviour and immobility (Buzsáki et al., 1992; Ylinen et al., 1995). These oscillations are essential to normal brain function as they contribute to cognitive processes such as encoding information, sensorimotor integration and memory consolidation by coordinating neuronal activity locally and in spatially distinct structures (Engel and da Silva, 2012). However, HFOs have also been detected in the EEG of patients with MTLE and in animal models mimicking this condition at the transition from interictal to ictal activity (Jacobs et al., 2009; Zijlmans et al., 2009). Since these oscillations originate from various neuronal populations, analysis of the relationship between HFOs and

seizure onset can reveal significant information regarding cellular mechanisms underlying ictogenesis.

HFOs have recently attracted much attention as a potential marker for excessive neuronal excitability (Jefferys et al., 2012b). HFOs are thought to reflect the activity of dysfunctional neural networks as they are recorded in regions of ictogenesis (Jacobs et al., 2012; Jefferys et al., 2012a, 2012b; Zijlmans et al., 2009). In addition, both clinical and experimental studies support the view that HFOs are better markers than interictal spikes to identify seizure onset zones (Jacobs et al., 2008, 2012; Jefferys et al., 2012a, 2012b; Jiruska et al., 2010a, 2010b; Urrestarazu et al., 2007). Two types of oscillations have been identified in the EEG of epileptic patients and in animal models of MTLE: ripples (80-200 Hz) and fast ripples (250-500 Hz). Ripples can be recorded in both physiological and pathological conditions (Bragin et al., 1999; Chrobak and Buzsáki, 1996) whereas fast ripples are only recorded in pathological conditions (Bragin et al., 1999; Buzsáki et al., 1992).

Excitatory and inhibitory synaptic interactions, intrinsic membrane oscillations, kinetics of intrinsic neuronal currents, out-of-phase firing in neuronal clusters, interneuronal coupling through gap junctions, and ephaptic interactions have been considered and continue to be investigated as underlying mechanisms of both physiological and pathological HFOs (Buzsáki and Chrobak, 1995; Jefferys et al., 2012c; Menendez de la Prida and Trevelyan, 2011; Ylinen et al., 1995). The exact role played by these mechanisms in generating pathologic HFOs remains undefined but it has been suggested that ripples reflect summated inhibitory postsynaptic potentials generated by principal cells in response to inhibitory interneuron firing (Buzsáki and Chrobak, 1995; Ylinen et al., 1995); in contrast, fast ripples are thought to reflect the synchronous firing of principal neurons (Bragin et al., 2011; Dzhala and Staley,

2004; Engel et al., 2009a) or the out-of-phase burst firing of principal cells in the hippocampus (Foffani et al., 2007; Ibarz et al., 2010).

The analysis of HFO patterns during spontaneous HYP and LVF seizures in the pilocarpine and kainic acid model of MTLE has suggested that these two patterns of seizure onset may rely on distinct mechanisms of initiation (Bragin et al., 2005a; Lévesque et al., 2012a). Indeed, it was shown that LVF seizures were mainly associated to activity in the ripple frequency range (Lévesque et al., 2012), thus suggesting that they may rely on the activity of interneuronal networks. In line with this hypothesis, Panuccio et al. (2012) have shown high rates of ripples along with the virtual absence of fast ripples during ictal-like events generated by piriform cortex networks following the administration of 4AP. HYP seizures may instead rely on the activity of principal cells of the glutamatergic networks since they were associated to fast ripples (Bragin et al., 2005; Lévesque et al., 2012).

1.6. Role of Limbic Structures in MTLE

Historically, research in MTLE has focused mainly on the contributions of the hippocampus proper while parahippocampal structures were largely ignored. Some of this evidence include: (i) the fact that the most obvious and consistent neuropathological alterations in this disorder are shown to be associated with this structure (Blümcke et al., 2002); (ii) that EEG recordings often point to the hippocampus as the seizure onset zone (Wieser, 1993); (iii) that satisfactory seizure relief can be attained by the surgical resection of the hippocampus (Spencer and Spencer, 1994). Despite these findings, recent studies have led to the realization that other structures within the limbic system also play major roles in MTLE. The pathogenicity of

medial temporal structures in MTLE was thus progressively recognized and surgical resection evolved accordingly (Spencer and Spencer, 1994).

Cellular, molecular, and pharmacological studies performed over the last few decades have led to remarkable progress in identifying the mechanisms and structures underlying epileptiform synchronization (Behr et al., 2014). Much of this evidence was obtained *in vitro* using brain slices comprising the hippocampus and parahippocampal structures including the EC (Avoli, 2013). For example, it has been shown that reciprocal anatomical connections from the hippocampus to the EC allow the control rather than reinforcement of epileptiform activity in the latter region (Barbarosie and Avoli, 1997). Furthermore, in patients and in animal models *in vivo,* both EC and CA3 regions are often associated with the seizure onset zone (Lévesque et al., 2012a) and since ictal discharges can be consistently recorded in the EC of tissue obtained from adult rodents, we focused our studies on this particular region. To understand the importance of the EC in epileptogenesis and ictogenesis, we must first look at the anatomical organization of this structure.

The EC is located in the anterior parahippocampal gyrus and is an important gateway between the hippocampus and the sensory cortex (Amaral et al., 1987). In the normal brain, this structure plays an important role in memory function, as it is both an input and an output region for the hippocampus (Sewards and Sewards, 2003). Anatomically, the EC is made up of six layers, which is separated by layer IV into superficial layers (I-III) and deep layers (V-VI) (Insausti et al., 1995). This limbic structure can also be divided into lateral and medial entorhinal cortices based on cell organization, morphology, and physiology as well as projections to and from neighboring structures (Uva et al., 2004). The main inputs of the EC come from the hippocampus and piriform cortex while it projects back to the hippocampus as

well as to the perirhinal, auditory, somatosensory, and visual cortices making it ideally placed to contribute to seizure propagation (Jones and Lambert, 1990; Vismer et al., 2015).

The EC is often involved in limbic seizures in MTLE patients (Gloor, 1997). Volumetric analysis studies have shown a correlation between reductions in EC and hippocampal volumes with the progression and duration of epilepsy (Bonilha et al., 2003). Furthermore, neuronal loss and gliosis have been documented in the EC of MTLE patients (Jung et al., 2009) and in animal models mimicking this disorder (Scholl et al., 2013). One study quantifying cell loss in the EC found that glutamatergic neurons of layer III are mostly affected rather than GABAergic interneurons (Drexel et al., 2012; Du et al., 1995). Contrarily, Kumar and Buckmaster found a major reduction in GABAergic interneurons and synapses (2006). Thus, it remains unclear whether a reduction in the inhibitory tone might be responsible for hyperexcitability in this structure. Regardless of the cell population affected, neuronal loss results in reorganization and rewiring, which can lead to increased excitability and epileptiform activity (Vismer et al., 2015). To investigate the contributions of various cell population of the EC to ictogenesis, we turned to the powerful optogenetic technique.

1.7. Optogenetic Technique

Optogenetics (combining ‘optics’ and ‘genetics’) is a novel biotechnology that goes beyond the limitations of traditional techniques and has revolutionized neuroscience, including epilepsy research, by allowing both temporal and spatial precision. This technique allows researchers to “bidirectionally” (i.e. depolarize or hyperpolarize) manipulate cellular systems to study the functional neuroanatomy in the brain, to examine the neural circuits, and to determine the etiology of neurological disorders such as epilepsy.

The technique involves introducing a light-sensitive protein, the opsin, to a specific cell type using viral gene delivery or transgenic technology. In the first method, the genetic construct is injected in a transgenic animal where Cre is expressed in a particular cell type that will drive opsin expression. In the latter method, the opsin is expressed in a particular cell type throughout the brain and this expression is maintained in the animals that are inbred. The targeted neuron then expresses the light-sensitive gene, which can be activated by optical illumination. Upon illumination, the ion channels undergo conformational change and allow specific ions to depolarize or hyperpolarize the cell. The discovery of opsins was crucial for the development of this technique. These are the light-sensitive channels that stimulate cells upon illumination. One class of opsins, used to depolarize target cells, includes channelrhodopsin-2 (ChR2) and its variants which are non-selective cation transporters (Nagel et al., 2002). The second class of opsins, used to hyperpolarize target cells, includes halorhodopsin-2 (i.e., a chloride pump), archaerhodopsin-3 (i.e., a proton pump), and their variants (Boyden et al., 2005; Deisseroth, 2015). The activity of particular cell populations can thus be bidirectionally and rapidly modulated in a given circuit.

The currently available options for the treatment of epilepsy are summarized here: (i) anti-epileptic drugs that must be taken regularly to provide non-specific seizure control for approximately one third of patients (Duncan et al., 2006); (ii) surgical treatments involving the resection of the seizure onset zone, if a single region can be identified, can render two thirds of the pharmaco-resistant patients seizure-free (Wiebe et al., 2001); (iii) deep-brain stimulation for modulating epileptiform activity in particular in MTLE patients (Nune et al., 2015). However, despite the temporal and spatial control offered by electrical or magnetic low-frequency stimulation (LFS), these procedures lack cell-specificity thus presumably

limiting their anti-ictogenic efficacy. This drawback can now be addressed using optogenetic techniques (Yizhar et al., 2011) that have been recently employed as potential therapeutic tools for controlling seizures (Bui et al., 2015; Wykes et al., 2015).

Although the application of optogenetic techniques in epilepsy research is a newly emerging field, exciting results have already been reported regarding the roles of specific cell types in ictogenesis and epileptogenesis as well as interventions that allow on-demand seizure control (Bui et al., 2015; Choy et al., 2016; Wykes et al., 2015). Overall, there are two approaches used in this context. One is to employ the optogenetic inhibition of excitatory principal cells expressing halorhodopsin; experiments using this approach have revealed attenuation of epileptiform activity *in vivo* (Krook-Magnuson et al., 2013) and in *in vitro* (Tønnesen et al., 2009) preparations. The second strategy is to increase the activity of inhibitory interneurons expressing ChR2; optogenetic activation of hippocampal interneurons has been shown to attenuate seizures *in vivo* (Krook-Magnuson et al., 2013), while low-frequency activation of GABAergic cells in the CA3 hippocampal subfield controls 4AP-induced ictal discharges *in vitro* (Ladas et al., 2015; Ledri et al., 2014).

Optogenetic seizure control shows a promising future for improved therapeutic approaches to treat epilepsy. However, there will be many challenges to overcome before the technique can be applied in the clinic. In the meanwhile, it can serve as a powerful tool for deciphering mechanisms of ictogenesis thus aiding to understand the etiology of the disease and to develop more effective drugs.

1.8. Research Rationale & Objectives

Largely driven by the enormous physical and social impact epilepsy has on the lives of those afflicted, much research in the last few decades has been dedicated to unveiling the mechanisms underlying ictogenesis and epileptogenesis. Contrary to the common view that considers decreased inhibition as the primary contributor to ictogenesis, many studies have demonstrated that GABAergic mechanisms (in addition to glutamatergic mechanisms) can actively contribute to pathological oscillations and thus to epileptiform activity. My graduate studies were focused on deciphering the contributions of different cell populations to epileptiform activity in the *in vitro* 4AP model using optogenetic approaches.

1.8.1. Objective 1: Contribution of PV cells to LVF onset seizures

It has been suggested that the GABAergic network is mainly responsible for the initiation of LVF onset seizures *in vivo* (Lévesque et al., 2012a). In the limbic system, there are two main classes of interneurons that innervate principal cells differently. Regular-spiking somatostatin (SOM)-expressing cells target the dendritic region whereas fast-spiking parvalbumin (PV)-expressing interneurons innervate the perisomatic compartments of pyramidal cells (DeFelipe et al., 2013; Freund and Buzsáki, 1996).

The first aim of my studies, elaborated in Chapter 2 of this thesis, was to test the hypothesis that synchronous activation of GABA releasing PV-positive interneurons (DeFelipe et al., 2013) can initiate seizures with an LVF onset pattern similar to those occurring spontaneously in the 4AP model by employing optogenetic control of PV-interneurons in the EC of brain slices obtained from mice constitutively expressing ChR2 in all PV cells in the brain. I also examined the pattern of HFO's during these events to test the hypothesis that ripple rates

predominate at the onset of LVF discharges. As a final component to this first investigation, I pharmacologically blocked GABAergic and glutamatergic neurotransmission in separate experiments to test the effects of PV-interneuron stimulation under such conditions.

1.8.2. Objective 2: Contribution of GABAergic cells to ictogenesis

Since previous studies have shown that GABA application to the dendrites induces depolarizing responses while its application to the soma results in hyperpolarization (Alger and Nicoll, 1982; Andersen et al., 1980; Misgeld et al., 1986; Perreault and Avoli, 1991), we anticipated differences in the ability of somatic-targeting PV and dendritic-targeting SOM interneurons to trigger ictal discharges in the EC network. In addition, PV interneurons innervate twice as many principal cells as other interneurons and receive more local excitatory input (Krook-Magnuson et al., 2013), therefore we expected these cells to play more preponderant roles compared to other interneuron types in triggering ictal discharges.

Therefore, in my next set of experiments, outlined in Chapter 3, I compared the role of PV-interneurons and SOM-interneurons in the initiation of LVF discharges. For this comparison, I confirmed the contribution of PV interneurons to LVF discharges using a novel strain of mice with a PV-Cre background in which we expressed the enhanced ChR2 opsin, ChETA, using a stereotaxic virus injection procedure. I then used the same procedure in a different transgenic line to obtain mice expressing the ChETA opsin in SOM-interneurons of the EC.

1.8.3. Objective 3: Contribution of glutamatergic cells to HYP onset seizures

It has been suggested that the glutamatergic network is mainly responsible for the initiation of HYP onset seizures *in vivo* and *in vitro* (Köhling et al., 2016; Lévesque et al., 2012a; Zhang et

al., 2012). In Chapter 3, I aimed to further test the hypothesis that distinct patterns of seizure onset (HYP and LVF) rely on the activity of different neuronal networks using the optogenetic control of calcium/calmodulin-dependent protein kinase II-positive (CaMKII) principal cells of the EC in the *in vitro* 4AP model. I also examined the pattern of HFOs during these events to test the hypothesis that fast ripple rates predominate at the onset of HYP discharges. Lastly, I pharmacologically blocked GABAergic and glutamatergic neurotransmission in separate experiments to test the effects of pyramidal cell activation under such conditions.

1.8.4. Objective 4: Optogenetic low-frequency stimulation

Having investigated the contributions of different cell populations to the onset of two common seizure-onset patterns observed in MTLE, I wanted to explore the ability of optogenetic LFS to abate seizures in real-time. The rationale for such intervention is supported by experimental evidence obtained from *in vivo* rodent models of MTLE where LFS of the ventral hippocampal commissure was shown to reduce seizure frequency (Kile et al., 2010; Rashid et al., 2012). Therefore, in the final part of my thesis, described in detail in Chapter 4, I used the optogenetic stimulation of CaMKII-positive principal cells and of PV- or SOM-positive interneurons at 1 Hz to compare, for the first time, the effects induced by activation of these specific cell subtypes on 4AP-induced ictal discharges generated from the EC of the transgenic mouse in an *in vitro* brain slice preparation.

Chapter 2: Interneuron activity leads to initiation of low-voltage fast-onset seizures

Shiri Z, Manseau F, Lévesque M, Williams S, Avoli M. *Annals of Neurology*, 2015, 77:541-546.

Seizures in temporal lobe epilepsy can be classified as hypersynchronous and low-voltage fast according to their onset patterns. Several *in vitro* and *in vivo* studies have suggested that low-voltage fast onset seizures result from the synchronization of GABAergic networks. We wanted to test this hypothesis using the temporal and spatial precision of the optogenetic technique *in vitro* by comparing the onset patterns of ictal-like discharges induced by 4-aminopyridine administration and those triggered by optogenetic stimulation of parvalbumin-positive interneurons in the entorhinal cortex. This work was published in 2015 in *Annals of Neurology* as a manuscript entitled “Interneuron activity leads to initiation of low-voltage fast-onset seizures”.

2.1. Abstract

Seizures in temporal lobe epilepsy can be classified as hypersynchronous and low-voltage fast according to their onset patterns. Experimental evidence suggests that low-voltage fast-onset seizures mainly result from the synchronous activity of GABA releasing cells. In this study, we tested this hypothesis using the optogenetic control of parvalbumin-positive interneurons in the entorhinal cortex, in the *in vitro* 4-aminopyridine model. We found that both spontaneous and optogenetically-induced seizures had similar low-voltage fast-onset patterns. In addition, both types of seizures presented with higher ripple than fast ripple rates. Our data demonstrate the involvement of interneuronal networks in the initiation of low-voltage fast-onset seizures.

2.2. Introduction

Patients with temporal lobe epilepsy (TLE) present with two distinct patterns of seizure-onset that have been termed low-voltage fast (LVF) and hypersynchronous (HYP) (Ogren et al., 2009b; Velasco et al., 2000b). Similar seizure onset types occur in animal models of TLE (Bragin et al., 2005a; Lévesque et al., 2012b). LVF seizures usually initiate with one or two interictal-like (hereafter referred to as 'interictal') spikes followed by low amplitude, high frequency activity whereas HYP onset is characterized by a series of (pre-ictal) focal spikes occurring at approximately 2 Hz. LVF and HYP seizures are thought to depend on the activity of distinct neural networks, and it has been shown that LVF ictal-like (hereafter referred to as 'ictal') discharges induced *in vitro* by the K^+ channel blocker 4-aminopyridine (4AP) are (i) initiated by spikes that may reflect the firing of GABA releasing cells, and (ii) sustained by $GABA_A$ receptor signaling (Avoli and de Curtis, 2011a). LVF seizures recorded in models of

temporal lobe epilepsy are also preferentially linked to ripples (i.e., high frequency oscillations at 80-200 Hz) (Lévesque et al., 2012b; Panuccio et al., 2012); ripples are thought to reflect IPSP populations generated by principal glutamatergic neurons entrained by networks of synchronously active interneurons (Aivar et al., 2014; Jefferys et al., 2012d). Moreover, modeling studies have suggested that LVF seizures are linked to the abnormal and continuous generation of IPSPs by inhibitory interneurons that impinge on principal cells (Wendling et al., 2002). We have therefore tested here the hypothesis that activation of GABA releasing parvalbumin (PV)-positive interneurons (DeFelipe et al., 2013) can initiate LVF seizures similar to those occurring spontaneously by employing the optogenetic control of PV-interneurons of the entorhinal cortex (EC) in the *in vitro* 4AP model.

2.3. Materials and Methods

2.3.1. Animals

We used 21 slices from 14 mice (30-39 days old) expressing Channelrhodopsin-2 (ChR2) in parvalbumin-expressing neurons. These animals were generated by breeding PV-Cre and R26-hChR2-EYFP homozygote mice (Jackson Laboratory: 008069 and 012569). Mice were deeply anesthetized with inhaled isoflurane and decapitated. Brains were quickly removed and immersed in ice-cold slicing solution containing (in mM): 252 sucrose, 10 glucose, 26 $NaHCO_3$, 2 KCl, 1.25 KH_2PO_4, 10 $MgCl_2$, and 0.1 $CaCl_2$ (pH 7.3, oxygenated with 95% O_2/5% CO_2). Horizontal sections (400 μm) containing the EC were cut using a vibratome (VT1000S, Leica) and kept for at least 1 hour prior to experimentation in a slice saver filled with artificial cerebrospinal fluid (ACSF) of the following composition (in mM): (125 NaCl, 25 glucose, 26 $NaHCO_3$, 2 KCl, 1.25 NaH_2PO_4, 2 $MgCl_2$, and 1.2 $CaCl_2$). All procedures

were performed according to protocols and guidelines approved by the McGill University Animal Care Committee and Canadian Council on Animal Care.

2.3.2. LFP, patch-clamp, and photostimulation

Slices were transferred to a submerged chamber with continuous perfusion of oxygenated ACSF (KCl and $CaCl_2$ adjusted to 4.5 and 2 mM, respectively) (30 ºC, 10 mL/min) and local field potentials (LFPs) were recorded using ACSF-filled microelectrodes (1-2 MΩ) positioned in the EC superficial layers. Signals were recorded with a differential AC amplifier (AM systems), filtered online (0.1-500 Hz), digitized with a Digidata 1440a (Axon Instruments) and sampled at 5 kHz using the pClamp software (Axon Instruments). In a subset of experiments (n = 3), whole-cell patch-clamp recordings were performed on visually identified interneurons in the EC. Patch electrodes (3–6MΩ) were filled with intrapipette solution containing the following (in mM): 144 K-gluconate, 3 $MgCl_2$, 10 HEPES, 0.2 EGTA, 2 Na_2ATP, and 0.3 GTP, pH7.3 (285-295 mOsm). Signals were amplified using a Multiclamp 700B patch-clamp amplifier (Molecular Devices), sampled at 20 kHz, and filtered at 10 kHz. For ChR2 excitation, blue light (473 nm, intensity 35 mW) was delivered through a custom-made LED system, where the LED (Luxeon) was coupled to a 3 mm wide optical-fiber (Edmund Optics) placed above the recording region. Light pulses (1 sec or 2 sec duration) were delivered at 0.2 Hz for 30 sec with a 130 sec interval between trains. The temperature of the bath was constantly monitored throughout the experiments and no change was observed during the stimulation. 4AP (150 μM) was bath applied in all experiments and in some slices (n = 5) we simultaneously added the $GABA_A$ receptor antagonist picrotoxin (50 μM), and the

$GABA_B$ receptor antagonist CGP55845 (4 μM) to the superfusing ACSF. All reagents were obtained from Sigma-Aldrich Canada, Ltd.

2.3.3. Analysis of high-frequency oscillations

LFPs were first low-pass filtered at 500 Hz and then down-sampled to 2000 Hz to prevent aliasing. A multiparametric algorithm was then used to identify oscillations in each frequency range, using routines based on standardized MATLAB signal processing functions (Mathworks). For each ictal discharge, raw LFP recordings were bandpass filtered in the 80–200 Hz and in the 250–500 Hz frequency range using a finite impulse response filter; zero-phase digital filtering was used to avoid phase distortion. A 10 sec artifact-free period (50–40 sec before ictal discharge onset) was selected as a reference for signal normalization. LFPs were thus normalized using their own reference period. To be considered as a high-frequency oscillation (HFO) candidate, oscillatory events in each frequency band had to show at least four consecutive cycles having an amplitude of 4 standard deviations above the mean of the reference period. The time lag between two consecutive cycles had to be between 5 msec and 12.5 msec for ripples and 2 msec and 4 msec for fast ripples. Furthermore, special care was taken to avoid the detection of false HFOs which may be caused by the filtering of sharp spikes.(Bénar et al., 2010) Rates of HFO (ripples, fast ripples) were computed based on 9 spontaneous and 10 evoked ictal discharges and compared using nonparametric Wilcoxon rank-sum tests followed by Bonferroni-Holm corrections for multiple comparisons. Statistical tests were performed in MATLAB using the Statistics Toolbox; the level of significance was set to $p < 0.05$.

2.4. Results

We analyzed a total of 255 ictal events that were recorded from the EC (n = 19 slices). Of these events, 138 occurred spontaneously, 77 were triggered by a train of 1 sec pulses and 40 were triggered by a train of 2 sec pulses. Both stimuli of 1 sec and 2 sec duration were equally successful (48%; data not shown) in triggering ictal events and were thus pooled together for analysis. Representative examples of spontaneous and evoked ictal events are shown in Figure 1A and B, respectively. In control experiments, the interval between spontaneous ictal discharges was 208.26 ± 11.39 s on average. We were able to trigger similar events at a shorter interval of 138.63 ± 5.75 s under the same conditions with optogenetic stimulation ($p < 0.01$). When the onset of an optically-induced ictal discharge was expanded (asterisk), the pattern was typical of an LVF seizure with one or two interictal spikes (arrow) leading to the ictal discharge. The same LVF pattern could be observed at the onset of spontaneous ictal discharges.

To ensure that the evoked discharges are dependent on interneuron activation only, we simultaneously bath applied the $GABA_A$ receptor antagonist Picrotoxin (50 μM), and $GABA_B$ receptor antagonist CGP55845 (4 μM). This pharmacological manipulation effectively abolished all spontaneous and light-induced ictal discharges (n = 5; Figure 1C). Under such GABA receptor-suppressing conditions, spontaneous rhythmic discharges (duration = 1-2 s) occured for the entire length of the recording (approx. 20 mins) and were not driven by the optogenetic stimulation (example expanded on right). As reported in previous studies (Avoli and de Curtis, 2011a), these presumptive glutamatergic epileptiform events were different from the interictal discharges recorded under 4AP conditions (example expanded on left).

Next, we wanted to test whether direct activation of PV-interneurons recorded in whole-cell configuration triggers ictal discharges in nearby field recordings. First, we set out to characterize the cells expressing the Channelrhodopsin (n = 3). Whole-cell current clamp recordings revealed typical firing activity of fast-spiking PV-interneurons (Figure 2A). Using optogenetic stimulation, we were able to repeatedly activate these interneurons (Figure 2B) and trigger ictal discharges with an LVF onset pattern (Figure 2C). These cells remained viable following optogenetic stimulation as they consistently responded to stimuli over time (Figure 2B).

We also examined the rate and pattern of HFO occurrence throughout the ictal discharges recorded in the EC (Figure 3A). Ripple rates were higher than fast ripple rates throughout both spontaneous and light-triggered ictal discharges as expected for an LVF discharge ($p < 0.01$) (Lévesque et al., 2012b). HFO rates were highest at the onset of the event in both spontaneous and stimulated ictal discharges and gradually decreased throughout the event (Figure 3B and C).

2.5. Discussion

The involvement of interneurons in the initiation of ictal discharges has been suggested based on *in vivo* (Grasse et al., 2013) and *in vitro* (Dzhala and Staley, 2003; Gnatkovsky et al., 2008; Zhang et al., 2012) results. Here, we show that GABA release due to the optogenetic activation of PV-interneurons could lead to LVF ictal discharges *in vitro*. First, we discovered that during bath application of 4AP, EC neuronal networks generate ictal discharges that are characterized by a LVF onset pattern and can occur both spontaneously or be triggered by PV-interneuron activation. Second, we triggered similar events in the whole-cell

configuration by optically activating PV-interneurons. Finally, we identified patterns of HFO occurrence that were similar during both types of ictal events and were predominated by ripple rates.

Our group has previously shown that the systemic administration of 4AP *in vivo* (Lévesque et al., 2013a) and its bath application *in vitro* (Avoli et al., 2013b) induce LVF type seizures with similar morphological features. Lévesque et al. (2013a) also reported that *in vivo* 4AP treatment induces sustained and rhythmic runs of theta oscillations that are thought to play a role in ictogenesis (Butuzova and Kitchigina, 2008). These theta oscillations are presumably caused by GABAergic inputs to pyramidal cells as they are abolished by the $GABA_A$ receptor antagonist, picrotoxin (Buzsáki, 2002). Other electrophysiological data have revealed a long-lasting GABAergic potential that reflects the synchronous activity of interneurons at the onset of LVF ictal discharges (Avoli and de Curtis, 2011a). Therefore, our study demonstrates that GABAergic mechanisms are responsible for LVF seizures since we could trigger ictal discharges with LVF onset patterns (similar to what is occurring spontaneously) by locally and transiently activating PV-positive EC interneurons.

It has been previously reported that in LVF seizures, the transition from interictal to ictal activity is characterized by higher ripple rates at seizure onset (Lévesque et al., 2012b). Indeed, we found higher ripple rates at the onset of both spontaneous and optogenetically-induced ictal discharges during 4AP application. Although the exact mechanisms underlying the generation of ripples is not known, it has been suggested that ripples reflect summated IPSPs generated by principal cells in response to the inhibitory action of interneurons. Therefore, our findings further highlight the involvement of interneuronal networks in

initiating LVF-onset seizures, which are then, at least partially, maintained by the persistent firing of principal cells.

Our findings clearly identify the pivotal involvement of GABAergic interneurons in the initiation and maintenance of LVF seizures in the limbic system. Additional studies should investigate whether activating glutamatergic principal cells in the EC leads to HYP onset seizures. Combining these results could help identify more efficacious antiepileptic strategies aimed specifically at targeting GABAergic or glutamatergic neuronal networks excitability.

Acknowledgement

This study was supported by the Canadian Institutes of Health Research (CIHR grants 8109 and 74609 to MA; and MOP119340 to SW).

Conflicts of interest

The authors have nothing to disclose.

2.6. Figures

Figure 2.1

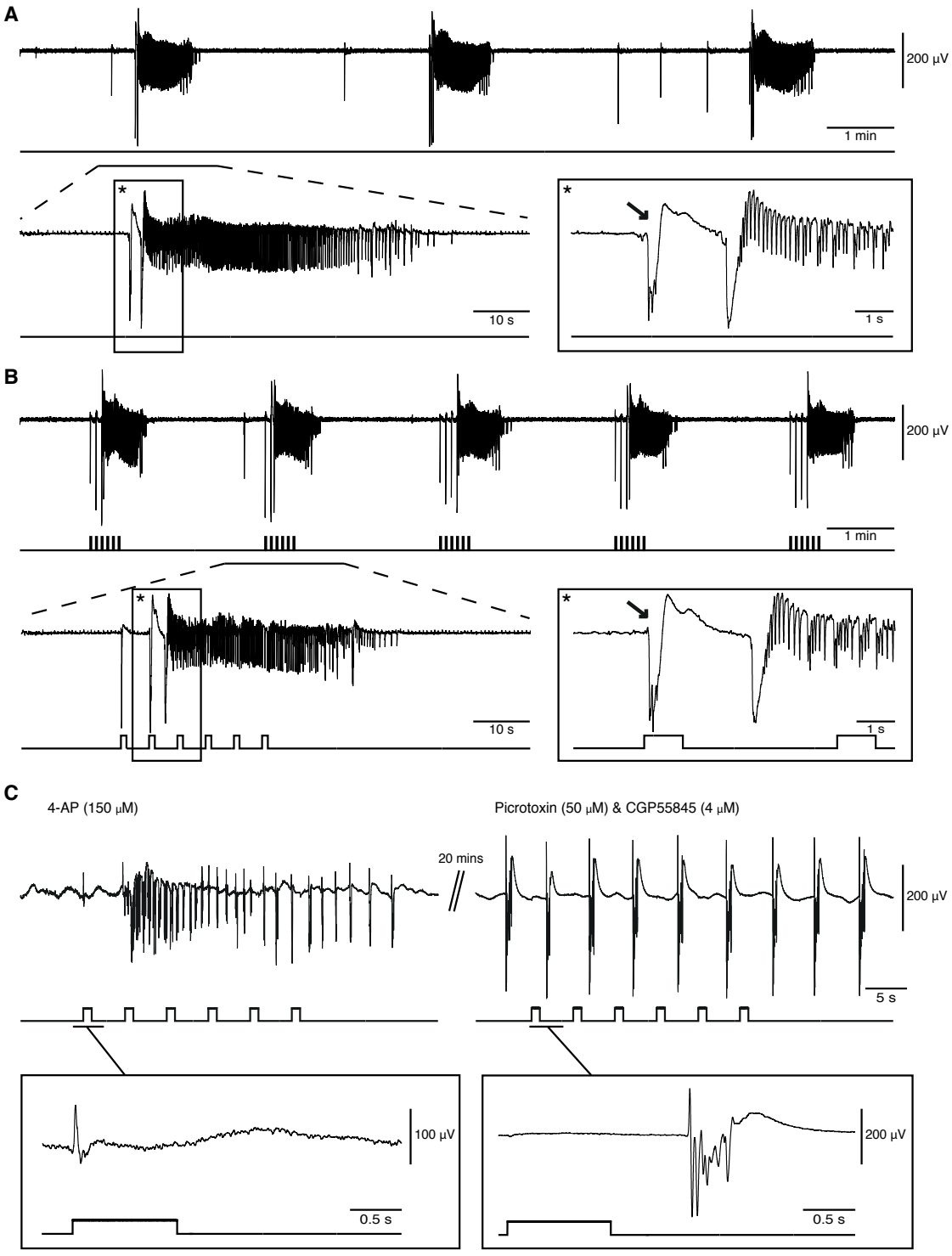

Figure 2.1. LVF ictal discharges can occur spontaneously or be triggered by optogenetic activation of PV-interneurons. **A:** Spontaneous ictal discharges occurring during bath application of 4AP; one of the events is further expanded to show the onset pattern (asterisk). **B:** Ictal discharges evoked by 1 sec light pulses during bath application of 4AP; one of the events is further expanded to compare the onset patterns (asterisk). Note that in both **A** and **B,** the ictal discharge is preceded by a negative-going interictal field potential (arrows). **C:** Changes induced by concomitant bath application of picrotoxin and CGP55845 on the ictal discharge evoked by a train of 1 sec light pulses (4AP, 150 μM panel). Note that under control conditions, the first light pulse induces a positive-going monospike (expanded example) that is followed by ictal synchronization while during $GABA_A$ and $GABA_B$ receptor antagonism both ictal discharge and the ability of light pulses to drive interictal events are abolished. Under these conditions, negative-going polyspikes (expanded example) occur regardless of the light pulses for at least 20 mins (maximum time recorded); note the different vertical scales in the expanded samples.

Figure 2.2

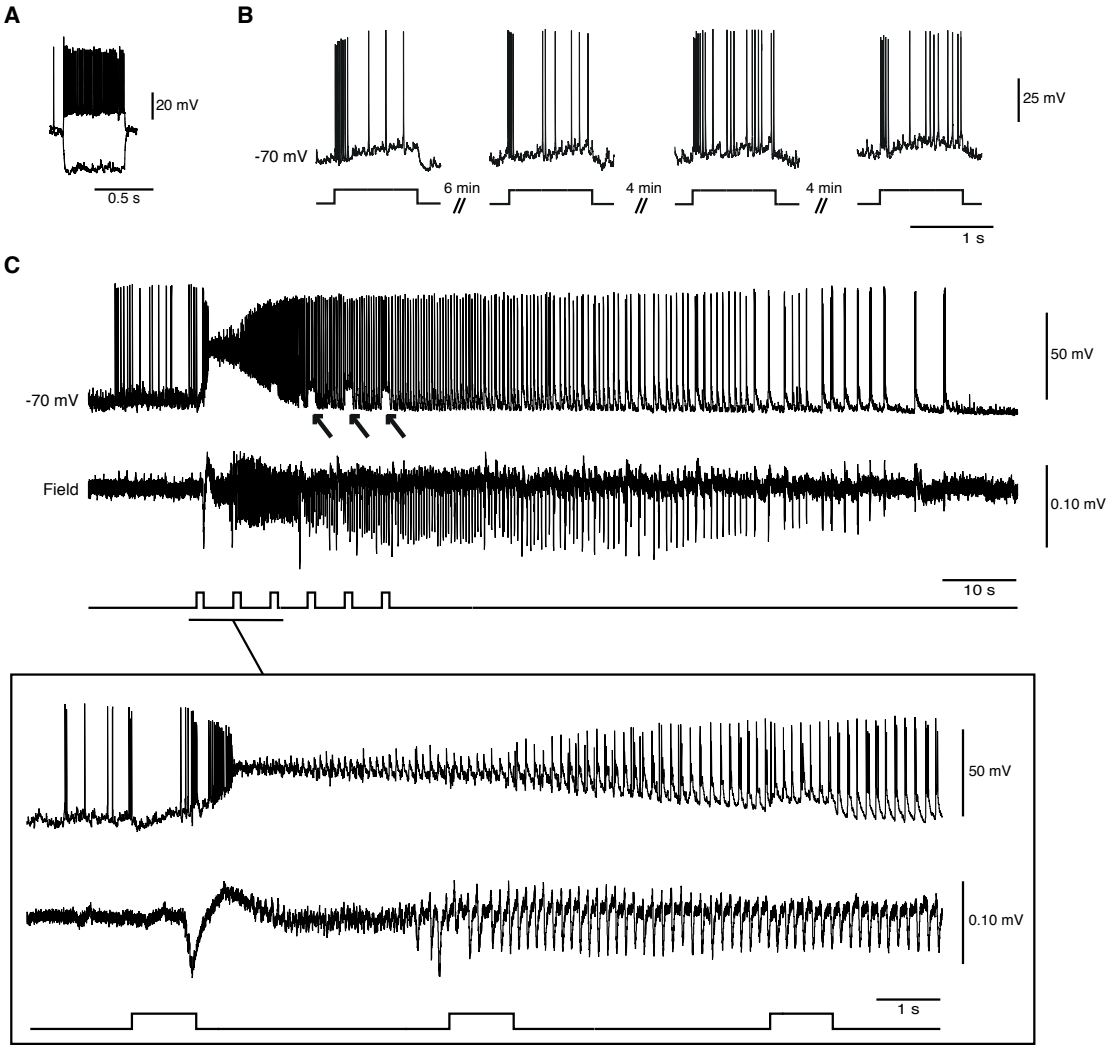
A
20 mV
0.5 s
B
-70 mV
25 mV
6 min
4 min
4 min
1 s
C
-70 mV
50 mV
Field
0.10 mV
10 s
50 mV
0.10 mV
1 s

Figure 2.2. Optogenetic activation of PV-interneurons in the whole-cell configuration triggers LVF ictal discharges. A: Electrophysiological characterization of an EC fast-spiking PV-interneuron during injection of hyperpolarizing and depolarizing current pulses (V_m = -70 mV; intracellular current pulses: 600 msec: -200 and 160 pA). **B:** Responses to 1 sec light pulses recorded from the same cell at four different time points. Note that similar action potential discharges are generated over time. **C:** Optogenetic activation of this interneuron (and of the concomitant LVF ictal discharge) by a train of 1 sec light pulses; note the arrows pointing to the pulse-induced depolarizations during the ictal discharge. The onset of the ictal event is expanded below to further reveal the LVF pattern.

Figure 2.3

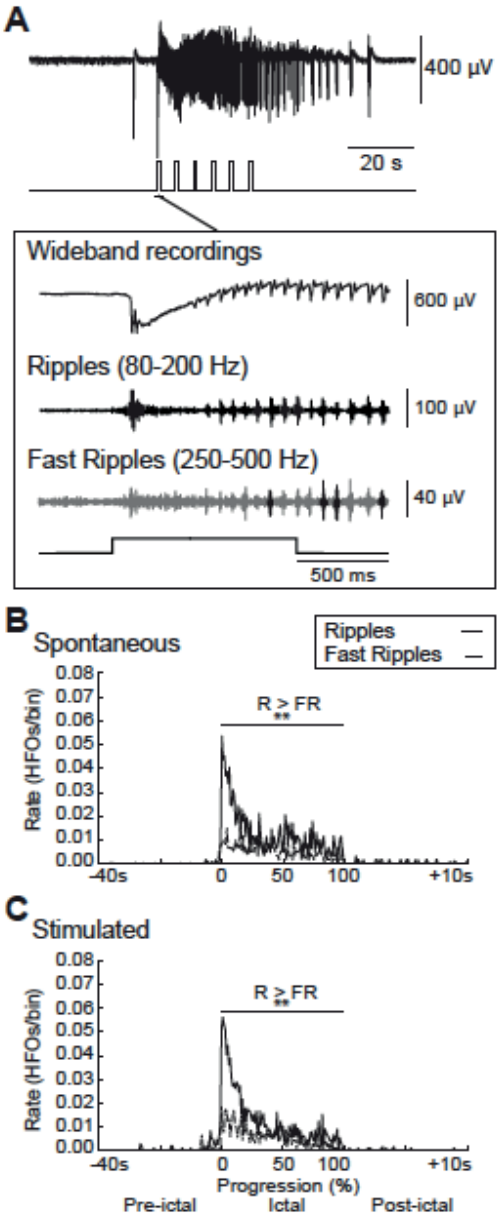
A
400 µV
20 s
Wideband recordings
600 µV
Ripples (80-200 Hz)
100 µV
Fast Ripples (250-500 Hz)
40 µV
500 ms
B
Spontaneous
Ripples
Fast Ripples
Rate (HFOs/bin)
0.08
0.07
0.06
0.05
0.04
0.03
0.02
0.01
0.00
R ≥ FR
**
-40s
0
50
100
+10s
C
Stimulated
Rate (HFOs/bin)
R ≥ FR
**
-40s
0
50
100
+10s
Progression (%)
Pre-ictal
Ictal
Post-ictal

Figure 2.3. Similar patterns of HFOs characterize spontaneous and light-triggered ictal discharges. A: Ictal discharge stimulated by a train of 1 sec light pulses and expanded onset illustrating wide-band recording and filtered traces of associated ripples and fast ripples that are highlighted in gray. **B** and **C:** Average rate of ripples (R) and fast ripples (FR) in the 40 sec preceding, during, and 10 sec following spontaneous (n = 9 events) and stimulated (n = 10 events) ictal discharges, respectively. The duration of the ictal discharges was normalized with 0 representing their start and 100 representing their end. Note that ripple rates are higher than fast ripple rates throughout spontaneous and stimulated ictal discharges as well as that both types of HFO are characterized by highest rates at the onset of the event and gradually decrease throughout the event; ** indicates $p < 0.01$.

Chapter 3: Activation of specific neuronal networks leads to different seizure onset types

Shiri Z, Manseau F, Lévesque M, Williams S, Avoli M. *Annals of Neurology*, 2016, 79:354-365.

Seizures in temporal lobe epilepsy can be classified as hypersynchronous and low-voltage fast according to their onset patterns. It has been suggested that low-voltage fast onset seizures are initiated by GABAergic mechanisms while glutamatergic networks are responsible for hypersynchronous onset seizures. In the previous chapter, we demonstrated the contribution of parvalbumin-positive interneurons to low-voltage fast-onset discharges in the entorhinal cortex. In this next study, we wanted to first compare the ability of somatic-targeting parvalbumin-positive and dendritic-targeting somatostatin-positive interneurons to contribute to low-voltage fast-onset seizures. Then we targeted the optogenetic stimulation to calcium/calmodulin-dependent protein kinase II-positive principal cells in entorhinal cortex to investigate their ability to trigger hypersynchronous discharges in the 4-aminopyridine model *in vitro.* This work was published in 2016 in *Annals of Neurology* as a manuscript entitled "Activation of specific neuronal networks leads to different seizure onset types".

3.1. Abstract

Objective: Ictal events occurring in temporal lobe epilepsy patients and in experimental models mimicking this neurological disorder can be classified based on their onset pattern, into low-voltage, fast and hypersynchronous onset seizures. It has been suggested that the low-voltage, fast onset pattern is mainly contributed by interneuronal (GABAergic) signalling while the hypersynchronous onset involves the activation of principal (glutamatergic) cells.

Methods: Here, we tested this hypothesis using the optogenetic control of parvalbumin-positive or somatostatin-positive interneurons and of calmodulin-dependent, protein kinase-positive, principal cells in the mouse entorhinal cortex in the *in vitro* 4-aminopyridine model of epileptiform synchronization.

Results: We found that during 4-aminopyridine application, both spontaneous seizure-like events and those induced by optogenetic activation of interneurons displayed low-voltage, fast onset patterns that were associated with a higher occurrence of ripples than of fast ripples. In contrast, seizures induced by the optogenetic activation of principal cells had a hypersynchronous onset pattern with fast ripple rates that were higher than those of ripples.

Interpretation: Our results firmly establish that under a similar experimental condition (i.e., bath application of 4-aminopyridine), the initiation of low-voltage, fast and of hypersynchronous onset seizures in the entorhinal cortex depends on the preponderant involvement of interneuronal and principal cell networks, respectively.

Keywords: Seizure onset pattern; interneurons; principal cells; high-frequency oscillations.

3.2. Introduction

Seizures in patients presenting with temporal lobe epilepsy (TLE) are mainly characterized by two distinct electrographic onset patterns defined as low-voltage fast (LVF) and hypersynchronous (HYP) (Ogren et al., 2009a; Velasco et al., 2000a). LVF seizures are characterized at onset by the occurrence of a sentinel spike followed by low amplitude, high frequency activity whereas the initiation of HYP seizures coincides with a series of focal (so-called pre-ictal) spiking at a frequency of approximately 2 Hz (Perucca et al., 2014). LVF and HYP seizures may mirror the activity of distinct limbic structures (Bragin et al., 2009). Accordingly, Velasco *et al.* (2000a) have reported that LVF seizures rest on the activity of hippocampal and parahippocampal networks whereas HYP seizures originate from local circuits in the hippocampal formation. In addition, TLE patients presenting with HYP seizures have histopathological patterns of atrophy that are consistent with hippocampal sclerosis whereas LVF seizures are linked to a more diffuse and bilateral distribution of atrophy (Ogren et al., 2009a). Finally, in animal models of TLE, LVF seizures more often initiate in parahippocampal structures while HYP seizure onset may be limited to the hippocampus (Bragin et al., 1999b; Lévesque et al., 2012b).

Recently, the analysis of high-frequency oscillations (HFOs) (ripples: 80-200 Hz, fast ripples: 250-500 Hz) during spontaneous HYP and LVF seizures in the pilocarpine and kainic acid model of TLE has suggested that these two seizure onset patterns may rely on distinct mechanisms of initiation. LVF seizures were found to be mainly associated with HFOs in the ripple frequency range (80-200 Hz), thus suggesting the predominant involvement of interneuronal (inhibitory) networks; in contrast, HYP seizures were mostly accompanied by fast ripple (250-500 Hz) occurrence thus highlighting the potential role of principal

(glutamatergic) networks (Bragin et al., 2005b; Lévesque et al., 2012b). Indeed, evidence obtained to date suggest that pathologic HFOs in the ripple band should represent population inhibitory postsynaptic potentials (IPSPs) generated by principal neurons entrained by synchronously active interneuron networks while those in the fast ripple band reflect the synchronous firing of abnormally active principal cells, and thus are not dependent on inhibitory processes (Engel et al., 2009b; Jefferys et al., 2012c; Ylinen et al., 1995).

It has been demonstrated that 4-aminopyridine (4AP) application induces LVF onset discharges in several limbic and para-limbic structures maintained *in vitro* (Avoli and de Curtis, 2011a). In addition, systemic injection of 4AP *in vivo* has been shown to induce LVF onset pattern seizures (Lévesque et al., 2013b; Salami et al., 2015b). Finally, we have found that optogenetic activation of parvalbumin (PV)-positive interneurons of entorhinal cortex (EC) in a constitutive model of channelrhodopsin-2 (ChR2) expression lead to the initiation of *in vitro* LVF seizures in the limbic system (Shiri et al., 2015). Therefore, in this study, we aimed to test the hypothesis that distinct (i.e., LVF and HYP) patterns of seizure onset rely on the activity of different neuronal networks in the *in vitro* 4AP model using the optogenetic control of PV-positive and somatostatin (SOM)-positive interneurons as well as of calmodulin-dependent protein kinase (CaMKII)-positive principal cells in the EC of mice where an enhanced ChR2 opsin was transcranially and locally injected.

3.3. Materials and Methods

3.3.1. Animals

All procedures were performed according to protocols and guidelines of the Canadian Council on Animal Care (http://ccac.ca/en/standards/guidelines) and were approved by the McGill

University Animal Care Committee. PV-Cre (Jackson Laboratory, B6;129P2-*Pvalb*$^{tm1(cre)Arbr}$/J, stock number 008069), SOM-Cre (Jackson Laboratory, *Ssttm2.1(cre)Zjh*/J, stock number 013044) and CaMKII-Cre (Jackson Laboratory, B6.Cg-Tg(Camk2a-cre)T29-1Stl/J, stock number 005359) homozygote mouse colonies were bred and maintained in house in order to generate pups that were used in this study.

3.3.2. Stereotaxic virus injections

Four PV-Cre, seven SOM-Cre, and eight CaMKII-Cre male or female pups were anesthetized at P15 using isoflurane and positioned in a stereotaxic frame (Stoelting). AAVdj-ChETA-eYFP virus (UNC Vector Core) was delivered in the EC (0.6 μL at a rate of 0.06 μL/min). Injection coordinates were: anteroposterior -4.00 mm from bregma, lateral +/- 3.60 mm, dorsoventral -4.00 mm. The transverse sinus was used as a point of reference, and the injection needle was inserted with a 2º anteroposterior angle. After completion of the surgery, pups were returned to their home cage.

3.3.3. Slice preparation

Mice were deeply anesthetized with inhaled isoflurane and decapitated at P30-40. Brains were quickly removed and immersed in ice-cold slicing solution containing (in mM): 25.2 sucrose, 10 glucose, 26 $NaHCO_3$, 2.5 KCl, 1.25 KH_2PO_4, 4 $MgCl_2$, and 0.1 $CaCl_2$ (pH 7.3, oxygenated with 95% O_2/5% CO_2). Horizontal brain sections (thickness = 400 μm) containing the EC were cut using a vibratome (VT1000S, Leica) and incubated for one hour or more in a slice saver filled with artificial cerebrospinal fluid (ACSF) of the following composition (in mM): 125 NaCl, 25 glucose, 26 $NaHCO_3$, 2 KCl, 1.25 NaH_2PO_4, 2 $MgCl_2$, and 1.2 $CaCl_2$.

3.3.4. Electrophysiological recordings and photostimulation

Slices were transferred to a submerged chamber where they were continuously perfused with oxygenated ACSF (KCl and $CaCl_2$ adjusted to 4.5 and 2 mM, respectively) (30 ºC, 10-15 mL/min). Field potentials were recorded using ACSF-filled microelectrodes (1-2 MΩ) positioned in the EC in the presence of 4AP. Signals were recorded with a differential AC amplifier (AM systems), filtered online (0.1-500 Hz), digitized with a Digidata 1440a (Molecular Devices) and sampled at 5 kHz using the pClamp software (Molecular Devices). In a subset of experiments, whole-cell patch-clamp recordings were performed on visually identified neurons from EC slices. Patch electrodes (2–3MΩ) were filled with a solution containing the following (in mM): 144 K-gluconate, 3 $MgCl_2$, 10 HEPES, 0.2 EGTA, 2 Na_2ATP, and 0.3 GTP, pH7.3 (285-295 mOsm). Signals were amplified using a Multiclamp 700B patch-clamp amplifier (Molecular Devices), sampled at 20 kHz, and filtered at 10 kHz.

For ChR2 excitation, blue light (473 nm, intensity 35 mW) was delivered through a custom-made LED system, where the LED (Luxeon) was coupled to a 3 mm or 1 mm wide fiber-optic for field or whole-cell recording experiments, respectively, (Edmund Optics) and was placed above the recording region. For optogenetic activation of PV- and SOM-positive interneurons, light pulses (1 s duration) were delivered at 0.2 Hz for 30 s with a 150 s interval between trains. For optogenetic activation of CaMKII-positive principal cells, light pulses (20 ms duration) were delivered at 2 Hz for 30 s with a 150 s interval between trains. All reagents were obtained from Sigma-Aldrich and were bath applied.

3.3.5. Analysis of HFOs

Field potentials were first low-pass filtered at 500 Hz and then down-sampled to 2000 Hz. For each ictal discharge, raw field potential signals were band-pass filtered in the 80-200 Hz and in the 250–500 Hz frequency range for identification of ripples and fast ripples, respectively; a more thorough description of this procedure is provided in Salami *et al.* (2015b) Rates of ripples and fast ripples were computed using average values obtained from all ictal discharges. The ictal period was arbitrarily divided in three equal parts, and rates of ripples and fast ripples in each part were compared using nonparametric Wilcoxon rank-sum tests followed by Bonferroni-Holm corrections for multiple comparisons. This allowed us to evaluate whether ripples or fast ripples predominated at specific moments of the ictal period. Statistical tests were performed in Matlab 7.11.0 (Mathworks) using the Statistics Toolbox. The level of significance was set to $p < 0.05$.

3.4. Results

3.4.1. Optogenetic activation of PV-positive interneurons leads to LVF onset seizures

We analysed a total of 182 ictal events recorded from the EC of PV-Cre mice transcranially injected with the enhanced ChR2 opsin, ChETA (n = 6 slices). Of these events, 142 occurred spontaneously and 40 were triggered using a 30 s train of 1 s light pulses at 0.2 Hz. Representative examples of spontaneous and light-triggered events are shown in Figure 1. When the onset of a spontaneous ictal-like event was expanded, a LVF onset pattern consistently initiated by an isolated spike became evident (Fig 1A; arrow). A similar LVF onset pattern was observed when the ictal events were triggered by optogenetic activation of PV-interneurons (Fig 1B; arrow). Spontaneously occurring events lasted 47.74 ± 1.34 s, a

duration that was similar to what was found for the optogenetically induced events (i.e., 45.57 ± 2.23 s) (Fig 1C) but spontaneous ictal discharges occurred every 156.61 ± 9.81 s, while during optogenetic PV-cell stimulation, we could reduce their interval of occurrence to 138.13 ± 4.89 s ($p < 0.05$; Fig 1D).

As shown in Figure 2, we also performed patch clamp recordings of fast-spiking, PV-positive interneurons in the whole-cell mode (n = 3). First, we characterized the patched cell by injecting intracellular depolarizing current pulses to reveal the typical firing activity of a fast-spiking PV-positive interneuron (Fig 2A) (DeFelipe et al., 2013). These interneurons reliably responded to optogenetic stimulation over time (Fig 2B). Moreover, as illustrated in Figure 2C (see also expanded trace), fast-spiking PV-positive interneurons generated a barrage of action potentials (delay of initial depolarization = 5.43 ± 0.51 ms; average spike frequency = 155.68 ± 10.99 Hz; average duration of barrage = 0.83 ± 0.06 s) in response to the optogenetic stimulus as well as in coincidence with the initial spike; then, they depolarized progressively undergoing a "firing depolarizing block" during the initial part of the LVF ictal discharge (n = 11 events). Later, during the subsequent "tonic" electrographic phase of the ictal discharge, these interneurons could resume action potential firing that occurred synchronously with each "clonic" field potential transient.

To ensure that the responses evoked by optogenetic stimuli were dependent on the release of GABA subsequent to interneuron discharge, we simultaneously blocked $GABA_A$ and $GABA_B$ receptors using picrotoxin (50 μM) and CGP55845 (4 μM), respectively. Under these pharmacological conditions, all spontaneous and stimulated ictal-like events as well as light-induced interictal events were abolished (n = 3 slices; data not shown but see (Shiri et al., 2015)).

3.4.2. Optogenetic activation of SOM-positive interneurons leads to LVF onset seizures

Next, we established whether the ability of interneuron activation to drive ictal discharges is linked exclusively to fast-spiking interneurons, or whether ictal discharges could also be triggered by activating regular-spiking SOM-positive interneurons. We analyzed a total of 224 ictal discharges recorded from the EC of Som-Cre mice that had been transcranially injected with ChETA (n = 11 slices). Of these events, 170 occurred spontaneously and 54 were stimulated by a 30 s train of 1 s light pulses at 0.2 Hz; this protocol was similar to the one employed in the PV-positive interneuron experiments. As illustrated in Fig 3A (arrow), the onset of an expanded spontaneous ictal-like event was characterized, in these experiments as well, by the occurrence of an isolated spike leading to an LVF onset pattern. Interestingly, the same pattern of field activity occurred at the onset of ictal events when they were triggered by activation of SOM-interneurons (Fig 3B; arrow). In these experiments, spontaneous ictal discharges lasted 64.39 ± 1.86 s and optogenetically-induced events had duration of 60.52 ± 2.30 s (Fig 3C). Spontaneous ictal discharges occurred regularly (every 130.31 ± 6.35 s) but could be driven at a more frequent rate during optogenetic stimulation of SOM-cells, i.e., every 105.42 ± 5.51 s ($p < 0.05$; Fig 3D). In these experiments as well, concomitant application of $GABA_A$ and $GABA_B$ receptor antagonists abolished all spontaneous and induced ictal-like events (n = 3 slices; Fig 3E). Under these conditions, presumptive glutamatergic field bursts occurred for the entire length of the recording but did not appear to follow the stimulation pattern (see expanded region).

3.4.3. Optogenetic activation of CaMKII-positive principal cells leads to HYP onset seizures

In this set of experiments we analysed a total of 293 ictal events that were recorded from the EC of brain slices expressing ChETA in CaMKII-positive principal cells. Of these ictal discharges, 141 occurred spontaneously while 152 events were triggered by a 30 s train of 20 ms light pulses at 2 Hz. Representative examples of spontaneous and light-triggered events are shown in Figure 4A and B. When the onset of a spontaneous ictal event was expanded, an LVF onset - which was preceded by a typical isolated spike - could be identified (Fig 4A; arrow). In contrast, the onset of ictal discharges triggered by principal cell activation was characterized by repeated spiking and thus resembled a HYP onset pattern (Fig 4B; arrow). We found that spontaneous ictal discharges lasted 44.95 ± 1.82 s whereas those induced by light pulses were significantly shorter (37.07 ± 0.72 s; $p < 0.01$) (Fig 4C). During 4AP application, ictal discharges occurred spontaneously every 121.16 ± 6.49 s but were driven at higher frequency by light stimulation (i.e., 111.23 ± 1.70 s; $p < 0.05$) (Fig 4D).

CaMKII-positive cells were also recorded in the whole-cell mode (n = 5) to analyze their electrophysiological properties, their responses to light stimuli and their activity during ictal discharges. As illustrated in Fig 5A, these neurons responded to injection of depolarizing current pulses by generating repetitive action potential firing with some degree of adaptation as reported for regular-spiking, principal cells in the EC (de Guzman et al., 2008) and in several cortical structures (McCormick et al., 1985; Schwartzkroin, 1975). We also found that these recorded neurons reliably responded to optogenetic stimulation with a short burst of action potentials when tested at different time points during the experiment (delay of initial depolarization = 6.37 ± 0.14 ms; Fig 5B). In the absence of optogenetic stimulation,

spontaneous, 4AP-induced ictal events with LVF onset patterns in the field recording were characterized intracellularly by a period of action potential quiescence at ictal onset while firing resumed during the late tonic phase of the discharge (n = 12 events; Fig 5C; see expanded onset). In contrast, as illustrated in Fig 5D, principal cell firing occurred in coincidence with the preictal spikes that were characteristic of optogenetically-induced HYP onset ictal discharges (duration of bursts = 0.27 s; n = 15 events; see expanded onset).

To further establish the contribution of principal glutamatergic cells to the evoked discharges, we simultaneously blocked the NMDA and non-NMDA receptors using 3-((*R*)-2-Carboxypiperazin-4-yl)-propyl-1-phosphonic acid (CPP) (5 μM) and 6-Cyano-7-nitroquinoxaline-2,3-dione (CNQX) (5 μM) in experiments in which we stimulated interneurons (n = 3; Fig 6A) or principal cells (n = 3; Fig 6B). Under these conditions, all spontaneous and stimulated ictal events were abolished; however, interneuron stimulation continued to evoke presumably GABAergic discharges while principal cell stimulation failed to induce such events. In the latter case, spontaneous GABAergic discharges could be recorded independently of the stimulation (Fig 6B; arrow).

3.4.4. HFOs associated with LVF and HYP onset seizures

Finally, we quantified the rate and pattern of HFO occurrence throughout the ictal discharges recorded in the EC (Fig 7). This analysis showed that ripple rates were higher than fast ripple rates ($p < 0.01$) at the onset of all spontaneous LVF onset ictal events as reported for LVF seizures recorded *in vivo* in the pilocarpine model of TLE (Lévesque et al., 2012b) and in the acute 4AP model (Salami et al., 2015b). A similar pattern of HFO distribution was associated with LVF onset seizures triggered by the activation of PV- and SOM-positive interneurons

and interestingly, this pattern was still observed in 4AP-induced spontaneous LVF seizures in CaMKII-Cre pups. These results therefore suggest that activation of interneuronal networks can trigger seizure-like events resembling human LVF seizures. In contrast, ictal discharges triggered by the activation of principal cells revealed higher fast ripple rates at seizure onset ($p < 0.01$) as reported to occur in HYP onset seizures occurring *in vivo* (Lévesque et al., 2012b; Salami et al., 2015b).

3.5. Discussion

The main findings of our study can be summarized as follows: (i) spontaneous ictal events recorded *in vitro* from the EC during 4AP application are characterized by an LVF onset pattern; (ii) similar LVF onset ictal discharges can be triggered by optical activation of PV- and SOM-positive interneurons; (iii) in contrast, ictal discharges triggered by CaMKII-pyramidal cell stimulation are associated with a HYP onset pattern; and (iv) specific HFO patterns characterized these two types of seizure onset as ripples predominated at the onset of LVF seizures while fast ripple rates were higher at the onset of HYP seizures.

3.5.1. Activation of the inhibitory or excitatory network can lead to ictal discharges

It is well established that 4AP blocks Kv1 channels thus increasing action potential duration in both excitatory and inhibitory neurons (Zhang and McBain, 1995), which leads to epileptiform activity (Smart et al., 1998). We have shown here that the EC networks under 4AP treatment can be activated by opsin stimulation in either interneurons or principal cells. However, we also discovered that activation of each specific cell population leads to ictal discharges with a different onset pattern. Namely, seizure-like events with an LVF onset

pattern can be triggered by interneuronal network activity; while triggering discharges with a HYP onset pattern requires synchronous activation of glutamatergic principal cells as previously suggested by *in vivo* studies (Bragin et al., 2005b; Lévesque et al., 2012b). These results have not been reported in other *in vitro* models.

Several studies performed in the 1970s and 1980s have proposed that the initiation of focal seizures depends on weakening or failure of inhibition, a process that should lead to an uncontrolled increase in glutamatergic excitation (Ben-Ari et al., 1979; Ayala et al., 1970). However, subsequent *in vitro* and *in vivo* experiments have shown that GABAergic interneurons are not simply responsible for providing inhibitory control on brain networks (Freund and Buzsáki, 1996); rather, GABAergic inhibitory signals can, paradoxically, favour seizure initiation (Avoli et al., 1996a; Gnatkovsky et al., 2008; Grasse et al., 2013; Schevon et al., 2012; Truccolo et al., 2011). Strong recruitment of interneurons, and the consequent activation of postsynaptic $GABA_A$ receptors, can indeed lead to epileptiform synchronization and ictogenesis via several mechanisms that result from intracellular Cl^- accumulation and include: (i) a positive shift in Cl^- reversal potential that makes $GABA_A$ receptor signalling excitatory (Khalilov et al., 2005); and (ii) an increase in extracellular $[K^+]$ that is caused by the activity of potassium chloride cotransporter-2 (KCC2) which extrudes both Cl^- and K^+ from the intraneuronal compartements (Viitanen et al., 2010). In addition, it has been reported that excessive interneuron firing can result in depolarization block (Ziburkus et al., 2006) and perhaps synchronize neuronal populations through rebound excitation (Gnatkovsky et al., 2008; Jefferys et al., 2012d). Therefore, excessive activation of interneurons can very well be sufficient to disrupt the excitation/inhibition balance within the neuronal network thus triggering ictal-like discharges.

3.5.2. Optogenetic activation of PV- and SOM-positive interneurons triggers LVF onset seizures

We have recently reported that PV interneuron activation in a constitutive model of ChR2 expression triggered LVF onset ictal discharges (Shiri et al., 2015). Here, we have confirmed the contribution of PV interneurons to LVF discharges using a novel strain with a PV-Cre background in which we provided the enhanced ChR2 opsin, ChETA, using a stereotaxic virus injection procedure. In addition, as recently reported by Yekhlef *et al.,* (2015), we found that the optogenetic activation of SOM interneurons in EC is also sufficient to trigger LVF onset events.

Since previous studies have shown that GABA application to the dendrites induces depolarizing responses while its application to the soma results in hyperpolarization, (Alger and Nicoll, 1982; Andersen et al., 1980; Misgeld et al., 1986; Perreault and Avoli, 1991) we anticipated differences in the ability of somatic-targeting PV and dendritic-targeting SOM interneurons to trigger ictal discharges in the EC network. In addition, PV interneurons innervate twice as many principal cells as other interneurons and receive more local excitatory input, (Krook-Magnuson et al., 2013) therefore we expected these cells to play more preponderant roles compared to other interneuron types in triggering of ictal discharges. However, we found that activation of either fast-spiking PV cells or non-fast-spiking SOM cells are equally effective in triggering ictal discharges with a LVF onset pattern. This may be partially explained by the fact that SOM interneurons are extensively coupled via gap junctions and fire more readily in response to convulsive agents like 4AP (Lillis et al., 2012). Also, Cl^- accumulation is greater and faster in smaller dendritic compartments in comparison

to larger somas, thus allowing GABAergic activity to become depolarizing (Ellender et al., 2014). Finally, activation of both PV and SOM interneurons leads to the release of GABA which has been shown to result in an increase in extracellular [K^+] regardless of target compartments (Barolet and Morris, 1991).

3.5.3. Optogenetic activation of CaMKII-positive neurons triggers HYP onset seizures

It has been proposed that LVF and HYP seizures depend on the activity of distinct neural networks (Bragin et al., 2009; Lévesque et al., 2012b; Memarian et al., 2015). Accordingly, we have recently reported that systemic injection of the $GABA_A$ receptor antagonist picrotoxin *in vivo* induces seizures characterized by a HYP onset pattern while seizures induced by 4AP in these experiments are most often characterized by an LVF seizure onset pattern (Salami et al., 2015b). This evidence is in line with *in vitro* work performed on human tissue where it was shown that pyramidal cell firing and therefore, glutamatergic mechanisms herald the onset of HYP seizures (Huberfeld et al., 2011). Indeed, we have shown here that repetitive optogenetic activation of CaMKII-positive principal cells in the EC is sufficient to switch the 4AP-induced LVF onset discharges to HYP onset discharges.

In line with the *in vivo* observations reported in the pilocarpine TLE model (Lévesque et al., 2012b), we found that LVF onset discharges lasted longer than HYP onset discharges. The cellular and pharmacological mechanisms responsible for such different duration remain to be elucidated; however, it has been proposed that this could result from the fact that HYP onset discharges often arise from the hippocampal region whereas LVF onset discharges often start in parahippocampal regions including the EC (Bragin et al., 2009; Memarian et al., 2015; Velasco et al., 2000a). Our data, obtained from the same structure, suggest that the

involvement of glutamatergic signalling results in shorter periods of epileptiform synchronization. Further studies are, however, needed to confirm this hypothesis.

It is worthy to note that LVF and HYP are not the only two seizure onset patterns identified in TLE (Alarcon et al., 1995; Pacia and Ebersole, 1997; Perucca et al., 2014; Wetjen et al., 2009). We also recorded spontaneous ictal events that did not clearly fall in either of these two categories; these ictal discharges were however rare and were thus excluded from our analysis as we were interested in the mechanisms underlying LVF and HYP seizure onset patterns.

3.5.4. High-frequency oscillations associated with LVF and HYP onset seizures

Evidence obtained from *in vitro* (Khosravani et al., 2005) and *in vivo* (Bragin et al., 2005b; Lévesque et al., 2012b) animal models as well as from epileptic patients (Zijlmans et al., 2009) indicate that HFO rate of occurrence increases shortly before the appearance of ictal activity and remains high throughout. Ripples occur when inhibitory interneurons entrain pyramidal cells and other interneurons into a rhythmic pattern of firing (Ylinen et al., 1995). Indeed, we found that optogenetic stimulation of interneurons that triggered LVF onset discharges were associated with higher ripple rates at onset. Fast ripples on the other hand are thought to rely on population spikes arising from hypersynchronous firing of small groups of principal neurons (Jiruska et al., 2010c). As expected, we found higher fast ripple rates at the onset of ictal discharges with a HYP pattern triggered by optogenetic activation of CaMKII-positive principal cells in the EC. Our results therefore suggest that HFOs in different frequency bands during distinct seizure onset patterns reflect dynamic processes that may rest on the functional organization of specific types of neuronal clusters (Bragin et al., 1999b;

Engel et al., 2009b; Lévesque et al., 2012b). However further investigation is required to confirm these presumptions since oscillatory frequency alone is not sufficient to distinguish between different pathological HFOs (Menendez de la Prida and Trevelyan, 2011).

3.6. Conclusions

Our results demonstrate the contribution of two types of GABAergic interneurons to LVF onset discharges. We also discovered the ability to switch 4AP-induced LVF onset discharges to HYP discharges by optogenetic activation of a local pool of principal glutamatergic cells in EC. These findings can provide insight for clinicians to delineate better therapeutic targets in the treatment of TLE depending on seizure onset patterns and the associated HFOs. Additional studies should investigate the effect of optogenetic inhibition of these interneurons or principal cells in modulating ictal discharge progression.

Acknowledgements

This study was supported by the Canadian Institutes of Health Research (CIHR grants 8109 and 74609 to MA; and MOP119340 to SW). Z. Shiri received a student scholarship from the Savoy Foundation for Epilepsy.

Conflicts of Interest

The authors have no conflicts of interest to declare.

3.7. Figures

Figure 3.1

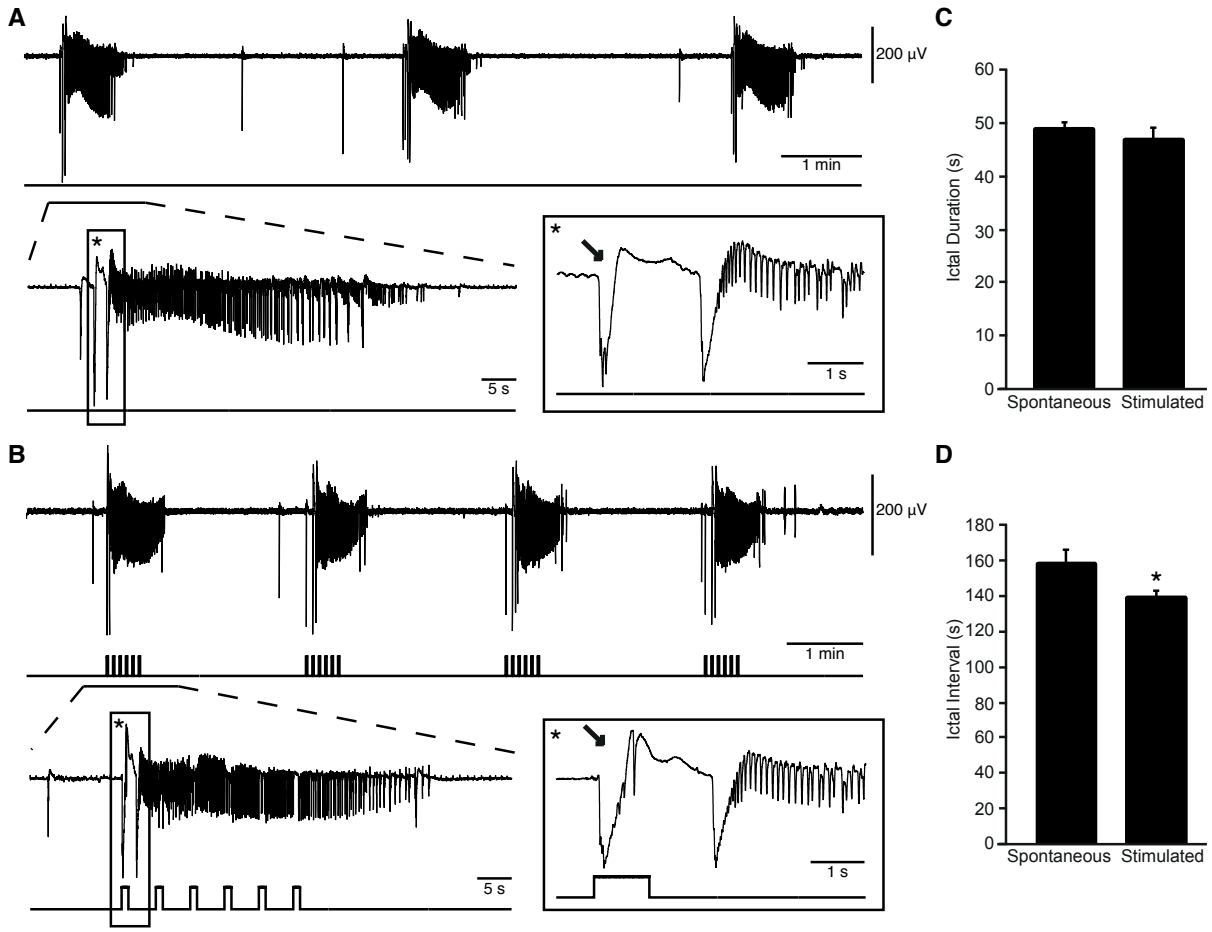

Figure 3.1. LVF ictal discharges can occur spontaneously or be triggered by optogenetic activation of PV-interneurons. **A**: Spontaneous ictal discharges occurring during bath application of 4AP; one event is further expanded to show the onset pattern (asterisk). **B**: Ictal discharges evoked by 1 s light pulses at 0.2 Hz during bath application of 4AP; one of these events is further expanded to compare the onset patterns (asterisk). Note that in both **A** and **B**, the ictal discharge is preceded by one or two negative-going interictal field potentials (arrows). **C** and **D**: Quantification of the duration and interval of occurrence of the spontaneous and stimulated ictal events recorded in these experiments (* indicates $p < 0.05$).

Figure 3.2

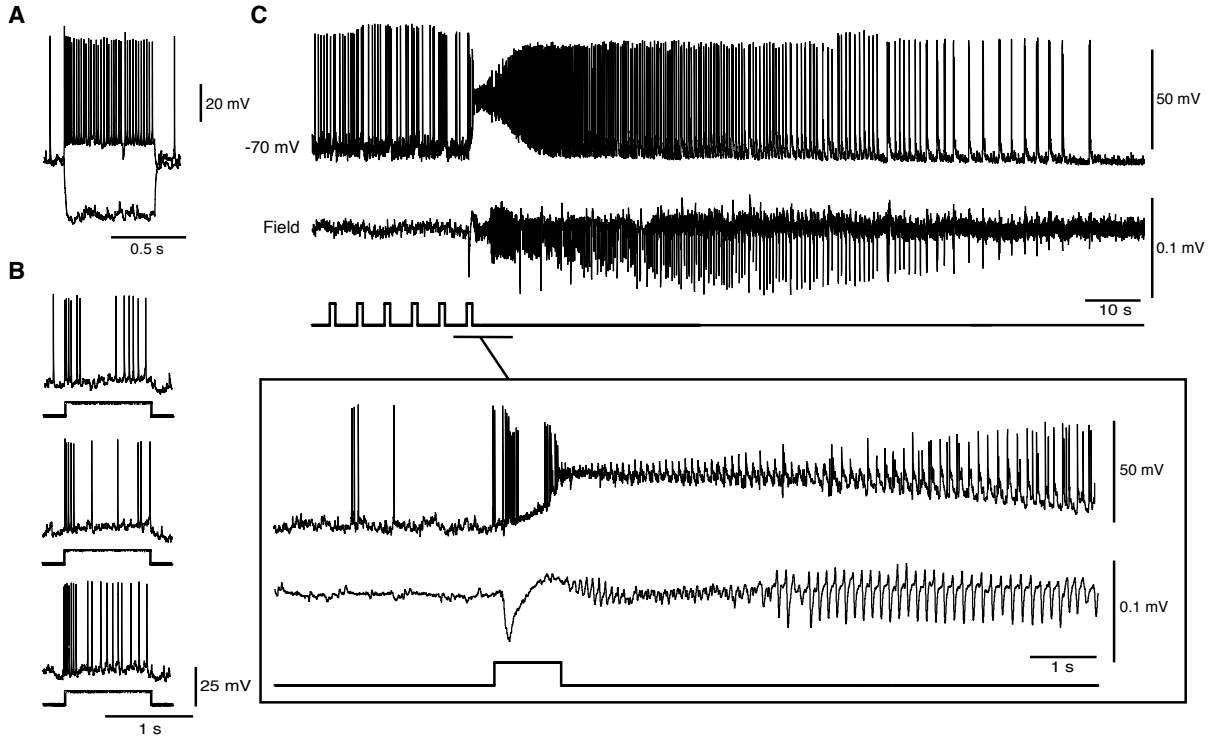

Figure 3.2. Optogenetic activation of PV-interneurons in the whole-cell configuration triggers LVF ictal discharges. **A**: Electrophysiological characterization of an EC fast-spiking PV-interneuron during injection of hyperpolarizing and depolarizing current pulses (membrane potential (Vm) = -70 mV; parameters of the intracellular current pulses = 600 ms, -200 and 160 pA; membrane resistance (R_m) = 121 MΩ; access resistance (R_a) = 36 MΩ). **B**: Responses generated by the same cell as in **A** to 1 s light pulses delivered at three-minute intervals. Note that similar action potential discharges are generated over time. **C**: Optogenetic activation of this interneuron (and of the concomitant LVF ictal discharge) by a train of 1 s light pulses at 0.2 Hz. The onset of the ictal event is expanded below to further reveal the LVF pattern.

Figure 3.3

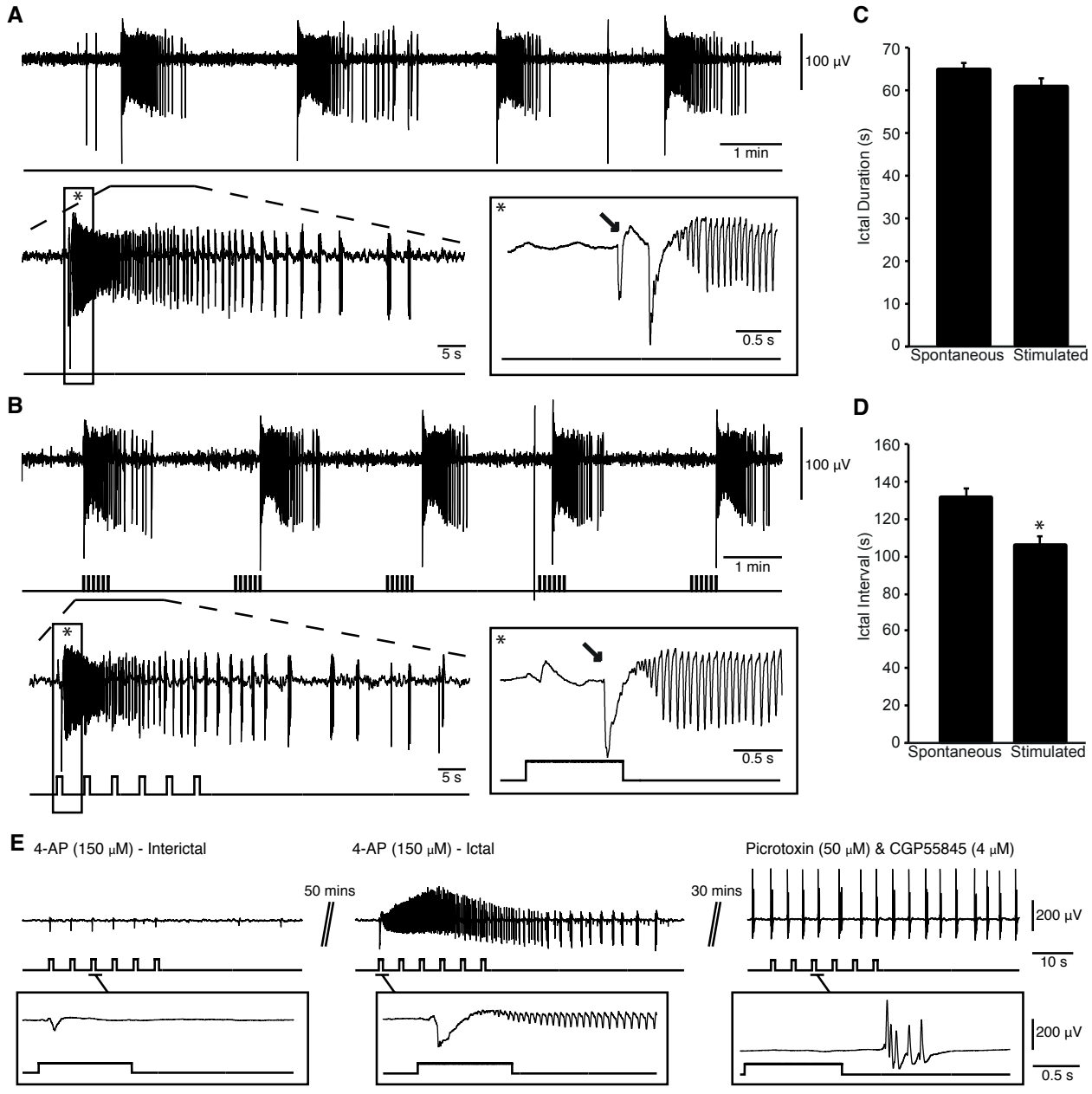
A
100 µV
1 min
5 s
0.5 s
B
100 µV
1 min
5 s
0.5 s
C
Ictal Duration (s)
70
60
50
40
30
20
10
0
Spontaneous
Stimulated
D
Ictal Interval (s)
160
140
120
100
80
60
40
20
0
Spontaneous
Stimulated
E
4-AP (150 µM) - Interictal
4-AP (150 µM) - Ictal
Picrotoxin (50 µM) & CGP55845 (4 µM)
50 mins
30 mins
200 µV
10 s
200 µV
0.5 s

Figure 3.3. LVF ictal discharges can also be triggered by optogenetic activation of SOM-interneurons. A: Spontaneous ictal discharges occurring during bath application of 4AP; one of the events is further expanded to show the onset pattern (asterisk). **B**: Ictal discharges evoked by a 30 s train of 1 s light pulses at 0.2 Hz during bath application of 4AP; one of the events is further expanded to compare the onset patterns (asterisk). Note that in both **A** and **B**, ictal discharges are preceded by one or two negative-going interictal field potential (arrows). **C** and **D**: Duration and interval of occurrence of spontaneous and stimulated ictal events are quantified (* indicates $p < 0.05$). Note that we were able to trigger ictal discharges at higher frequencies that what occurs spontaneously. **E**: Example 4AP-induced interictal discharges and ictal discharge triggered by trains of 1 s light pulses; bath application of 50 μM picrotoxin and 4 μM CGP55845 blocked all ictal discharges and responses to stimuli (see expanded example).

Figure 3.4

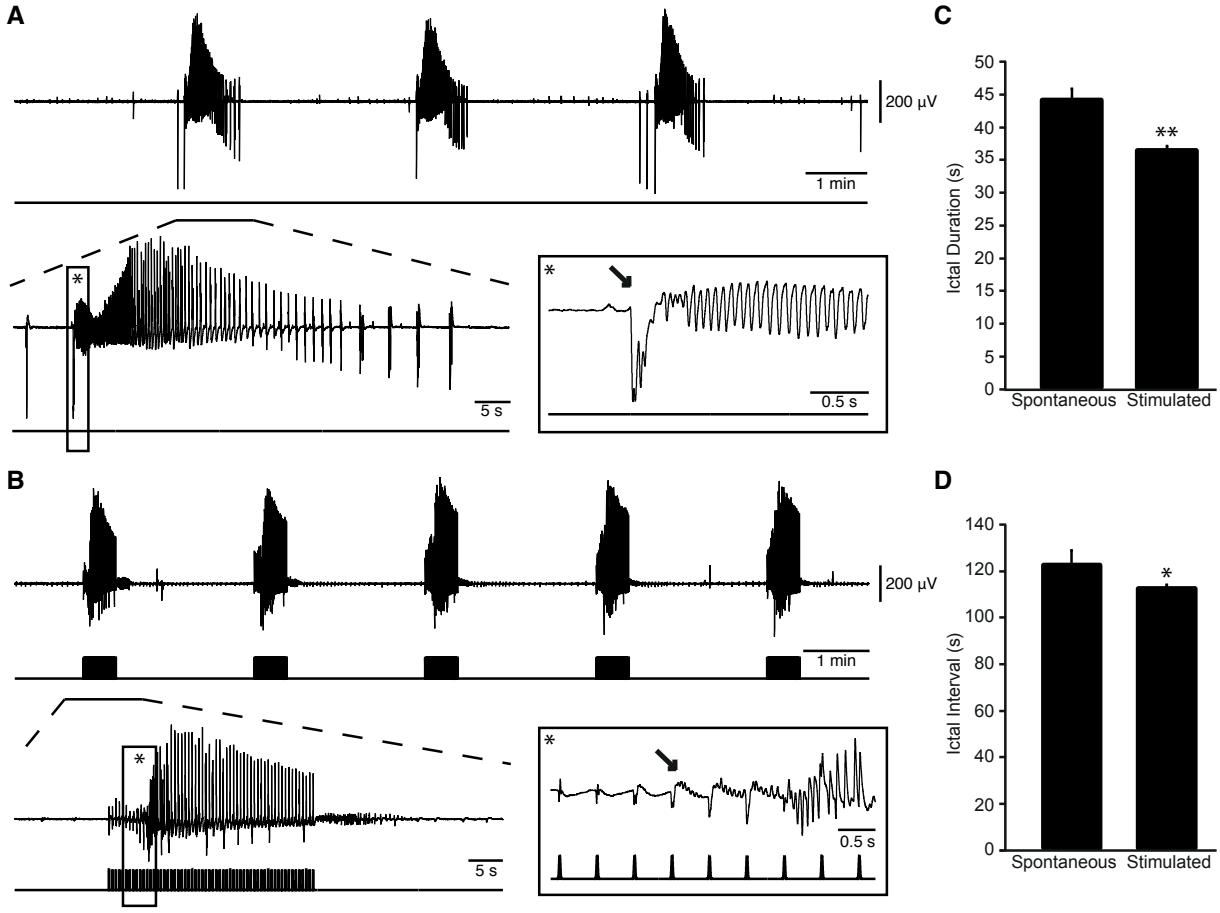
A
200 µV
1 min
*
5 s
*
0.5 s
B
200 µV
1 min
*
5 s
*
0.5 s
C
Ictal Duration (s)
50
45
40
35
30
25
20
15
10
5
0
**
Spontaneous
Stimulated
D
Ictal Interval (s)
140
120
100
80
60
40
20
0
*
Spontaneous
Stimulated

Figure 3.4. HYP ictal discharges can be triggered by optogenetic activation of CaMKII-principal neurons. **A**: Spontaneous ictal discharges occurring during bath application of 4AP; one of the events is further expanded to show the onset pattern (asterisk). **B**: Ictal discharges evoked by 20 ms light pulses at 2 Hz during bath application of 4AP; one of these events is further expanded to compare the onset pattern (asterisk). Note that in **B**, the ictal discharge is preceded by repeated spiking that are characteristic of HYP seizure onset (one of these spikes is indicated by an arrow). **C** and **D**: Plots of the duration and interval of occurrence of spontaneous and stimulated ictal events. Note that the stimulated HYP onset discharges were shorter than the spontaneous LVF discharges (* indicates $p < 0.05$; ** indicates $p < 0.01$).

Figure 3.5

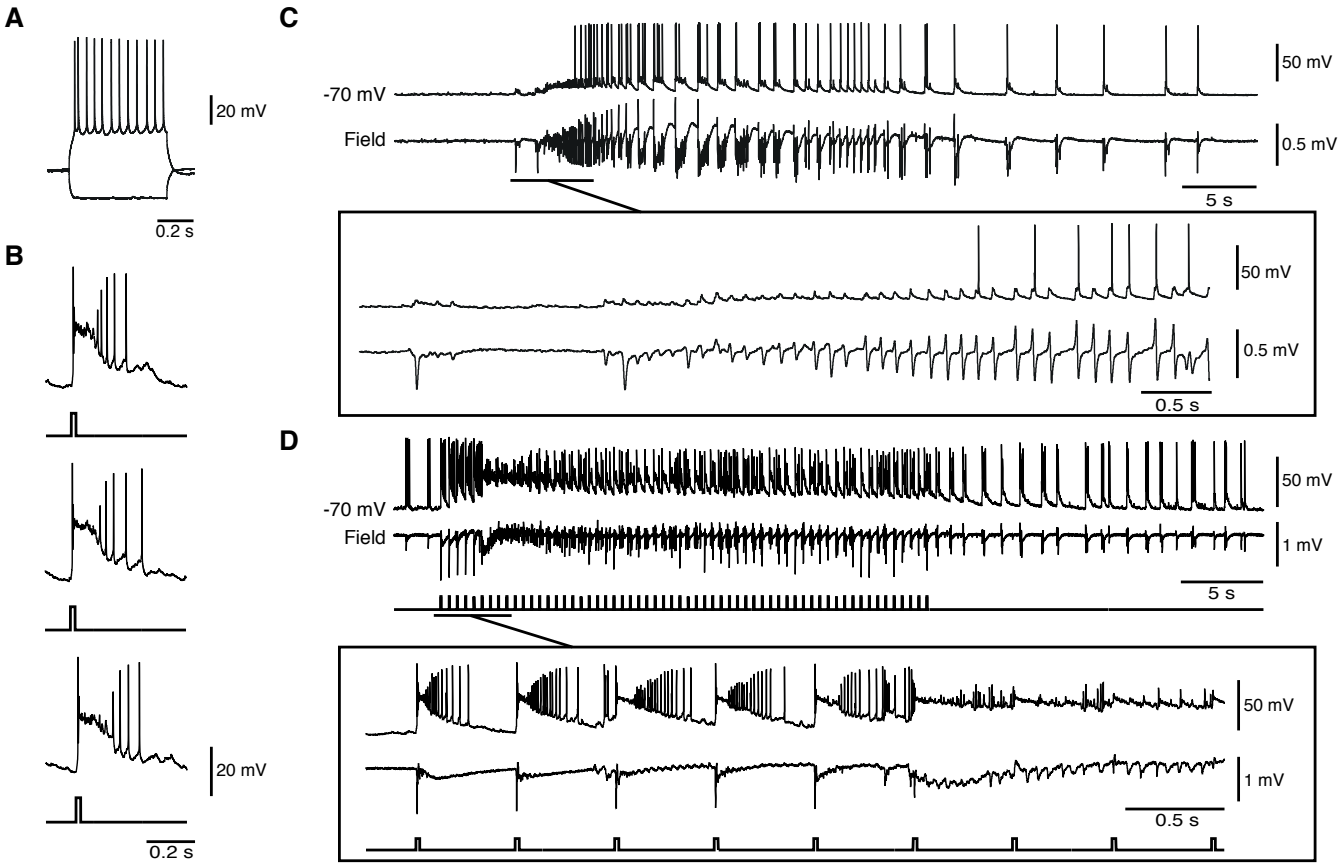
A
20 mV
0.2 s
B
20 mV
0.2 s
C
-70 mV
Field
50 mV
0.5 mV
5 s
50 mV
0.5 mV
0.5 s
D
-70 mV
Field
50 mV
1 mV
5 s
50 mV
1 mV
0.5 s

Figure 3.5. Optogenetic activation of CaMKII-principal cells in the whole-cell configuration triggers HYP ictal discharges. A: Electrophysiological characterization of an EC CaMKII-neuron during injection of hyperpolarizing and depolarizing current pulses (Vm = -70 mV; characteristics of the intracellular current pulses = 600 ms: -200 and 160 pA; R_m = 87 MΩ; R_a = 26 MΩ). **B**: Successive responses to 20 ms light pulses recorded from the same cell at three-minute intervals. Note that similar action potential discharges are generated over time. **C**: Firing pattern of a principal cell during a 4AP-induced spontaneous LVF onset ictal discharge. Note that the principal cell is quiescent at the onset of the LVF discharge. **D**: Optogenetic activation of a CaMKII-positive neuron (and of the concomitant HYP ictal discharge) by a train of 20 ms light pulses at 2 Hz. The onset of the ictal event is expanded below to further reveal the HYP pattern.

Figure 3.6

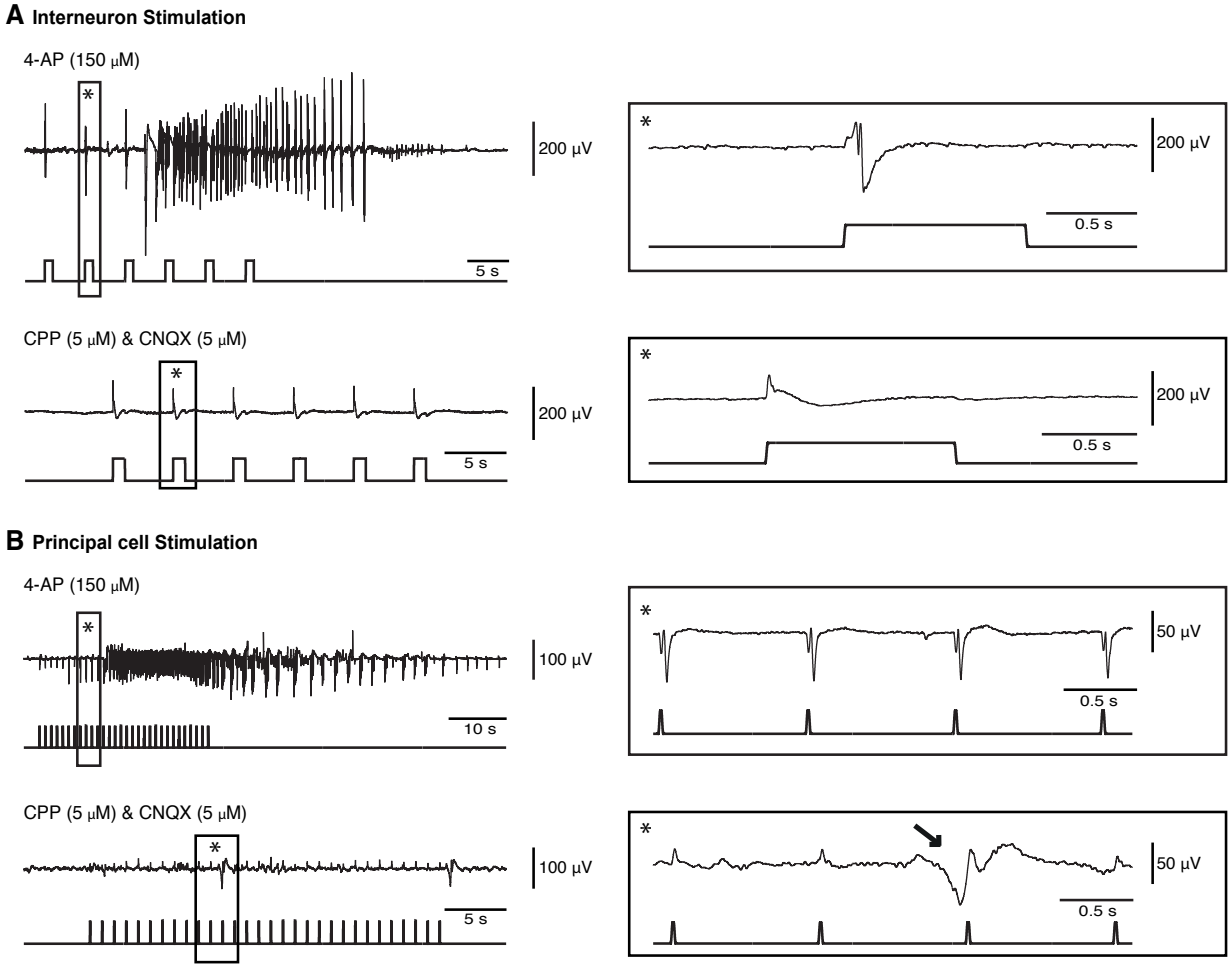
A Interneuron Stimulation
4-AP (150 μM)
200 μV
5 s
200 μV
0.5 s
CPP (5 μM) & CNQX (5 μM)
200 μV
5 s
200 μV
0.5 s
B Principal cell Stimulation
4-AP (150 μM)
100 μV
10 s
50 μV
0.5 s
CPP (5 μM) & CNQX (5 μM)
100 μV
5 s
50 μV
0.5 s

Figure 3.6. Blockade of glutamatergic neurotransmission abolishes both spontaneously occurring and optogenetic-induced ictal events. A: Example of an ictal discharge induced by a train of 1 s light pulses at 0.2 Hz that activate PV-positive interneurons in the EC during bath application of 4AP; a light-induced interictal discharge is expanded on the right (asterisk). Note that bath application of 5 μM CPP and 5 μM CNQX block all ictal discharges while light-driven presumptive GABAergic interictal event could be still evoked. **B**: Example of an ictal discharge induced by a train of 20 ms light pulses at 1 Hz activating CaMKII-positive principal cells in the EC during bath application of 4AP; part of the trace is further expanded to show the direct responses to stimuli (asterisk). In this experiment as well, bath application of 5 μM CPP and 5 μM CNQX abolishes spontaneous and light-induced ictal discharges; under these condition, spontaneous GABAergic discharges could however be recorded (arrow). Note that the small deflections in the field potential trace coinciding with stimuli are stimulation artefacts.

Figure 3.7

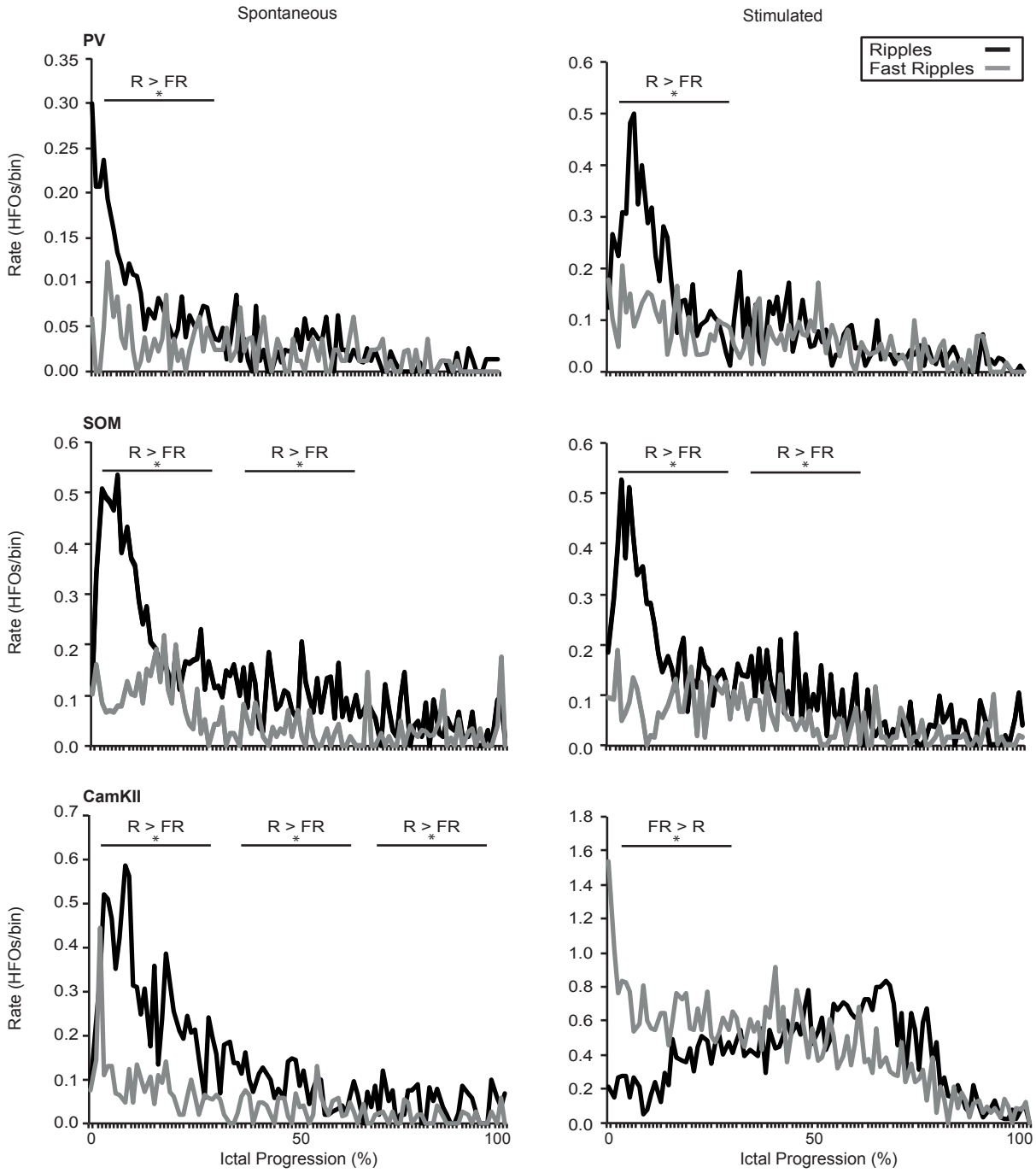
Spontaneous
Stimulated
PV
SOM
CamKII
Ripples
Fast Ripples
Rate (HFOs/bin)
R > FR
FR > R
*
Ictal Progression (%)
0
50
100

Figure 3.7. Specific patterns of HFOs characterize LVF and HYP onset ictal discharges. Average rate of ripples (R) and fast ripples (FR) are plotted over time for spontaneous 4AP-induced (left) and optogenetically stimulated (right) ictal discharges in PV, SOM, and CaMKII slices (n = 10 events for each plot). Wideband recordings of spontaneous and stimulated ictal discharges were filtered to detect HFOs throughout the event from the onset (0 % Progression) to the end of the ictal discharge (100% progression). Note that ripple rates predominate in the LVF onset discharges; whereas fast ripple rates are higher at the onset of HYP discharges triggered by CaMKII-cell stimulation (* indicates $p < 0.01$).

Chapter 4: Optogenetic low-frequency stimulation of specific neuronal populations abates ictogenesis

Shiri Z, Lévesque M, Frédéric Manseau, Guillaume Etter, Williams S, Avoli M. *Journal of Neuroscience*, submitted.

In Chapters 2 and 3, I investigated the contributions of different cell populations to the onset of common seizure patterns observed in mesial temporal lobe epilepsy. For the final study included in my thesis, I wanted to slightly shift gears and explore the ability of optogenetic low-frequency stimulation to abate seizures in real-time. The rationale for such intervention is supported by experimental evidence obtained from *in vivo* rodent models of mesial temporal lobe epilepsy where low-frequency stimulation of the ventral hippocampal commissure was shown reduce seizure frequency. Therefore, here we used the optogenetic stimulation of calcium/calmodulin-dependent protein kinase II-positive principal cells and of parvalbumin- or somatostatin-positive interneurons at 1 Hz to compare, for the first time, the effects induced by activation of these specific cell subtypes on 4-aminopyridine-induced ictal discharges generated from the entorhinal cortex in an *in vitro* brain slice preparation. This work has been submitted to *Journal of Neuroscience* as a manuscript entitled "Optogenetic low-frequency stimulation of specific neuronal populations abates ictogenesis".

4.1. Abstract

Despite many advances made in understanding the pathophysiology of epileptic disorders, seizures remain poorly controlled in approximately one third of mesial temporal lobe epilepsy patients. Here, we established the efficacy of cell type-specific low-frequency stimulation (LFS) in controlling ictogenesis in the mouse entorhinal cortex (EC) in an *in vitro* brain slice preparation. Specifically, we used 1 Hz optogenetic stimulation of Ca^{2+}/calmodulin-dependent protein kinase II-positive principal cells as well as of parvalbumin- or somatostatin-positive interneurons to study the effects of such repetitive activation on epileptiform discharges induced by 4-aminopyridine. We found that 1 Hz stimulation of any of these cell types reduced the frequency and duration of ictal discharges in some trials, while completely blocking them in others. The field responses evoked by the stimulation of each cell type revealed that their duration and amplitude were higher when principal cells were targeted. Furthermore, following a short period of silence ranging from 67 to 135 s, ictal discharges were re-established with similar duration and frequency as before stimulation; however, this period of silence was longer following principal cell stimulation compared to parvalbumin- or somatostatin-positive interneuron stimulation. Our results show that LFS of either excitatory or inhibitory cell networks in EC are effective in controlling ictogenesis. Although optogenetic stimulation of either cell type significantly reduced the occurrence of ictal discharges, principal cell stimulation resulted in a more prolonged suppression of ictogenesis and thus, it may constitute a better approach for controlling seizures.

4.2. Introduction

Mesial temporal lobe epilepsy is the most common form of focal epilepsy in adulthood and involves seizures arising from limbic structures such as the hippocampus and the rhinal cortices (Gloor, 1997). It is also one of the most refractory forms of epilepsy since up to 75% of patients do not achieve adequate seizure control through medication (Jallon, 1997); therefore, costly, at times impractical, surgical resection of the epileptic tissue remains the only therapeutic alternative in these cases (Blume and Parrent, 2006; Wiebe, 2004). An alternative approach for treating patients with intractable epilepsy rests on low-frequency stimulation (LFS) that can be delivered through either transcranial magnetic or deep-brain electrical procedures (Fisher and Velasco, 2014). The rationale for such intervention is supported by experimental evidence obtained from *in vivo* rodent models of mesial temporal lobe epilepsy where LFS of the ventral hippocampal commissure reduces seizure frequency (Kile et al., 2010; Rashid et al., 2012).

It is also known that CA3-driven interictal activity controls the entorhinal cortex (EC) propensity to generate ictal discharges *in vitro* (Barbarosie and Avoli, 1997; Bragdon et al., 1992). In addition, when inputs from the CA3 are removed by cutting the Schaffer collaterals, electrical stimuli delivered in the subiculum at frequencies similar to those of CA3-driven interictal discharges decrease epileptiform synchronization in the EC (Barbarosie and Avoli, 1997); indeed, it has been shown that 1 Hz stimulation frequency exhibits maximal efficacy in reducing ictogenesis in the EC (D'Arcangelo et al., 2005). However, despite the temporal and spatial control offered by electrical or magnetic LFS, these procedures lack cell-specificity thus presumably limiting their anti-ictogenic efficacy. This drawback can now be addressed using optogenetic techniques (Yizhar et al., 2011) that have been recently employed as

potential therapeutic tools for controlling seizures (Bui et al., 2015; Wykes et al., 2015). Overall, there are two approaches used in this context. One is to employ the optogenetic inhibition of excitatory principal cells expressing halorhodopsin; experiments using this approach have revealed attenuation of epileptiform activity *in vivo* (Krook-Magnuson et al., 2013) and *in vitro* (Tønnesen et al., 2009) preparations. The second strategy is to increase the activity of inhibitory interneurons expressing channelrhodopsin-2 (Kokaia et al., 2013); optogenetic activation of hippocampal interneurons has been shown to attenuate seizures *in vivo* (Krook-Magnuson et al., 2013), while low-frequency activation of GABAergic cells in the CA3 hippocampal subfield controls 4-aminopyridine (4AP)-induced ictal discharges *in vitro* (Ladas et al., 2015; Ledri et al., 2014).

It remains to be established whether low frequency activation of principal cells results in attenuation or strengthening of ictal synchronization. Also, most of the studies reviewed above focused on the effects of optogenetic stimulation on epileptiform activity in the hippocampus, and thus it is unknown whether optogenetic activation of specific neuron subtypes in parahippocampal structures such as the EC can control epileptiform synchronization as well. The EC is an epileptogenic area that is highly interconnected with the hippocampus (Canto et al., 2008; Gloor, 1997; Rutecki et al., 1989). Therefore, in this study we used optogenetic stimulation of Ca^{2+}/calmodulin-dependent protein kinase II (CaMKII)-positive principal cells and of parvalbumin (PV)- or somatostatin (SOM)- positive interneurons at 1 Hz to compare, for the first time, the effects induced by activation of these specific cell subtypes on 4AP-induced ictal discharges generated from the transgenic mouse EC in an *in vitro* brain slice preparation.

4.3. Materials and Methods

4.3.1. Animals

All procedures were performed according to protocols and guidelines of the Canadian Council on Animal Care and were approved by the McGill University Animal Care Committee. CaMKII-Cre (Jackson Laboratory, B6.Cg-Tg(Camk2a-cre)T29-1Stl/J, stock number 005359), PV-Cre (Jackson Laboratory, B6;129P2-*pvalb*$^{tm1(cre)Arbr}$/J, stock number 008069), and SOM-Cre (Jackson Laboratory, *Ssttm2.1(cre)Zjh*/J, stock number 013044) homozygote mouse colonies were bred and maintained in house in order to generate pups that were used in this study.

4.3.2. Stereotaxic virus injections

Six CaMKII-Cre, seven PV-Cre, and four SOM-Cre male or female pups were anesthetized at P15 using isoflurane and positioned in a stereotaxic frame (Stoelting). AAVdj-ChETA-eYFP virus (UNC Vector Core) was delivered in the EC (0.6 µL at a rate of 0.06 µL/min). Injection coordinates were: AP -4.00 mm , ML +/- 3.60 mm, DV -4.00 mm. The transverse sinus was used as a point of reference, and the injection needle was inserted with a 2º anteroposterior angle. After completion of the surgery, pups were given a single injection of carprofen (20 mg/kg, SC) and placed on a heat pad for 30 minutes to allow recovery. Pups were then returned to their home cage.

4.3.3. Slice preparation

Mice were deeply anesthetized with inhaled isoflurane and decapitated at P30-40. Brains were quickly removed and immersed in ice-cold slicing solution containing (in mM): 25.2 sucrose,

10 glucose, 26 $NaHCO_3$, 2.5 KCl, 1.25 KH_2PO_4, 4 $MgCl_2$, and 0.1 $CaCl_2$ (pH 7.3, oxygenated with 95% O_2/5% CO_2). Horizontal brain slices (thickness = 400 μm) containing the EC were cut using a vibratome (VT1000S, Leica) and incubated for one hour or more at room temperature in a slice saver filled with oxygenated artificial cerebrospinal fluid (aCSF) of the following composition (in mM): 125 NaCl, 25 glucose, 26 $NaHCO_3$, 2 KCl, 1.25 NaH_2PO_4, 2 $MgCl_2$, and 1.2 $CaCl_2$.

4.3.4. Electrophysiological recordings and photostimulation

Brain slices were transferred to a submerged chamber where they were perfused with oxygenated aCSF (KCl and $CaCl_2$ adjusted to 4.5 and 2 mM, respectively) at a rate of 10-15 mL/min atn 30 ºC. Field potentials were recorded with aCSF-filled microelectrodes (1-2 MΩ) positioned in the EC deep layers in the presence of 4AP. Signals were recorded with a differential AC amplifier (AM systems), filtered online (0.1-500 Hz), digitized with a Digidata 1440a (Molecular Devices) and sampled at 5 kHz using the pClamp software (Molecular Devices). For ChETA excitation, blue light (473 nm, intensity 35 mW) was delivered through a custom-made LED (Luxeon) system coupled to a 3 mm wide fiber optic (Edmund Optics), placed above the recorded area. For optogenetic activation of CaMKII-positive principal cells and PV- or SOM- positive cells, light pulses (1 ms duration) were delivered at 1 Hz for 180 s with a 220 s interval between stimulating protocols. Reagents were obtained from Sigma-Aldrich.

4.3.5. Data analysis

Rate of ictal discharges were computed based on the number of ictal discharges (per min) that occurred during 1 Hz stimulation compared to the number of ictal discharges (per min) that occurred during periods of no stimulation. Ictal recovery time was measured from the end of the last optogenetic pulse to the start of the next ictal discharge. To quantify the responses to optogenetic pulses, we measured the delay, amplitude, and duration of each response. The delay of each response was measured from the time the LED was on until the time the first deflection from baseline occurred. The negligible artifacts that occurred during the 1 ms pulse were not considered in the response onset. The amplitude of each response was measured as the peak minus the trough of the resulting waveform. The duration of the response was measured from the first deflection from baseline until the return to baseline.

4.4. Results

As described in Shiri et al. (2016), 4AP application in slices obtained from the three types of transgenic mice induced spontaneous epileptiform activity with similar electrographic characteristics. The average intervals of spontaneous ictal discharge occurrence were 110.23 ± 6.24, 153.46 ± 9.51, and 145.43 ± 11.14 s in CaMKII, PV, and SOM mice, respectively (not significantly different). Furthermore, the average duration of ictal discharges obtained from approximately 140 events per transgenic type were 52.85 ± 1.58, 56.45 ± 1.31, and 55.67 ± 1.02 s in CaMKII, PV, and SOM mice, respectively (not significantly different).

4.4.1. Optogenetic activation of CaMKII-positive neurons

First, we used brain slices (n = 7) obtained from transgenic mice expressing the ChETA opsin in CaMKII-positive principle cells in the EC; spontaneous ictal discharges were recorded in all experiments during continuous perfusion with 4AP-containing aCSF (Figure 1Aa). Optogenetic stimulation of CaMKII-positive principal cells using 1 ms light pulses at 1 Hz for 180 s disrupted this ictal activity and significantly reduced its rate of occurrence from 0.31 ± 0.06 to 0.11 ± 0.03 discharges per min (60% reduction; $p < 0.05$; Figure 1B). In 51% of the optogenetic stimulation trials (n = 21), an initial ictal discharge of shorter duration ($p < 0.01$; Figure 1C) was elicited and was followed by stimulation-induced field potentials (Figure 1Ab). In the remaining recordings (n = 20), 1 Hz stimulation of principal cells was effective in blocking ictal discharges for the entire duration of the session (Figure 1Ac). It should be emphasized that partial or full blockade of ictal discharges during stimulation of CaMKII-positive principal cells could occur in different sessions performed in the same slice. Following termination of this stimulation paradigm, ictal activity recovered to control (pre-stimulation) conditions within 135.35 ± 12.49 s in both outcomes with similar duration, rate of occurrence, and electrographic pattern (Figures 1A and 4).

4.4.2. Optogenetic activation of PV-positive interneurons

Next, we used brain slices (n = 7) obtained from transgenic mice expressing the opsin in PV-positive interneurons in the EC. As illustrated in Figure 2, optogenetic stimulation of PV-positive interneurons using the same stimulation paradigm as for principal cell stimulation (1 ms light pulses at 1 Hz for 180 s) significantly reduced the rate of spontaneous ictal discharges from 0.25 ± 0.01 to 0.12 ± 0.01 discharges per min (51% reduction; $p < 0.01$;

Figure 2B). PV-positive interneuron stimulation resulted in ictal discharges of shorter duration ($p < 0.01$; Figure 2C) followed by direct responses to optogenetic stimulation in 17% of trials ($n = 4$; Figure 2Ab). In 83% of trials ($n = 19$), optogenetic stimulation of PV-interneurons only elicited brief field potentials while blocking ictal events for the duration of the recording (Figure 2Ac). Ictal activity in this series of experiments recovered within 67.93 ± 6.90 s (Figure 4) with a similar rate of occurrence and a shorter duration ($p < 0.05$).

4.4.3. Optogenetic activation of SOM-positive interneurons

In a final set of experiments, we used slices ($n = 6$) obtained from transgenic mice expressing the opsin in SOM-positive interneurons in the EC. Optogenetic stimulation of SOM-positive interneurons using 1 ms light pulses at 1 Hz for 180 s significantly reduced the rate of 4AP-induced ictal discharges from 0.34 ± 0.04 to 0.16 ± 0.03 discharges per min (49% reduction; $p < 0.01$; Figure 3B). In all successful trials ($n = 15$), 1 Hz stimulation of SOM-interneurons was effective in blocking ictal discharges for the entire duration of the recording (Figure 3Ab). Following this stimulation paradigm, ictal activity recovered on average within 70.45 ± 23.50 s and with a similar duration and pattern of occurrence as seen before stimulation (Figure 3A and 4). As illustrated in Figure 4, ictal discharges reappeared significantly earlier following PV-interneuron ($p < 0.01$) and SOM-interneuron ($p < 0.05$) stimulation compared to principal cell stimulation.

4.4.4. Characterization of field responses to optogenetic stimulation

To examine the electrographic properties of the field potentials evoked by the different optogenetic stimulation procedures, we superimposed 180 consecutive responses per group

(grey traces; Figure 5A). The average delay of the responses from stimulation onset was comparable in each group (Figure 5B). The average field potential amplitude was highest ($p < 0.01$) in the CaMKII group at 0.41 ± 0.02 mV and lowest ($p < 0.01$) in the SOM group at 0.02 ± 0.00 mV (Figure 5C). The average durations of the responses were 0.20 ± 0.01 s in the CaMKII group, 0.26 ± 0.02 s in the PV group ($p < 0.01$), and 0.19 ± 0.02 s in the SOM group (Figure 5C).

4.5. Discussion

We used an optogenetic approach of LFS in the EC to investigate the role of local interneuron subtypes and for the first time, of principal cells, in the process of stimulus-induced suppression of ictogenesis during application of 4AP. The main findings of our study can be summarized as follows: (i) 4AP-induced ictal discharges had similar features in slices obtained from the three transgenic mice used in this study; (ii) using the same experimental parameters, optogenetic LFS of CaMKII-positive principal cells and PV- or SOM-positive interneurons in EC significantly reduced the rate of 4AP-induced ictal discharges; (iii) optogenetic stimulation applied to principal cells had a longer lasting effect in suppressing ictal discharges once stimulation was aborted.

Evidence obtained from rodent models of temporal lobe epilepsy have shown that LFS can reduce both excitability and seizure frequency (Barbarosie and Avoli, 1997; D'Arcangelo et al., 2005; Kile et al., 2010; Rashid et al., 2012). However, it remained unclear whether this effect could be attributed to excitatory or inhibitory neurons or other cells of the central nervous system, as electric stimuli do not discriminate between different cell types. Using

optogenetic stimulation, we showed that activation of either principal cells or interneurons is effective in disrupting synchronicity and reducing seizure activity in the 4AP model *in vitro*.

We have found here that 4AP-induced ictogenicity in EC is depressed by repetitive stimulation of interneurons using 1 ms pulses at 1 Hz. These results are in line with other *in vitro* studies where it was shown that electrical stimuli (Barbarosie and Avoli, 1997; Barbarosie et al., 2002; Benini et al., 2003) and optogenetic stimuli (Krook-Magnuson et al., 2013; Ladas et al., 2015; Ledri et al., 2014) delivered at low frequencies can reduce and block ictal discharge generation. The novel finding of our study however, is that low frequency stimulation of principal cells in the EC is also effective in temporarily blocking ictal discharges. This finding is rather surprising as other studies have previously shown that inhibition of excitatory cells in the hippocampus results in an anti-ictogenic action (Krook-Magnuson et al., 2013; Tønnesen et al., 2009). Specifically, Tønnesen et al. (2009) demonstrated that selective hyperpolarization of CaMKII-positive neurons in the hippocampus is effective in attenuating stimulation-train induced bursting. The differences observed in these studies and ours may be attributed to the different models of hyperexcitability used and the different structures being studied.

It may seem untenable that repeated stimulation of both principal cells and interneurons can play a protective role against ictal discharge generation. However, the common feature in these experiments is that we are increasing neuronal spatial synchrony by stimulating at low frequencies and thus protecting against ictogenesis (Schindler et al., 2007; Timofeev and Steriade, 2004). Selective activation of interneuron subtypes or principal cells induces rebound or direct excitatory bursting in the principal cell network thus causing entrainment and consequently an overall suppression of hyperactivity (Ladas et al., 2015). Furthermore,

previous studies have shown that repetitive stimulation can restrain ictal discharge generation in EC by clamping GABA-mediated potentials that lead to large elevations in extracellular potassium levels which can then initiate ictal discharges (Barbarosie et al., 2002; Eng and Kocsis, 1987). This hypothesis is supported by experiments that showed elevations in extracellular potassium induced by electrical stimulation delivered at 0.5 Hz is significantly lower than those induced by stimuli delivered at or lower than 0.1 Hz (Avoli et al., 2013a). These transient increases in extracellular potassium due to $GABA_A$ receptor activation can be reproduced theoretically with any of the three procedures used in this study, either directly (through interneuron stimulation) or indirectly (through principal cell stimulation).

Our results show that recovery of spontaneous 4AP-induced ictal discharges took longer in experiments where the optogenetic stimulation targeted principal cells rather than interneurons. This may be due to the morphology of interneurons and the large pool of local principal cells that they target (Vereczki et al., 2016) which presumably causes a larger rebound activation and synchronization in the target excitatory cells. This orchestrated synchronization could explain why ictal discharges recover sooner in experiments where interneurons are the target of stimulation.

In conclusion, we have discovered that LFS of specific cell populations, principal cells or interneuron subtypes, can reliably shorten or delay seizures *in vitro* presumably by disrupting synchronicity. It remains unclear whether these stimulation paradigms can control ictogenesis when applied to other *in vitro* models and more importantly whether low-frequency optogenetic stimulation can modulate ictogenesis and epileptogenesis in models *in vivo*. However, our work suggests that optogenetic LFS targeting a single cell population at a time

can address the limitations of classic LFS techniques and may thus constitute a more reliable means for controlling seizures in patients that present with focal seizures.

4.6. Figures

Figure 4.1

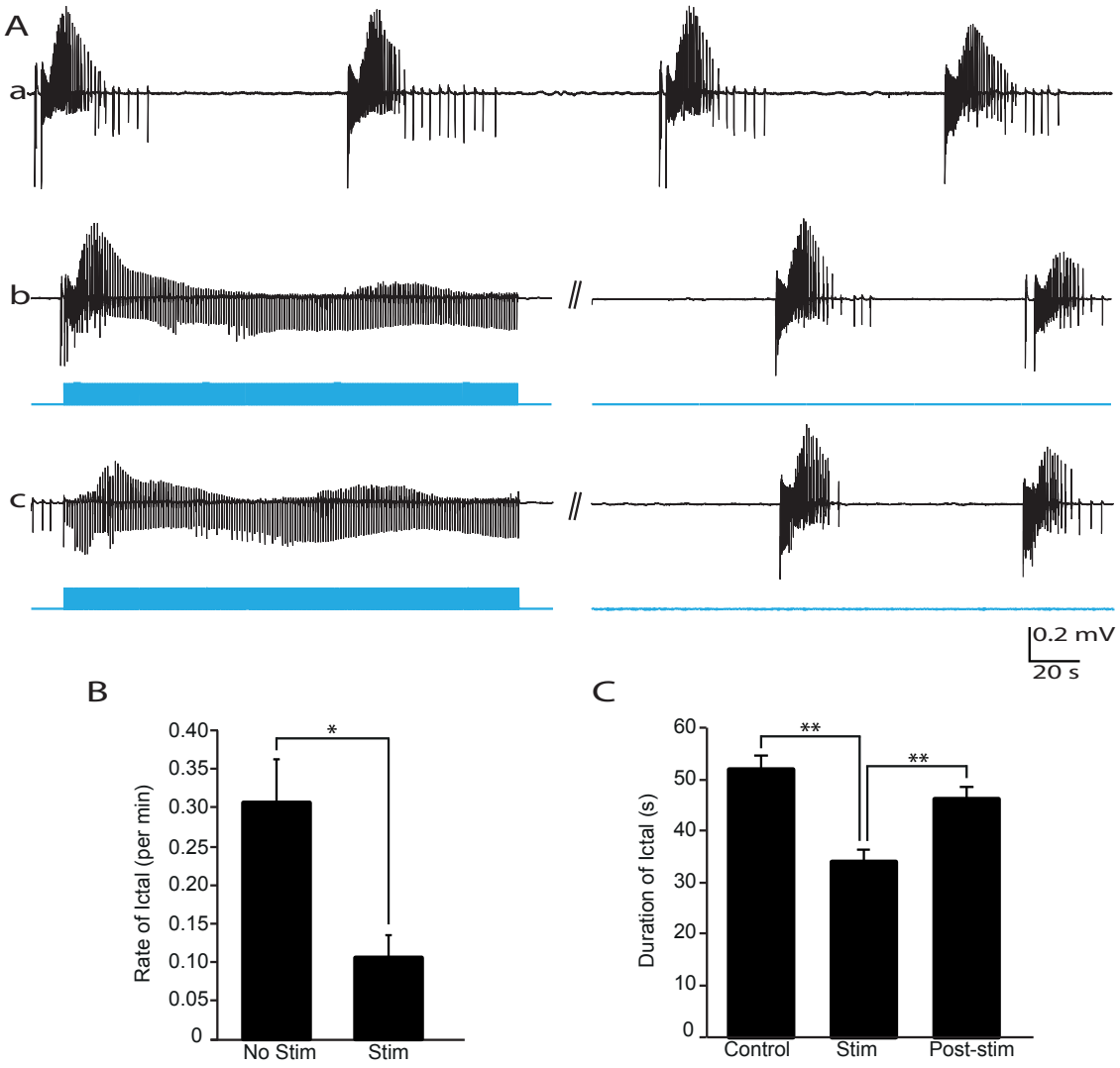

Figure 4.1. Optogenetic activation of CaMKII-positive principal cells reduces ictal discharges. A: (a) Spontaneous ictal discharges can be recorded from the EC following 4AP administration (Control). A series of 200 s protocols were applied sequentially where we stimulated CaMKII cells using 1 ms pulses at 1 Hz for 180 s (Stim) followed by gap-free recordings of similar duration where we recorded the post-stimulus 4AP-induced network activity (Post-stim); **(b)** in 51% of stimulation trials, a brief ictal discharge was elicited followed by stimulation-induced field potentials (n = 21). The gap between the stimulation and post-stimulation recordings was 4 s; **(c)** in 49% of stimulation trials, ictal discharges were completely blocked (n = 20). The gap between the stimulation and post-stimulation recordings was 3 s. In both (b) and (c), the network fully recovers once the optogenetic stimulation is aborted and can generate ictal discharges once again. **B:** The rate of ictal discharges was 0.31 ± 0.06 discharges per min in the control and post-stim recordings and 0.11 ± 0.03 discharges per min in the stim recordings. **C:** The duration of ictal discharges in control and post-stim conditions were 51.94 ± 2.63 s and 46.08 ± 2.42 s respectively. The duration of ictal discharges that occurred during stim were significantly shorter at 34.13 ± 2.21 s (* signifies $p < 0.05$; ** signifies $p < 0.01$).

Figure 4.2

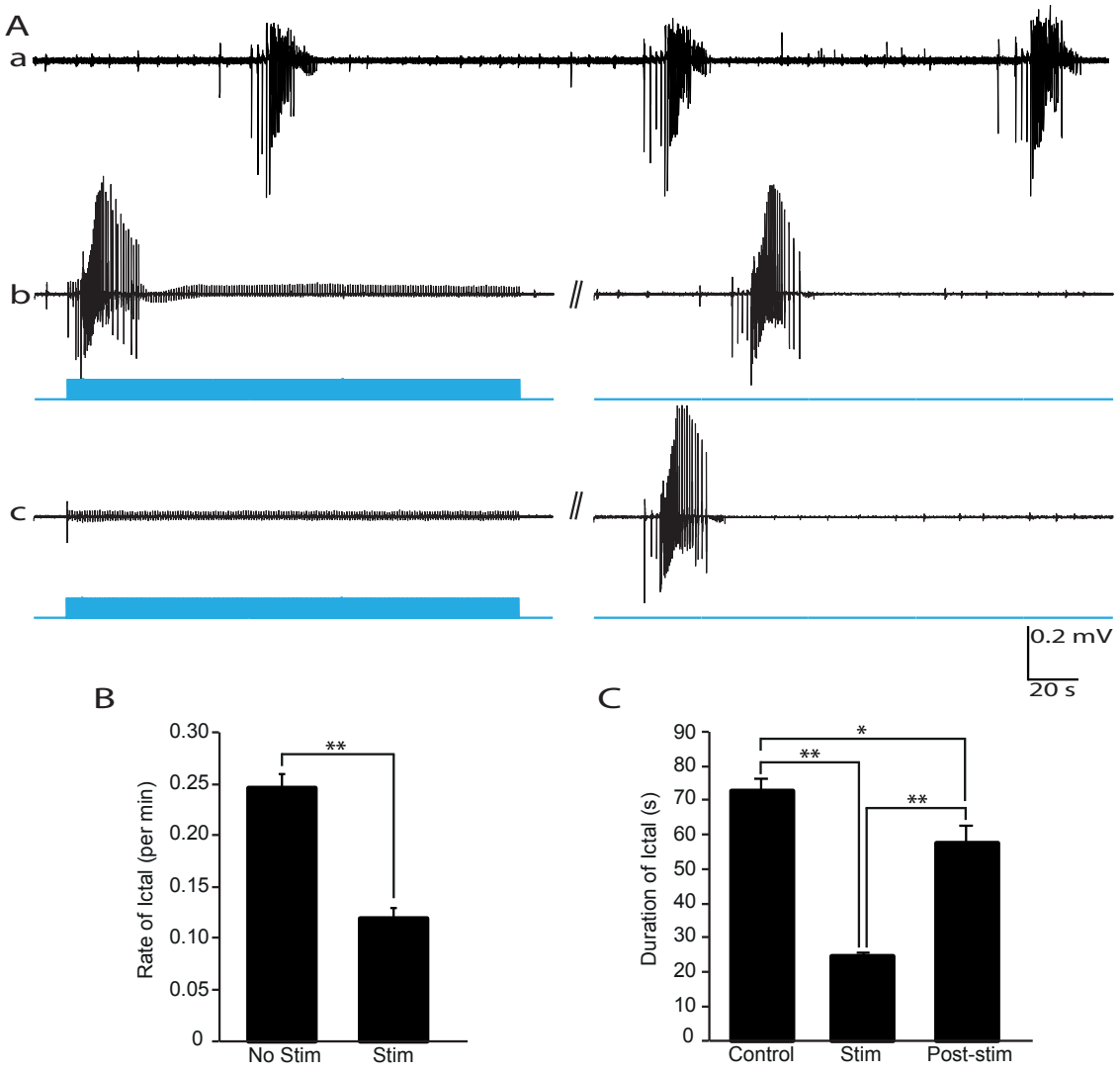
A
a
b
c
0.2 mV
20 s
B
Rate of Ictal (per min)
0.30
0.25
0.20
0.15
0.10
0.05
0
**
No Stim
Stim
C
Duration of Ictal (s)
90
80
70
60
50
40
30
20
10
0
*
**
**
Control
Stim
Post-stim

Figure 4.2. Optogenetic activation of PV-positive interneurons reduces ictal activity. A: (a) Spontaneous (Control) ictal discharges recorded from the EC are shown. A series of 200 s protocols were applied sequentially where we stimulated PV cells using 1 ms pulses at 1 Hz for 180 s (Stim) followed by gap-free recordings of similar duration where we recorded the post-stimulus 4AP-induced network activity (Post-stim); **(b)** in 17% of stimulation trials, a brief ictal discharge was elicited (n = 4). The gap between the stimulation and post-stimulation recordings was 3 s; **(c)** in 83% of stimulation trials, ictal discharges were completely blocked (n = 19). The gap between the stimulation and post-stimulation recordings was 3 s. In both (b) and (c), the network fully recovers once the optogenetic stimulation is aborted and can generate ictal discharges once again. **B:** The rate of ictal discharges was 0.25 ± 0.01 discharges per min in the control and post-stim recordings and 0.12 ± 0.01 discharges per min in the stim recordings. **C:** The duration of ictal discharges was 72.55 ± 3.78 s in control, 24.67 ± 1.20 s in stim, and 57.40 ± 5.03 s in post-stim conditions (* signifies $p < 0.05$; ** signifies $p < 0.01$).

Figure 4.3

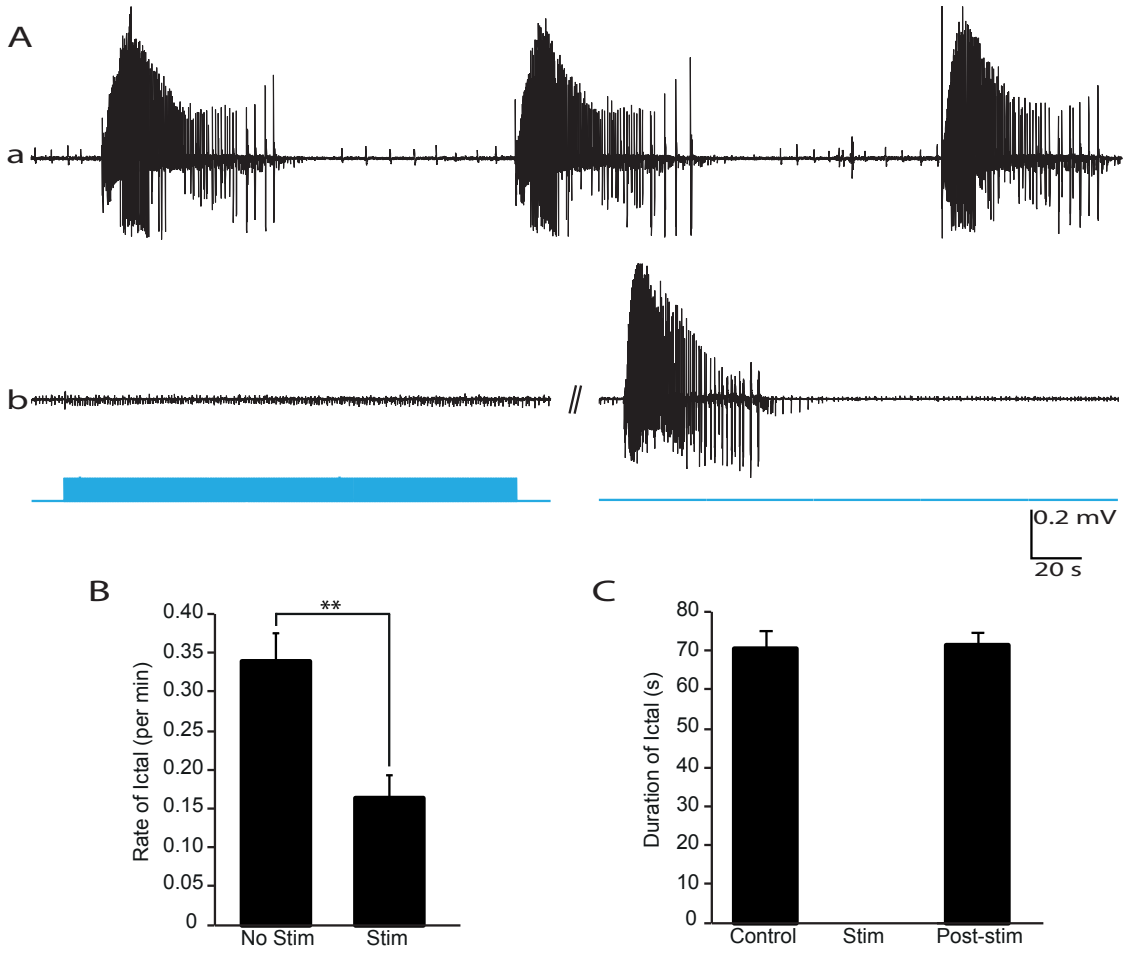
A
a
b
0.2 mV
20 s
B
Rate of Ictal (per min)
0.40
0.35
0.30
0.25
0.20
0.15
0.10
0.05
0
**
No Stim
Stim
C
Duration of Ictal (s)
80
70
60
50
40
30
20
10
0
Control
Stim
Post-stim

Figure 4.3. Optogenetic activation of SOM-positive interneurons reduces ictal activity. **A: (a)** Spontaneous (Control) ictal discharges recorded from the EC are shown. A series of 200 s protocols were applied sequentially where we stimulated SOM cells using 1 ms pulses at 1 Hz for 180 s (Stim) followed by gap-free recordings of similar duration where we recorded the post-stimulus 4AP-induced network activity (Post-stim); **(b)** in all stimulation trials, ictal discharges were completely blocked (n = 15). The gap between the stimulation and post-stimulation recordings was 4 s. Following stimulation, the network fully recovers and can generate ictal discharges once again. **B:** The rate of ictal discharges was 0.34 ± 0.04 discharges per min in the control and post-stim recordings and 0.17 ± 0.03 discharges per min in the stim recordings. **C:** The duration of ictal discharges was 70.40 ± 4.49 s in control and 71.35 ± 3.44 s in post-stim conditions (** signifies $p < 0.01$).

Figure 4.4

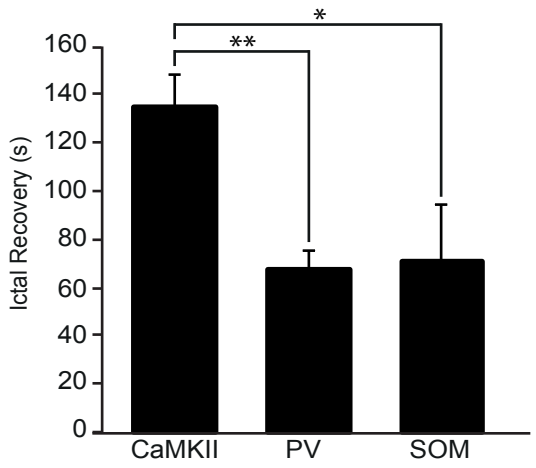

Figure 4.4. Recovery of ictal discharges. Bar graph depicting the average amount of time taken for ictal discharges to reappear following repetitive optogenetic stimulation of CaMKII, PV, or SOM neurons. Note that ictal discharges recovered significantly sooner when interneurons were the target of stimulation (* signifies $p < 0.05$; ** signifies $p < 0.01$).

Figure 4.5

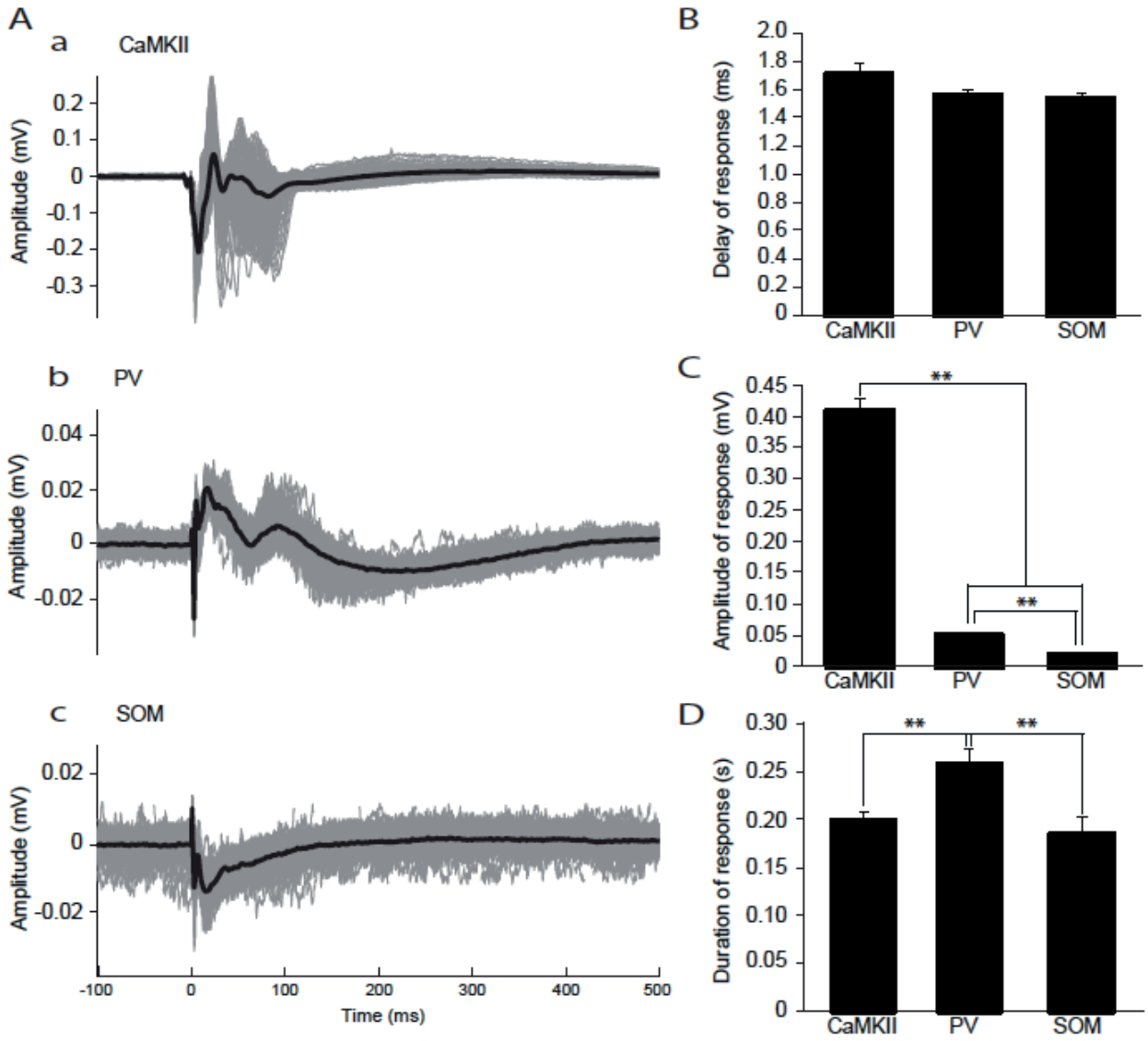
A
a
CaMKII
Amplitude (mV)
0.2
0.1
0
-0.1
-0.2
-0.3
b
PV
Amplitude (mV)
0.04
0.02
0
-0.02
c
SOM
Amplitude (mV)
0.02
0
-0.02
-100
0
100
200
300
400
500
Time (ms)
B
Delay of response (ms)
2.0
1.8
1.6
1.4
1.2
1.0
0.8
0.6
0.4
0.2
0
CaMKII
PV
SOM
C
Amplitude of response (mV)
0.45
0.40
0.35
0.30
0.25
0.20
0.15
0.10
0.05
0
**
**
CaMKII
PV
SOM
D
Duration of response (s)
0.30
0.25
0.20
0.15
0.10
0.05
0
**
**
CaMKII
PV
SOM

Figure 4.5. LFP transients evoked by optogenetic stimulation. A: Overlap (grey traces) and average (black trace) of 180 consecutive field responses to **(a)** CaMKII-cell stimulation, **(b)** PV-cell stimulation, and **(c)** SOM-cell stimulation using 1 ms light pulses. **B:** Bar graph showing the average delay of the field responses measured from the onset of the light pulses. **C:** Bar graph showing the amplitude of field responses evoked by 1 ms light pulses in each group. **D:** Bar graphs showing the duration of optogenetically induced field responses in each group (** signifies $p < 0.01$).

Chapter 5: General Discussion

In this final chapter, I will summarize the main findings reported in my thesis. First, I will discuss the significance of my findings as well as the limitations of the experiments that I have performed. Second, I will define possible directions for future studies.

5.1. Summary of the findings

Contrary to the common, original view that considers a decrease or loss of inhibition as the primary contributor to ictogenesis, many studies have repeatedly demonstrated that GABAergic mechanisms in addition to glutamatergic mechanisms can actively contribute to pathological oscillations and epileptiform activity. Indeed, there is a growing body of evidence that distinct cellular mechanisms and brain regions mediate different seizure onset patterns. My graduate studies were focused on deciphering the contributions of different cell populations to epileptiform activity in the *in vitro* 4AP model using the powerful optogenetic technique. The main findings of my studies can be summarized as follows:

1. In Chapter 2 of this manuscript, I showed that GABA release due to the optogenetic activation of PV-interneurons leads to LVF ictal discharges *in vitro*. First, I demonstrated that during bath application of 4AP, EC neuronal networks generate ictal discharges that are characterized in field recordings by an LVF onset pattern and can occur both spontaneously or be triggered by PV-interneuron activation. Second, I triggered similar events in the whole-cell configuration by optically activating PV-interneurons. Third, I identified patterns of HFO occurrence that were similar during both types of ictal events and were predominated by ripple rates. Finally, I showed that under conditions of

GABAergic neurotransmission blockade, PV-interneuron stimulation could no longer generate ictal discharges.

2. In Chapter 3 of my dissertation, I compared the role of somatic-targeting PV-interneurons and dendritic-targeting SOM-interneurons in the initiation of LVF onset ictal discharges (Freund and Buzsáki, 1996). Interestingly, I found that optogenetic stimulation of either interneuron subtype using the same stimulation paradigm can trigger ictal discharges with LVF onset pattern features. In contrast, ictal discharges triggered by optogenetic stimulation of CaMKII-positive principal cells in the same experimental conditions presented with a HYP onset pattern. Furthermore, whole-cell recordings of a principal cell during 4AP-induced LVF discharges show a brief period of quiescence at ictal onset followed by increased cell firing; in contrast, robust principal cell firing can be recorded at the onset of optogenetically-induced HYP discharges. Finally, I discovered that ripple rates are higher than fast ripple rates at the onset of both spontaneous and optogenetically-induced LVF onset events while fast ripple rates predominate at the onset of optogenetically-induced HYP onset ictal discharges.
3. For the final study of my graduate work, elaborated in Chapter 4 of this thesis, I used an optogenetic approach of LFS in the EC to investigate the role of local interneuron subtypes and for the first time, of principal cells, in the process of stimulus-induced suppression of ictogenesis during application of 4AP. Indeed, I found that using the same experimental parameters, optogenetic LFS of CaMKII-positive principal cells, PV- or SOM-positive interneurons in EC significantly reduced the rate of 4AP-induced ictal discharges. Interestingly, optogenetic stimulation applied to principal cells had a longer

lasting effect in suppressing ictal discharges once stimulation was aborted, as ictal discharges took longer to recur in these experiments.

Collectively, my results demonstrate that under similar experimental conditions (i.e. during 4AP application): (i) the initiation of LVF and of HYP onset seizures in the EC depends on the preponderant involvement of interneuronal and principal cell networks, respectively, and that (ii) optogenetic LFS of either interneurons or principal cells can control 4AP-induced ictogenesis *in vitro*.

5.2. GABAergic network and LVF onset discharges

Ictogenesis has classically been attributed to a shift in the balance between excitatory and inhibitory neuronal activity towards more excitation. However, the mechanisms that underlie this transition to seizure are not well understood. Several studies performed in the 1970s and 1980s have proposed that the initiation of focal seizures depends on weakening or failure of inhibition, a process that should lead to an uncontrolled increase in glutamatergic excitation (Ben-Ari et al., 1979; Avoli and Krnjević, 2016; Ayala et al., 1970; Krnjević et al., 1970). However, subsequent *in vitro* and *in vivo* experiments have shown that GABAergic interneurons are not simply responsible for providing inhibitory control on brain networks (Freund and Buzsáki, 1996); rather, GABAergic inhibitory signals can, paradoxically, favor seizure initiation (Avoli et al., 1996a; Gnatkovsky et al., 2008; Grasse et al., 2013; Schevon et al., 2012; Truccolo et al., 2011).

Evidence gathered in the last three decades suggests that an interplay between principal cells and interneurons is key in the emergence of seizures. Indeed, simultaneous whole-cell recordings of excitatory and inhibitory neurons obtained from rat hippocampal slices *in vitro*

(Ziburkus et al., 2006) and single unit recordings *in vivo* (Toyoda et al., 2015) have shown that both cell types are active at specific time points throughout seizures. However, these patterns of activity may differ between ictal discharges with different onset patterns and this should be considered when administering anti-epileptic drugs (de Curtis and Gnatkovsky, 2009).

Our group has previously shown that the systemic administration of 4AP *in vivo* (Lévesque et al., 2013a) and its bath application *in vitro* (Avoli et al., 2013b) induce LVF type seizures with similar morphological features. Lévesque et al. (2013a) also reported that *in vivo*, 4AP treatment induces sustained and rhythmic runs of theta oscillations that are thought to play a role in ictogenesis (Butuzova and Kitchigina, 2008). These theta oscillations are presumably caused by GABAergic inputs to pyramidal cells as they are abolished by the $GABA_A$ receptor antagonist, picrotoxin (Buzsáki, 2002). Electrophysiological data have also revealed a long-lasting GABAergic potential that reflects the synchronous activity of interneurons at the onset of LVF ictal discharges (Avoli and de Curtis, 2011a).

In Chapters 2 and 3, we showed that GABA release due to the local optogenetic activation of PV or SOM-interneurons in the EC could trigger LVF ictal discharges with similar features as those occurring spontaneously in the presence of 4AP. Strong recruitment of interneurons, and the subsequent activation of postsynaptic $GABA_A$ receptors, can thus lead to epileptiform synchronization and ictogenesis via several mechanisms that result from intracellular Cl^- accumulation and include: (i) a positive shift in Cl^- reversal potential that makes $GABA_A$ receptor signaling excitatory (Khalilov et al., 2005); and (ii) an increase in extracellular $[K^+]$ that is caused by the activity of potassium chloride cotransporter-2 which extrudes both Cl^- and K^+ from the intraneuronal compartments (Viitanen et al., 2010). In addition, it has been

reported that excessive interneuron firing can result in depolarization block (Ziburkus et al., 2006) and perhaps synchronize neuronal populations through rebound excitation (Gnatkovsky et al., 2008; Jefferys et al., 2012d). Therefore, excessive activation of interneurons can very well be sufficient to disrupt the excitation/inhibition balance within the neuronal network thus triggering ictal-like discharges.

5.3. Glutamatergic network and HYP onset discharges

It has been proposed that LVF and HYP seizures depend on the activity of distinct neural networks (Bragin et al., 2009; Lévesque et al., 2012b; Memarian et al., 2015). Accordingly, it has been recently reported that systemic injection of the $GABA_A$ receptor antagonist picrotoxin *in vivo* induces seizures characterized by a HYP onset pattern while seizures induced by 4AP in these experiments are most often characterized by an LVF seizure onset pattern (Salami et al., 2015b). This evidence is in line with *in vitro* work performed on human tissue where it was shown that pyramidal cell firing and therefore, glutamatergic mechanisms herald the onset of HYP seizures (Huberfeld et al., 2011).

The development of optogenetic techniques has allowed researchers to drive specific cell populations with the aim of studying their contributions to seizure initiation in real-time. Indeed, recent work has shown that repetitive optogenetic stimulation of hippocampal CaMKII-positive neurons can evoke seizure-like after-discharges in an anesthetized rat model (Osawa et al., 2013; Weitz et al., 2015). As elaborated in Chapter 3, I have demonstrated that repetitive optogenetic activation of CaMKII-positive principal cells in the EC is sufficient to switch the 4AP-induced LVF onset discharges to HYP onset events supporting the hypothesis

that glutamatergic mechanisms are largely at work in the emergence of these seizure onset types.

My findings thus clearly identify the pivotal involvement of GABAergic interneurons in the initiation and maintenance of LVF seizures and of glutamatergic neurons in the initiation and maintenance of HYP seizures in the limbic system. This information can be of utmost importance in designing more reliable and better-adapted treatments for controlling seizures in MTLE patients, as these two patterns of ictal onset constitute the majority of patterns detected in these patients. It is important to note that HYP onset events make up a very small proportion of spontaneous ictal discharges detected in the *in vitro* 4AP model (but see Köhling et al., 2016), which can potentially limit the translatability of my findings as they are obtained from this very model. However, the broader implication of the study is to demonstrate, using the powerful optogenetic technique, the existence of different mechanisms underlying different ictal onset patterns which have been suggested based on various models of ictogenesis and epileptogenesis. Future studies of these phenomena should pay closer attention to the type(s) of ictal onset pattern(s) generated by the model being used so the results can be interpreted in a clinically meaningful manner.

5.4. Optogenetic LFS hinders ictogenesis

Evidence obtained from rodent models of temporal lobe epilepsy have shown that LFS can reduce both excitability and seizure frequency (Barbarosie and Avoli, 1997; D'Arcangelo et al., 2005; Kile et al., 2010; Rashid et al., 2012). However, it remained unclear whether this effect could be attributed to excitatory or inhibitory neurons or other cells of the central nervous system, as electric stimuli do not discriminate between different cell types. As

described in Chapter 4, I used a novel optogenetic method of low-frequency stimulation in the EC to investigate the role of cortical principal cells or interneurons in disrupting synchronicity and reducing seizure activity in the 4AP model *in vitro*. This approach was used as an analogue to the classical electrical stimulation techniques used to control ictogenesis, with the advantage of cell-type specificity to allow a closer examination of the mechanisms involved in LFS-mediated network suppression.

Using this approach, I found that 4AP-induced ictogenicity in EC is depressed by repetitive stimulation of interneurons using 1 ms pulses at 1 Hz. These results are in line with previous *in vitro* studies where it was shown that electrical stimuli (Barbarosie and Avoli, 1997; Barbarosie et al., 2002; Benini et al., 2003) and optogenetic stimuli in different limbic areas (Krook-Magnuson et al., 2013; Ladas et al., 2015; Ledri et al., 2014) delivered at low frequencies can reduce and block ictal discharge generation. The novel finding of my study however, is that low frequency stimulation of principal cells in the EC is also effective in temporarily blocking ictal discharges.

It may seem untenable that repeated stimulation of both principal cells and interneurons can play a protective role against ictal discharge generation. However, the common feature in these experiments is that we are increasing neuronal spatial synchrony by stimulating at low frequencies and thus protecting against ictogenesis (Schindler et al., 2007; Timofeev and Steriade, 2004). Selective activation of interneuron subtypes or principal cells induces rebound or direct excitatory bursting in the principal cell network thus causing entrainment and consequently an overall suppression of hyperactivity (Ladas et al., 2015). Furthermore, previous studies have shown that repetitive stimulation can restrain ictal discharge generation in EC by clamping GABA-mediated potentials that lead to large elevations in extracellular

potassium levels which can then initiate ictal discharges (Barbarosie et al., 2002; Eng and Kocsis, 1987). These transient increases in extracellular potassium due to $GABA_A$ receptor activation can be reproduced theoretically with any of the three procedures used in this study, either directly (through interneuron stimulation) or indirectly (through principal cell stimulation).

I have discovered that LFS of specific cell populations, principal cells or interneuron subtypes, can reliably shorten or delay seizures *in vitro* presumably by disrupting synchronicity. It remains unclear whether these stimulation paradigms can control ictogenesis when applied to other *in vitro* models and more importantly whether low-frequency optogenetic stimulation can modulate ictogenesis and epileptogenesis in *in vivo* models. However, this work suggests that optogenetic LFS targeting a single cell population at a time can address the limitations of classic LFS techniques and may thus constitute a more reliable means for controlling seizures in patients that present with focal seizures.

5.5. Concluding remarks

My findings clearly identify the pivotal involvement of GABAergic interneurons in the initiation and maintenance of LVF seizures and glutamatergic neurons in the initiation and maintenance of HYP seizures in the limbic system. Furthermore, using a different stimulation paradigm in the same model, I demonstrated the ability of optogenetic LFS of either interneurons or principal cells to control ictogenesis and to reduce the overall rate of ictal discharges. Combining these results could help identify more efficacious antiepileptic strategies aimed specifically at targeting GABAergic or glutamatergic neuronal networks. In MTLE, seizure activity starts in a restricted region of the brain before evolving to the

convulsive stage where the seizure manifests itself. This delayed progression provides a time window for intervention before seizure onset. If the early seizure activity is detected, one could optogenetically manipulate principal cells or interneurons to balance the network in real-time and thus to potentially prevent seizure generation.

The *in vitro* slice preparation is a powerful tool that allows electrophysiologists to study specific circuits and brain networks while controlling various experimental parameters, visualizing brain structures, and applying pharmacological agents. In this way, experiments conducted in brain slices allow a researcher to think outside the box and freely manipulate a relatively steady setup. However, the brain slice preparation is undeniably oversimplified and cannot be directly compared to *in vivo* models. First, the brain network under study is incomplete and many projections are severed in this configuration. Second, slicing procedures can be damaging to the tissue. Third, the artificial cerebrospinal fluid used to maintain these slices *in vitro* do not mimic all the components of the natural milieu of the brain. Therefore, the results obtained using this model and those presented in this thesis need to be confirmed in other *in vitro* models, or better yet, in *in vivo* models using an intact brain in its natural environment.

Nevertheless, my findings have helped clarify the mechanisms and neural connections involved in generating different patterns of ictal activity and can aid in establishing better treatments for epilepsy. In addition, paying attention to seizure onset patterns can potentially lead to more efficacious anti-epileptic drugs and thus reduce the amount of trial and error involved in this process. Alternatively, in the long run, the identification of optogenetic stimulation protocols capable of influencing ictogenesis and epileptogenesis represents a new window to the treatment of epilepsy. Although translating these results to humans is presently

a distant reality, on-going advancements in the development of optogenetic approaches suggests that such strategies might not be unlikely in the future.

References

Aivar, P., Valero, M., Bellistri, E., and Prida, L.M. de la (2014). Extracellular Calcium Controls the Expression of Two Different Forms of Ripple-Like Hippocampal Oscillations. J. Neurosci. *34*, 2989–3004.

Alarcon, G., Binnie, C.D., Elwes, R.D., and Polkey, C.E. (1995). Power spectrum and intracranial EEG patterns at seizure onset in partial epilepsy. Electroencephalogr. Clin. Neurophysiol. *94*, 326–337.

Alger, B.E., and Nicoll, R.A. (1982). Pharmacological evidence for two kinds of GABA receptor on rat hippocampal pyramidal cells studied in vitro. J. Physiol. *328*, 125–141.

Amaral, D.G., Insausti, R., and Cowan, W.M. (1987). The entorhinal cortex of the monkey: I. Cytoarchitectonic organization. J. Comp. Neurol. *264*, 326–355.

Andersen, P., Dingledine, R., Gjerstad, L., Langmoen, I.A., and Laursen, A.M. (1980). Two different responses of hippocampal pyramidal cells to application of gamma-amino butyric acid. J. Physiol. *305*, 279–296.

Avoli, M. (1996). GABA-mediated synchronous potentials and seizure generation. Epilepsia *37*, 1035–1042.

Avoli, M. (2013). Mechanisms of Epileptiform Synchronization in Cortical Neuronal Networks. Curr. Med. Chem.

Avoli, M., and de Curtis, M. (2011a). GABAergic synchronization in the limbic system and its role in the generation of epileptiform activity. Prog. Neurobiol. *95*, 104–132.

Avoli, M., and de Curtis, M. (2011b). GABAergic synchronization in the limbic system and its role in the generation of epileptiform activity. Prog. Neurobiol. *95*, 104–132.

Avoli, M., and Krnjević, K. (2016). The Long and Winding Road to Gamma-Amino-Butyric Acid as Neurotransmitter. Can. J. Neurol. Sci. *43*, 219–226.

Avoli, M., Barbarosie, M., Lücke, A., Nagao, T., Lopantsev, V., and Köhling, R. (1996a). Synchronous GABA-Mediated Potentials and Epileptiform Discharges in the Rat Limbic System In Vitro. J. Neurosci. *16*, 3912–3924.

Avoli, M., Louvel, J., Kurcewicz, I., Pumain, R., and Barbarosie, M. (1996b). Extracellular free potassium and calcium during synchronous activity induced by 4-aminopyridine in the juvenile rat hippocampus. J. Physiol. *493 (Pt 3)*, 707–717.

Avoli, M., de Curtis, M., and Köhling, R. (2013a). Does interictal synchronization influence ictogenesis? Neuropharmacology *69*, 37–44.

Avoli, M., Panuccio, G., Herrington, R., D'Antuono, M., de Guzman, P., and Lévesque, M. (2013b). Two different interictal spike patterns anticipate ictal activity in vitro. Neurobiol. Dis. *52*, 168–176.

Ayala, G.F., Matsumoto, H., and Gumnit, R.J. (1970). Excitability changes and inhibitory mechanisms in neocortical neurons during seizures. J. Neurophysiol. *33*, 73–85.

Ayala, G.F., Dichter, M., Gumnit, R.J., Matsumoto, H., and Spencer, W.A. (1973). Genesis of epileptic interictal spikes. New knowledge of cortical feedback systems suggests a neurophysiological explanation of brief paroxysms. Brain Res. *52*, 1–17.

Barbarosie, M., and Avoli, M. (1997). CA3-driven hippocampal-entorhinal loop controls rather than sustains in vitro limbic seizures. J. Neurosci. Off. J. Soc. Neurosci. *17*, 9308–9314.

Barbarosie, M., Louvel, J., D'Antuono, M., Kurcewicz, I., and Avoli, M. (2002). Masking synchronous GABA-mediated potentials controls limbic seizures. Epilepsia *43*, 1469–1479.

Barolet, A.W., and Morris, M.E. (1991). Changes in extracellular K+ evoked by GABA, THIP and baclofen in the guinea-pig hippocampal slice. Exp. Brain Res. *84*, 591–598.

Bartolomei, F., Wendling, F., Régis, J., Gavaret, M., Guye, M., and Chauvel, P. (2004). Pre-ictal synchronicity in limbic networks of mesial temporal lobe epilepsy. Epilepsy Res. *61*, 89–104.

Behr, C., D'Antuono, M., Hamidi, S., Herrington, R., Lévesque, M., Salami, P., Shiri, Z., Köhling, R., and Avoli, M. (2014). Limbic networks and epileptiform synchronization: the view from the experimental side. Int. Rev. Neurobiol. *114*, 63–87.

Beierlein, M., Gibson, J.R., and Connors, B.W. (2000). A network of electrically coupled interneurons drives synchronized inhibition in neocortex. Nat. Neurosci. *3*, 904–910.

Ben-Ari, Y., Krnjević, K., and Reinhardt, W. (1979). Hippocampal seizures and failure of inhibition. Can J Physiol Pharmacol *57*, 1462–1466.

Bénar, C.G., Chauvière, L., Bartolomei, F., and Wendling, F. (2010). Pitfalls of high-pass filtering for detecting epileptic oscillations: a technical note on "false" ripples. Clin. Neurophysiol. Off. J. Int. Fed. Clin. Neurophysiol. *121*, 301–310.

Benini, R., D'Antuono, M., Pralong, E., and Avoli, M. (2003). Involvement of amygdala networks in epileptiform synchronization in vitro. Neuroscience *120*, 75–84.

Blümcke, I., Thom, M., and Wiestler, O.D. (2002). Ammon's horn sclerosis: a maldevelopmental disorder associated with temporal lobe epilepsy. Brain Pathol. Zurich Switz. *12*, 199–211.

Blume, W.T., and Parrent, A.G. (2006). Assessment of patients with intractable epilepsy for surgery. Adv. Neurol. *97*, 537–548.

Boido, D., Jesuthasan, N., de Curtis, M., and Uva, L. (2014). Network dynamics during the progression of seizure-like events in the hippocampal-parahippocampal regions. Cereb. Cortex N. Y. N 1991 *24*, 163–173.

Bonilha, L., Kobayashi, E., Rorden, C., Cendes, F., and Li, L.M. (2003). Medial temporal lobe atrophy in patients with refractory temporal lobe epilepsy. J. Neurol. Neurosurg. Psychiatry *74*, 1627–1630.

Boyden, E.S., Zhang, F., Bamberg, E., Nagel, G., and Deisseroth, K. (2005). Millisecond-timescale, genetically targeted optical control of neural activity. Nat. Neurosci. *8*, 1263–1268.

Bragdon, A.C., Kojima, H., and Wilson, W.A. (1992). Suppression of interictal bursting in hippocampus unleashes seizures in entorhinal cortex: a proepileptic effect of lowering [K+]o and raising [Ca2+]o. Brain Res. *590*, 128–135.

Bragin, A., Engel, J., Jr, Wilson, C.L., Vizentin, E., and Mathern, G.W. (1999a). Electrophysiologic analysis of a chronic seizure model after unilateral hippocampal KA injection. Epilepsia *40*, 1210–1221.

Bragin, A., Engel, J., Jr, Wilson, C.L., Vizentin, E., and Mathern, G.W. (1999b). Electrophysiologic analysis of a chronic seizure model after unilateral hippocampal KA injection. Epilepsia *40*, 1210–1221.

Bragin, A., Azizyan, A., Almajano, J., Wilson, C.L., and Engel, J., Jr (2005a). Analysis of chronic seizure onsets after intrahippocampal kainic acid injection in freely moving rats. Epilepsia *46*, 1592–1598.

Bragin, A., Azizyan, A., Almajano, J., Wilson, C.L., and Engel, J. (2005b). Analysis of chronic seizure onsets after intrahippocampal kainic acid injection in freely moving rats. Epilepsia *46*, 1592–1598.

Bragin, A., Azizyan, A., Almajano, J., and Engel, J. (2009). The cause of the imbalance in the neuronal network leading to seizure activity can be predicted by the electrographic pattern of the seizure onset. J. Neurosci. Off. J. Soc. Neurosci. *29*, 3660–3671.

Bragin, A., Benassi, S.K., Kheiri, F., and Engel Jr., J. (2011). Further evidence that pathologic high-frequency oscillations are bursts of population spikes derived from recordings of identified cells in dentate gyrus. Epilepsia *52*, 45–52.

Brodie, M.J. (2010). Antiepileptic drug therapy the story so far. Seizure *19*, 650–655.

Bui, A.D., Alexander, A., and Soltesz, I. (2015). Seizing Control: From Current Treatments to Optogenetic Interventions in Epilepsy. The Neuroscientist.

Butuzova, M.V., and Kitchigina, V.F. (2008). Repeated blockade of GABAA receptors in the medial septal region induces epileptiform activity in the hippocampus. Neurosci. Lett. *434*, 133–138.

Buzsáki, G. (2002). Theta Oscillations in the Hippocampus. Neuron *33*, 325–340.

Buzsáki, G., and Chrobak, J.J. (1995). Temporal structure in spatially organized neuronal ensembles: a role for interneuronal networks. Curr. Opin. Neurobiol. *5*, 504–510.

Buzsáki, G., and Draguhn, A. (2004). Neuronal oscillations in cortical networks. Science *304*, 1926–1929.

Buzsáki, G., Horváth, Z., Urioste, R., Hetke, J., and Wise, K. (1992). High-frequency network oscillation in the hippocampus. Science *256*, 1025–1027.

Canto, C.B., Wouterlood, F.G., and Witter, M.P. (2008). What Does the Anatomical Organization of the Entorhinal Cortex Tell Us? Neural Plast. *2008*, e381243.

Capogna, M., Gähwiler, B.H., and Thompson, S.M. (1993). Mechanism of mu-opioid receptor-mediated presynaptic inhibition in the rat hippocampus in vitro. J. Physiol. *470*, 539–558.

Chen, L.-L., Feng, H.-F., Mao, X.-X., Ye, Q., and Zeng, L.-H. (2013). One hour of pilocarpine-induced status epilepticus is sufficient to develop chronic epilepsy in mice, and is associated with mossy fiber sprouting but not neuronal death. Neurosci. Bull. *29*, 295–302.

Choy, M., Duffy, B.A., and Lee, J.H. (2016). Optogenetic study of networks in epilepsy. J. Neurosci. Res.

Chrobak, J.J., and Buzsáki, G. (1996). High-frequency oscillations in the output networks of the hippocampal-entorhinal axis of the freely behaving rat. J. Neurosci. Off. J. Soc. Neurosci. *16*, 3056–3066.

Curia, G., Longo, D., Biagini, G., Jones, R.S.G., and Avoli, M. (2008). The pilocarpine model of temporal lobe epilepsy. J. Neurosci. Methods *172*, 143–157.

De Curtis, M., and Avanzini, G. (2001). Interictal spikes in focal epileptogenesis. Prog. Neurobiol. *63*, 541–567.

De Curtis, M., and Avoli, M. (2016). GABAergic networks jump-start focal seizures. Epilepsia *57*, 679–687.

De Curtis, M., and Gnatkovsky, V. (2009). Reevaluating the mechanisms of focal ictogenesis: The role of low-voltage fast activity. Epilepsia *50*, 2514–2525.

D'Arcangelo, G., Panuccio, G., Tancredi, V., and Avoli, M. (2005). Repetitive low-frequency stimulation reduces epileptiform synchronization in limbic neuronal networks. Neurobiol. Dis. *19*, 119–128.

DeFelipe, J., López-Cruz, P.L., Benavides-Piccione, R., Bielza, C., Larrañaga, P., Anderson, S., Burkhalter, A., Cauli, B., Fairén, A., Feldmeyer, D., et al. (2013). New insights into the classification and nomenclature of cortical GABAergic interneurons. Nat. Rev. Neurosci. *14*, 202–216.

Deisseroth, K. (2015). Optogenetics: 10 years of microbial opsins in neuroscience. Nat. Neurosci. *18*, 1213–1225.

Derchansky, M., Jahromi, S.S., Mamani, M., Shin, D.S., Sik, A., and Carlen, P.L. (2008). Transition to seizures in the isolated immature mouse hippocampus: a switch from dominant phasic inhibition to dominant phasic excitation. J. Physiol. *586*, 477–494.

Drexel, M., Preidt, A.P., and Sperk, G. (2012). Sequel of spontaneous seizures after kainic acid-induced status epilepticus and associated neuropathological changes in the subiculum and entorhinal cortex. Neuropharmacology *63*, 806–817.

Du, F., Eid, T., Lothman, E.W., Köhler, C., and Schwarcz, R. (1995). Preferential neuronal loss in layer III of the medial entorhinal cortex in rat models of temporal lobe epilepsy. J. Neurosci. Off. J. Soc. Neurosci. *15*, 6301–6313.

Duncan, J.S., Sander, J.W., Sisodiya, S.M., and Walker, M.C. (2006). Adult epilepsy. Lancet Lond. Engl. *367*, 1087–1100.

Dzhala, V.I., and Staley, K.J. (2003). Transition from Interictal to Ictal Activity in Limbic Networks In Vitro. J. Neurosci. *23*, 7873–7880.

Dzhala, V.I., and Staley, K.J. (2004). Mechanisms of fast ripples in the hippocampus. J. Neurosci. Off. J. Soc. Neurosci. *24*, 8896–8906.

Ellender, T.J., Raimondo, J.V., Irkle, A., Lamsa, K.P., and Akerman, C.J. (2014). Excitatory effects of parvalbumin-expressing interneurons maintain hippocampal epileptiform activity via synchronous afterdischarges. J. Neurosci. Off. J. Soc. Neurosci. *34*, 15208–15222.

Eng, D.L., and Kocsis, J.D. (1987). Activity-dependent changes in extracellular potassium and excitability in turtle olfactory nerve. J. Neurophysiol. *57*, 740–754.

Engel, J., Jr (2001). Mesial temporal lobe epilepsy: what have we learned? Neurosci. Rev. J. Bringing Neurobiol. Neurol. Psychiatry *7*, 340–352.

Engel, J., Jr (2005). Natural History of Mesial Temporal Lobe Epilepsy with Hippocampal Sclerosis. In Kindling 6, M.E. Corcoran, and S.L. Moshé, eds. (Springer US), pp. 371–384.

Engel, J., and Ackermann, R.F. (1980). Interictal EEG spikes correlate with decreased, rather than increased, epileptogenicity in amygdaloid kindled rats. Brain Res. *190*, 543–548.

Engel, J., Jr, and da Silva, F.L. (2012). High-frequency oscillations - where we are and where we need to go. Prog. Neurobiol. *98*, 316–318.

Engel, J., Pedley, T.A., and Aicardi, J. (2008). Epilepsy: A Comprehensive Textbook (Lippincott Williams & Wilkins).

Engel, J., Jr, Bragin, A., Staba, R., and Mody, I. (2009a). High-frequency oscillations: what is normal and what is not? Epilepsia *50*, 598–604.

Engel, J., Jr, Bragin, A., Staba, R., and Mody, I. (2009b). High-frequency oscillations: what is normal and what is not? Epilepsia *50*, 598–604.

Fisher, R.S., and Velasco, A.L. (2014). Electrical brain stimulation for epilepsy. Nat. Rev. Neurol. *10*, 261–270.

Foffani, G., Uzcategui, Y.G., Gal, B., and Menendez de la Prida, L. (2007). Reduced Spike-Timing Reliability Correlates with the Emergence of Fast Ripples in the Rat Epileptic Hippocampus. Neuron *55*, 930–941.

Freund, T.F., and Buzsáki, G. (1996). Interneurons of the hippocampus. Hippocampus *6*, 347–470.

Gelinas, J.N., Khodagholy, D., Thesen, T., Devinsky, O., and Buzsáki, G. (2016). Interictal epileptiform discharges induce hippocampal-cortical coupling in temporal lobe epilepsy. Nat. Med. *22*, 641–648.

Gloor, P. (1990). Experiential Phenomena of Temporal Lobe Epilepsy Facts and Hypotheses. Brain *113*, 1673–1694.

Gloor, P. (1997). The temporal lobe and limbic system (New York: Oxford University Press).

Gnatkovsky, V., Librizzi, L., Trombin, F., and de Curtis, M. (2008). Fast activity at seizure onset is mediated by inhibitory circuits in the entorhinal cortex in vitro. Ann. Neurol. *64*, 674–686.

Grasse, D.W., Karunakaran, S., and Moxon, K.A. (2013). Neuronal synchrony and the transition to spontaneous seizures. Exp. Neurol. *248*, 72–84.

De Guzman, P., Inaba, Y., Baldelli, E., de Curtis, M., Biagini, G., and Avoli, M. (2008). Network hyperexcitability within the deep layers of the pilocarpine-treated rat entorhinal cortex. J. Physiol. *586*, 1867–1883.

Huberfeld, G., Menendez de la Prida, L., Pallud, J., Cohen, I., Le Van Quyen, M., Adam, C., Clemenceau, S., Baulac, M., and Miles, R. (2011). Glutamatergic pre-ictal discharges emerge at the transition to seizure in human epilepsy. Nat. Neurosci. *14*, 627–634.

Ibarz, J.M., Foffani, G., Cid, E., Inostroza, M., and Menendez de la Prida, L. (2010). Emergent Dynamics of Fast Ripples in the Epileptic Hippocampus. J. Neurosci. *30*, 16249–16261.

Insausti, R., Tuñón, T., Sobreviela, T., Insausti, A.M., and Gonzalo, L.M. (1995). The human entorhinal cortex: a cytoarchitectonic analysis. J. Comp. Neurol. *355*, 171–198.

Jacobs, J., LeVan, P., Chander, R., Hall, J., Dubeau, F., and Gotman, J. (2008). Interictal high-frequency oscillations (80-500 Hz) are an indicator of seizure onset areas independent of spikes in the human epileptic brain. Epilepsia *49*, 1893–1907.

Jacobs, J., Zelmann, R., Jirsch, J., Chander, R., Dubeau, C.-E.C.F., and Gotman, J. (2009). High frequency oscillations (80-500 Hz) in the preictal period in patients with focal seizures. Epilepsia *50*, 1780–1792.

Jacobs, J., Staba, R., Asano, E., Otsubo, H., Wu, J.Y., Zijlmans, M., Mohamed, I., Kahane, P., Dubeau, F., Navarro, V., et al. (2012). High-frequency oscillations (HFOs) in clinical epilepsy. Prog. Neurobiol. *98*, 302–315.

Jallon, P. (1997). The problem of intractability: the continuing need for new medical therapies in epilepsy. Epilepsia *38 Suppl 9*, S37–S42.

Jefferys, J.G. (1995). Nonsynaptic modulation of neuronal activity in the brain: electric currents and extracellular ions. Physiol. Rev. *75*, 689–723.

Jefferys, J.G., and Haas, H.L. (1982). Synchronized bursting of CA1 hippocampal pyramidal cells in the absence of synaptic transmission. Nature *300*, 448–450.

Jefferys, J.G.R., Jiruska, P., de Curtis, M., and Avoli, M. (2012a). Limbic Network Synchronization and Temporal Lobe Epilepsy. In Jasper's Basic Mechanisms of the Epilepsies, J.L. Noebels, M. Avoli, M.A. Rogawski, R.W. Olsen, and A.V. Delgado-Escueta, eds. (Bethesda (MD): National Center for Biotechnology Information (US)),.

Jefferys, J.G.R., Menendez de la Prida, L., Wendling, F., Bragin, A., Avoli, M., Timofeev, I., and Lopes da Silva, F.H. (2012b). Mechanisms of physiological and epileptic HFO generation. Prog. Neurobiol. *98*, 250–264.

Jefferys, J.G.R., Menendez de la Prida, L., Wendling, F., Bragin, A., Avoli, M., Timofeev, I., and Lopes da Silva, F.H. (2012c). Mechanisms of physiological and epileptic HFO generation. Prog. Neurobiol. *98*, 250–264.

Jefferys, J.G.R., Jiruska, P., de Curtis, M., and Avoli, M. (2012d). Limbic Network Synchronization and Temporal Lobe Epilepsy. In Jasper's Basic Mechanisms of the Epilepsies, J.L. Noebels, M. Avoli, M.A. Rogawski, R.W. Olsen, and A.V. Delgado-Escueta, eds. (Bethesda (MD): National Center for Biotechnology Information (US)),.

Jensen, M.S., and Yaari, Y. (1988). The relationship between interictal and ictal paroxysms in an in vitro model of focal hippocampal epilepsy. Ann. Neurol. *24*, 591–598.

Jiruska, P., Powell, A.D., Chang, W.-C., and Jefferys, J.G.R. (2010a). Electrographic high-frequency activity and epilepsy. Epilepsy Res. *89*, 60–65.

Jiruska, P., Csicsvari, J., Powell, A.D., Fox, J.E., Chang, W.-C., Vreugdenhil, M., Li, X., Palus, M., Bujan, A.F., Dearden, R.W., et al. (2010b). High-frequency network activity, global increase in neuronal activity, and synchrony expansion precede epileptic seizures in vitro. J. Neurosci. Off. J. Soc. Neurosci. *30*, 5690–5701.

Jiruska, P., Finnerty, G.T., Powell, A.D., Lofti, N., Cmejla, R., and Jefferys, J.G.R. (2010c). Epileptic high-frequency network activity in a model of non-lesional temporal lobe epilepsy. Brain J. Neurol. *133*, 1380–1390.

Jiruska, P., de Curtis, M., Jefferys, J.G.R., Schevon, C.A., Schiff, S.J., and Schindler, K. (2013). Synchronization and desynchronization in epilepsy: controversies and hypotheses. J. Physiol. *591*, 787–797.

Jones, R.S., and Lambert, J.D. (1990). Synchronous discharges in the rat entorhinal cortex in vitro: site of initiation and the role of excitatory amino acid receptors. Neuroscience *34*, 657–670.

Jung, K.-H., Chu, K., Lee, S.-T., Kim, J.-H., Kang, K.-M., Song, E.-C., Kim, S.-J., Park, H.-K., Kim, M., Lee, S.K., et al. (2009). Region-specific plasticity in the epileptic rat brain: a hippocampal and extrahippocampal analysis. Epilepsia *50*, 537–549.

Khalilov, I., Le Van Quyen, M., Gozlan, H., and Ben-Ari, Y. (2005). Epileptogenic actions of GABA and fast oscillations in the developing hippocampus. Neuron *48*, 787–796.

Khosravani, H., Pinnegar, C.R., Mitchell, J.R., Bardakjian, B.L., Federico, P., and Carlen, P.L. (2005). Increased high-frequency oscillations precede in vitro low-Mg seizures. Epilepsia *46*, 1188–1197.

Kile, K.B., Tian, N., and Durand, D.M. (2010). Low frequency stimulation decreases seizure activity in a mutation model of epilepsy. Epilepsia *51*, 1745–1753.

Köhling, R., D'Antuono, M., Benini, R., de Guzman, P., and Avoli, M. (2016). Hypersynchronous ictal onset in the perirhinal cortex results from dynamic weakening in inhibition. Neurobiol. Dis. *87*, 1–10.

Kokaia, M., Andersson, M., and Ledri, M. (2013). An optogenetic approach in epilepsy. Neuropharmacology *69*, 89–95.

Krnjević, K., Reiffenstein, R.J., and Silver, A. (1970). Inhibition and paroxysmal activity in long-isolated cortical slabs. Electroencephalogr. Clin. Neurophysiol. *29*, 283–294.

Krook-Magnuson, E., Armstrong, C., Oijala, M., and Soltesz, I. (2013). On-demand optogenetic control of spontaneous seizures in temporal lobe epilepsy. Nat. Commun. *4*, 1376.

Kumar, S.S., and Buckmaster, P.S. (2006). Hyperexcitability, interneurons, and loss of GABAergic synapses in entorhinal cortex in a model of temporal lobe epilepsy. J. Neurosci. Off. J. Soc. Neurosci. *26*, 4613–4623.

Ladas, T.P., Chiang, C.-C., Gonzalez-Reyes, L.E., Nowak, T., and Durand, D.M. (2015). Seizure reduction through interneuron-mediated entrainment using low frequency optical stimulation. Exp. Neurol. *269*, 120–132.

Ledri, M., Madsen, M.G., Nikitidou, L., Kirik, D., and Kokaia, M. (2014). Global optogenetic activation of inhibitory interneurons during epileptiform activity. J. Neurosci. Off. J. Soc. Neurosci. *34*, 3364–3377.

Lévesque, M., and Avoli, M. (2013). The kainic acid model of temporal lobe epilepsy. Neurosci. Biobehav. Rev. *37*, 2887–2899.

Lévesque, M., Salami, P., Gotman, J., and Avoli, M. (2012a). Two seizure-onset types reveal specific patterns of high-frequency oscillations in a model of temporal lobe epilepsy. J. Neurosci. *32*, 13264–13272.

Lévesque, M., Salami, P., Gotman, J., and Avoli, M. (2012b). Two seizure-onset types reveal specific patterns of high-frequency oscillations in a model of temporal lobe epilepsy. J. Neurosci. Off. J. Soc. Neurosci. *32*, 13264–13272.

Lévesque, M., Salami, P., Behr, C., and Avoli, M. (2013a). Temporal lobe epileptiform activity following systemic administration of 4-aminopyridine in rats. Epilepsia *54*, 596–604.

Lévesque, M., Salami, P., Behr, C., and Avoli, M. (2013b). Temporal lobe epileptiform activity following systemic administration of 4-aminopyridine in rats. Epilepsia *54*, 596–604.

Lillis, K.P., Kramer, M.A., Mertz, J., Staley, K.J., and White, J.A. (2012). Pyramidal cells accumulate chloride at seizure onset. Neurobiol. Dis. *47*, 358–366.

Lopantsev, V., and Avoli, M. (1998). Participation of GABAA-Mediated Inhibition in Ictallike Discharges in the Rat Entorhinal Cortex. J. Neurophysiol. *79*, 352–360.

Mann, E.O., and Mody, I. (2008). The multifaceted role of inhibition in epilepsy: seizure-genesis through excessive GABAergic inhibition in autosomal dominant nocturnal frontal lobe epilepsy. Curr. Opin. Neurol. *21*, 155–160.

McCormick, D.A., Connors, B.W., Lighthall, J.W., and Prince, D.A. (1985). Comparative electrophysiology of pyramidal and sparsely spiny stellate neurons of the neocortex. J. Neurophysiol. *54*, 782–806.

McNamara, J.O. (1994). Cellular and molecular basis of epilepsy. J. Neurosci. Off. J. Soc. Neurosci. *14*, 3413–3425.

Memarian, N., Madsen, S.K., Macey, P.M., Fried, I., Engel, J., Thompson, P.M., and Staba, R.J. (2015). Ictal depth EEG and MRI structural evidence for two different epileptogenic networks in mesial temporal lobe epilepsy. PloS One *10*, e0123588.

Menendez de la Prida, L., and Trevelyan, A.J. (2011). Cellular mechanisms of high frequency oscillations in epilepsy: On the diverse sources of pathological activities. Epilepsy Res. *97*, 308–317.

Misgeld, U., Deisz, R.A., Dodt, H.U., and Lux, H.D. (1986). The role of chloride transport in postsynaptic inhibition of hippocampal neurons. Science *232*, 1413–1415.

Mormann, F., Kreuz, T., Andrzejak, R.G., David, P., Lehnertz, K., and Elger, C.E. (2003). Epileptic seizures are preceded by a decrease in synchronization. Epilepsy Res. *53*, 173–185.

Morris, M.E., Obrocea, G.V., and Avoli, M. (1996). Extracellular K+ accumulations and synchronous GABA-mediated potentials evoked by 4-aminopyridine in the adult rat hippocampus. Exp. Brain Res. *109*, 71–82.

Nagel, G., Ollig, D., Fuhrmann, M., Kateriya, S., Musti, A.M., Bamberg, E., and Hegemann, P. (2002). Channelrhodopsin-1: a light-gated proton channel in green algae. Science *296*, 2395–2398.

Nune, G., DeGiorgio, C., and Heck, C. (2015). Neuromodulation in the Treatment of Epilepsy. Curr. Treat. Options Neurol. *17*, 375.

Ogren, J.A., Wilson, C.L., Bragin, A., Lin, J.J., Salamon, N., Dutton, R.A., Luders, E., Fields, T.A., Fried, I., Toga, A.W., et al. (2009a). Three-dimensional surface maps link

local atrophy and fast ripples in human epileptic hippocampus. Ann. Neurol. *66*, 783–791.

Ogren, J.A., Wilson, C.L., Bragin, A., Lin, J.J., Salamon, N., Dutton, R.A., Luders, E., Fields, T.A., Fried, I., Toga, A.W., et al. (2009b). Three-dimensional surface maps link local atrophy and fast ripples in human epileptic hippocampus. Ann. Neurol. *66*, 783–791.

Osawa, S.-I., Iwasaki, M., Hosaka, R., Matsuzaka, Y., Tomita, H., Ishizuka, T., Sugano, E., Okumura, E., Yawo, H., Nakasato, N., et al. (2013). Optogenetically induced seizure and the longitudinal hippocampal network dynamics. PloS One *8*, e60928.

Pacia, S.V., and Ebersole, J.S. (1997). Intracranial EEG substrates of scalp ictal patterns from temporal lobe foci. Epilepsia *38*, 642–654.

Panuccio, G., Sanchez, G., Lévesque, M., Salami, P., de Curtis, M., and Avoli, M. (2012). On the ictogenic properties of the piriform cortex in vitro. Epilepsia *53*, 459–468.

Perreault, P., and Avoli, M. (1991). Physiology and pharmacology of epileptiform activity induced by 4-aminopyridine in rat hippocampal slices. J. Neurophysiol. *65*, 771–785.

Perreault, P., and Avoli, M. (1992). 4-aminopyridine-induced epileptiform activity and a GABA-mediated long-lasting depolarization in the rat hippocampus. J. Neurosci. Off. J. Soc. Neurosci. *12*, 104–115.

Perucca, P., Dubeau, F., and Gotman, J. (2014). Intracranial electroencephalographic seizure-onset patterns: effect of underlying pathology. Brain *137*, 183–196.

Pitkänen, A., and Sutula, T.P. (2002). Is epilepsy a progressive disorder? Prospects for new therapeutic approaches in temporal-lobe epilepsy. Lancet Neurol. *1*, 173–181.

Rashid, S., Pho, G., Czigler, M., Werz, M.A., and Durand, D.M. (2012). Low frequency stimulation of ventral hippocampal commissures reduces seizures in a rat model of chronic temporal lobe epilepsy. Epilepsia *53*, 147–156.

Rutecki, P.A., Grossman, R.G., Armstrong, D., and Irish-Loewen, S. (1989). Electrophysiological connections between the hippocampus and entorhinal cortex in patients with complex partial seizures. J. Neurosurg. *70*, 667–675.

Salami, P., Lévesque, M., Gotman, J., and Avoli, M. (2015a). Distinct EEG seizure patterns reflect different seizure generation mechanisms. J. Neurophysiol. *113*, 2840–2844.

Salami, P., Lévesque, M., Gotman, J., and Avoli, M. (2015b). Distinct EEG seizure patterns reflect different seizure generation mechanisms. J. Neurophysiol. jn.00031.2015.

Schevon, C.A., Weiss, S.A., McKhann, G., Goodman, R.R., Yuste, R., Emerson, R.G., and Trevelyan, A.J. (2012). Evidence of an inhibitory restraint of seizure activity in humans. Nat. Commun. *3*, 1060.

Schindler, K., Elger, C.E., and Lehnertz, K. (2007). Increasing synchronization may promote seizure termination: evidence from status epilepticus. Clin. Neurophysiol. Off. J. Int. Fed. Clin. Neurophysiol. *118*, 1955–1968.

Scholl, E.A., Dudek, F.E., and Ekstrand, J.J. (2013). Neuronal degeneration is observed in multiple regions outside the hippocampus after lithium pilocarpine-induced status epilepticus in the immature rat. Neuroscience *252*, 45–59.

Schwartzkroin, P.A. (1975). Characteristics of CA1 neurons recorded intracellularly in the hippocampal in vitro slice preparation. Brain Res. *85*, 423–436.

Sewards, T.V., and Sewards, M.A. (2003). Input and output stations of the entorhinal cortex: superficial vs. deep layers or lateral vs. medial divisions? Brain Res. Brain Res. Rev. *42*, 243–251.

Shiri, Z., Manseau, F., Lévesque, M., Williams, S., and Avoli, M. (2015). Interneuron activity leads to initiation of low-voltage fast-onset seizures. Ann. Neurol. *77*, 541–546.

Shiri, Z., Manseau, F., Lévesque, M., Williams, S., and Avoli, M. (2016). Activation of specific neuronal networks leads to different seizure onset types. Ann. Neurol. *79*, 354–365.

Smart, S.L., Lopantsev, V., Zhang, C.L., Robbins, C.A., Wang, H., Chiu, S.Y., Schwartzkroin, P.A., Messing, A., and Tempel, B.L. (1998). Deletion of the KV1.1 Potassium Channel Causes Epilepsy in Mice. Neuron *20*, 809–819.

Spencer, D.D., and Spencer, S.S. (1994). Hippocampal resections and the use of human tissue in defining temporal lobe epilepsy syndromes. Hippocampus *4*, 243–249.

Stanton, P.K., Jones, R.S., Mody, I., and Heinemann, U. (1987). Epileptiform activity induced by lowering extracellular [Mg2+] in combined hippocampal-entorhinal cortex slices: modulation by receptors for norepinephrine and N-methyl-D-aspartate. Epilepsy Res. *1*, 53–62.

Swartzwelder, H.S., Lewis, D.V., Anderson, W.W., and Wilson, W.A. (1987). Seizure-like events in brain slices: suppression by interictal activity. Brain Res. *410*, 362–366.

Swartzwelder, H.S., Anderson, W.W., and Wilson, W.A. (1988). Mechanism of electrographic seizure generation in the hippocampal slice in Mg2+-free medium: the role of GABAa inhibition. Epilepsy Res. *2*, 239–245.

Timofeev, I., and Steriade, M. (2004). Neocortical seizures: initiation, development and cessation. Neuroscience *123*, 299–336.

Timofeev, I., Bazhenov, M., Seigneur, J., and Sejnowski, T. (2012). Neuronal Synchronization and Thalamocortical Rhythms in Sleep, Wake and Epilepsy. In Jasper's Basic Mechanisms of the Epilepsies, J.L. Noebels, M. Avoli, M.A. Rogawski, R.W. Olsen, and A.V. Delgado-Escueta, eds. (Bethesda (MD): National Center for Biotechnology Information (US)),.

Tønnesen, J., Sørensen, A.T., Deisseroth, K., Lundberg, C., and Kokaia, M. (2009). Optogenetic control of epileptiform activity. Proc. Natl. Acad. Sci. U. S. A. *106*, 12162–12167.

Toyoda, I., Fujita, S., Thamattoor, A.K., and Buckmaster, P.S. (2015). Unit Activity of Hippocampal Interneurons before Spontaneous Seizures in an Animal Model of Temporal Lobe Epilepsy. J. Neurosci. *35*, 6600–6618.

Traub, R.D., and Wong, R.K. (1982). Cellular mechanism of neuronal synchronization in epilepsy. Science *216*, 745–747.

Truccolo, W., Donoghue, J.A., Hochberg, L.R., Eskandar, E.N., Madsen, J.R., Anderson, W.S., Brown, E.N., Halgren, E., and Cash, S.S. (2011). Single-neuron dynamics in human focal epilepsy. Nat. Neurosci. *14*, 635–641.

Urrestarazu, E., Chander, R., Dubeau, F., and Gotman, J. (2007). Interictal high-frequency oscillations (100-500 Hz) in the intracerebral EEG of epileptic patients. Brain J. Neurol. *130*, 2354–2366.

Uva, L., Grüschke, S., Biella, G., De Curtis, M., and Witter, M.P. (2004). Cytoarchitectonic characterization of the parahippocampal region of the guinea pig. J. Comp. Neurol. *474*, 289–303.

Velasco, A.L., Wilson, C.L., Babb, T.L., and Engel, J., Jr (2000a). Functional and anatomic correlates of two frequently observed temporal lobe seizure-onset patterns. Neural Plast. *7*, 49–63.

Velasco, A.L., Wilson, C.L., Babb, T.L., and Engel, J., Jr (2000b). Functional and anatomic correlates of two frequently observed temporal lobe seizure-onset patterns. Neural Plast. *7*, 49–63.

Vereczki, V.K., Veres, J.M., Müller, K., Nagy, G.A., Rácz, B., Barsy, B., and Hájos, N. (2016). Synaptic Organization of Perisomatic GABAergic Inputs onto the Principal Cells of the Mouse Basolateral Amygdala. Front. Neuroanat. *10*.

Viitanen, T., Ruusuvuori, E., Kaila, K., and Voipio, J. (2010). The K+-Cl cotransporter KCC2 promotes GABAergic excitation in the mature rat hippocampus. J. Physiol. *588*, 1527–1540.

Vismer, M.S., Forcelli, P.A., Skopin, M.D., Gale, K., and Koubeissi, M.Z. (2015). The piriform, perirhinal, and entorhinal cortex in seizure generation. Front. Neural Circuits *9*, 27.

Voskuyl, R.A., and Albus, H. (1985). Spontaneous epileptiform discharges in hippocampal slices induced by 4-aminopyridine. Brain Res. *342*, 54–66.

Weitz, A.J., Fang, Z., Lee, H.J., Fisher, R.S., Smith, W.C., Choy, M., Liu, J., Lin, P., Rosenberg, M., and Lee, J.H. (2015). Optogenetic fMRI reveals distinct, frequency-dependent networks recruited by dorsal and intermediate hippocampus stimulations. NeuroImage *107*, 229–241.

Wendling, F., Bartolomei, F., Bellanger, J.J., and Chauvel, P. (2002). Epileptic fast activity can be explained by a model of impaired GABAergic dendritic inhibition. Eur. J. Neurosci. *15*, 1499–1508.

Wetjen, N.M., Marsh, W.R., Meyer, F.B., Cascino, G.D., So, E., Britton, J.W., Stead, S.M., and Worrell, G.A. (2009). Intracranial electroencephalography seizure onset patterns and surgical outcomes in nonlesional extratemporal epilepsy. J. Neurosurg. *110*, 1147–1152.

Wiebe, S. (2004). Effectiveness and safety of epilepsy surgery: what is the evidence? CNS Spectr. *9*, 120–122, 126–132.

Wiebe, S., Blume, W.T., Girvin, J.P., Eliasziw, M., and Effectiveness and Efficiency of Surgery for Temporal Lobe Epilepsy Study Group (2001). A randomized, controlled trial of surgery for temporal-lobe epilepsy. N. Engl. J. Med. *345*, 311–318.

Wieser, H. (1993). Surgically remediable temporal lobe syndromes. Surg. Treat. Epilepsies 49–63.

Wirrell, E.C. (2010). Prognostic significance of interictal epileptiform discharges in newly diagnosed seizure disorders. J. Clin. Neurophysiol. Off. Publ. Am. Electroencephalogr. Soc. *27*, 239–248.

Wykes, R.C., Kullmann, D.M., Pavlov, I., and Magloire, V. (2015). Optogenetic approaches to treat epilepsy. J. Neurosci. Methods.

Yamamoto, J., Ikeda, A., Kinoshita, M., Matsumoto, R., Satow, T., Takeshita, K., Matsuhashi, M., Mikuni, N., Miyamoto, S., Hashimoto, N., et al. (2006). Low-frequency electric cortical stimulation decreases interictal and ictal activity in human epilepsy. Seizure *15*, 520–527.

Yekhlef, L., Breschi, G.L., Lagostena, L., Russo, G., and Taverna, S. (2015). Selective activation of parvalbumin- or somatostatin-expressing interneurons triggers epileptic seizurelike activity in mouse medial entorhinal cortex. J. Neurophysiol. *113*, 1616–1630.

Yizhar, O., Fenno, L.E., Davidson, T.J., Mogri, M., and Deisseroth, K. (2011). Optogenetics in neural systems. Neuron *71*, 9–34.

Ylinen, A., Bragin, A., Nadasdy, Z., Jando, G., Szabo, I., Sik, A., and Buzsaki, G. (1995). Sharp wave-associated high-frequency oscillation (200 Hz) in the intact hippocampus: network and intracellular mechanisms. J. Neurosci. *15*, 30–46.

Zhang, L., and McBain, C.J. (1995). Potassium conductances underlying repolarization and after-hyperpolarization in rat CA1 hippocampal interneurones. J. Physiol. *488*, 661–672.

Zhang, Z.J., Koifman, J., Shin, D.S., Ye, H., Florez, C.M., Zhang, L., Valiante, T.A., and Carlen, P.L. (2012). Transition to seizure: ictal discharge is preceded by exhausted presynaptic GABA release in the hippocampal CA3 region. J. Neurosci. *32*, 2499–2512.

Ziburkus, J., Cressman, J.R., Barreto, E., and Schiff, S.J. (2006). Interneuron and pyramidal cell interplay during in vitro seizure-like events. J. Neurophysiol. *95*, 3948–3954.

Zijlmans, M., Jacobs, J., Zelmann, R., Dubeau, F., and Gotman, J. (2009). High frequency oscillations and seizure frequency in patients with focal epilepsy. Epilepsy Res. *85*, 287–292.